Chapter 5. The Eocene Subduction-Obduction Complex of New Caledonia

Chapter 5 The Eocene Subduction-Obduction Complex

*P. Maurizot[1], D. Cluzel[2], M. Patriat[3], J. Collot[1], M. Iseppi[1], S. Lesimple[1], A. Secchiari[4], D. Bosch[5], A. Montanini[4], P. Macera[6], H.L. Davies[7].

1. Service Géologique de Nouvelle-Calédonie (New Caledonia Geological Survey), BP 465, 98 845, Noumea, New Caledonia.
2. University of New Caledonia, ISEA-EA 7484, BP R4, 98851, Noumea, New Caledonia.
3. Institut Français de Recherche pour l'Exploitation de la Mer (Ifremer), Délégation de Nouvelle-Calédonie, Unité de Recherche Géosciences Marines, 101 Promenade R. Laroque, 98800, Noumea, New Caledonia.
4. Department of Chemistry, Life Sciences and Environmental Sustainability, Parco Area delle Scienze 157/a, 43124 Parma, Italy.
5. Géosciences Montpellier, Université de Montpellier, Place Eugène Bataillon, 34095 Montpellier, France.
6. Earth Science Department, Pisa University, Via S Maria 53, 56126 Pisa, Italy
7. University of Papua New Guinea, PO Box 414, Papua New Guinea

Corresponding author (pierre.maurizot@gouv.nc)

26990 words
238 references
24 figures
1 table

Abbreviated title: Eocene Subduction-Obduction Complex

Abstract
Convergence and subduction started in the Late Palaeocene, to the east of New Caledonia, in the South Loyalty Basin/Loyalty Basin, leading to the formation of the Subduction-Obduction Complex of Grande Terre. Convergence during the Eocene consumed the oceanic South Loyalty Basin, and the north easternmost margin of Zealandia (the Norfolk Ridge). The attempted subduction of the Norfolk Ridge led eventually to the end-Eocene obduction. Intra-oceanic subduction started in the South Loyalty Basin, as indicated by high-temperature amphibolite (56 Ma), boninite- and adakite-series dykes (55-50 Ma), and changes in sedimentation regime (55 Ma). The South Loyalty Basin and its margin were dragged to a maximum depth of 70 km, forming the high pressure – low temperature Pouébo Terrane and the Diahot-Panié Metamorphic Complex, before being exhumed at 38-34 Ma. The obduction complex was formed by the stacking from NE to SW of several allochthonous units over autochthonous Zealandia, which include the Montagnes Blanches Nappe (Norfolk Ridge crust), the Poya Terrane (crust of the South Loyalty Basin), and the Peridotite Nappe (mantle lithosphere of the Loyalty Basin). A model of continental subduction accepted by most authors is proposed and discussed. Offshore continuations and comparable units in Papua-New Guinea and New Zealand are presented.

Key-words
New Caledonia, Norfolk Ridge, Loyalty Basin, Zealandia, ophiolite, ophiolitic melange, obduction, subduction, supra-subduction, exhumation, palaeo-transform fault, HP-LT metamorphism, basal sole, amphibolite, peridotite, lherzolite, boninite, adakite, eclogite, blueschist, serpentinite, tremolite, antigorite, lizardite.

Chapter 5 The Eocene Subduction-Obduction Complex 1
Montagnes Blanches Nappe 5
Poya Terrane 6
Poya Terrane Basalts (PTB) 6
Koné Facies 8
Eocene Metamorphic Belt 10
Diahot-Panié Metamorphic Complex 12
Pouébo Terrane 13
Metamorphism, structure, and age 13
Peridotite Nappe 15
Lithology 17
Fabric 18
High-temperature shear zones 19
Petrology and geochemistry 20
Age 22
Dykes 22
HT amphibolites (metamorphic sole) 24
Serpentinization and fracture development 24
Offshore extent 25
Geodynamic model 26
Discussion 28
Foreland basin 28
Montagnes Blanches Nappe 28
Poya Terrane 28
HP-LT Metamorphic Belt 29
Peridotite Nappe 30
Mechanism 32
Regional correlations 34
Conclusions 36
Acknowledgements 36
Figure captions 37
References 40

The Subduction-Obduction Complex of Grande Terre, the main island of New Caledonia, is one of the most studied features of the geology of the country. The association in the same island of a large ultramafic unit, the Peridotite Nappe, and an extensive high pressure - low temperature (HP-LT) metamorphic belt, had drawn already the attention of geologists in the 1970s, when plate tectonics was still a new theory. The term 'subduction' was first defined in the European Alps by Amstutz (1951), but at the time was outside the conceptual framework of plate tectonics. It was only in the 1970s that it was recognized as the process of consumption of an oceanic lithosphere under an oceanic or continental lithosphere at convergent plate boundaries. Conversely, 'obduction', the reverse process of overthrusting of a dense oceanic lithosphere (an ophiolite) onto a lighter continental lithosphere, was defined by Coleman (1971), with the examples of the Papuan Ultrabasic Belt, and the Peridotite Nappe of New Caledonia. Later, the gradual improvement of knowledge on the geology of New Caledonia and its surrounding marine domain, showed that both Peridotite Nappe, HP-LT Metamorphic Belt, and some other units, were part of a single set, herein termed the Subduction-Obduction Complex, accreted during Palaeogene convergence.

The Subduction-Obduction Complex comprises several allochthonous units (Fig. 1 and Fig. 2) stacked over the autochthonous Norfolk Ridge, north easternmost continental margin of Zealandia (Luyendyk 1995; Mortimer et al. 2017). These units are successively, in their order of superposition (with first reference), i) the Montagnes Blanches Nappe (Maurizot 2011). ii) the Poya Terrane (Cluzel *et al.* 1994). iii) the Peridotite Nappe (Avias 1967). In the north-eastern part of Grande Terre, the HP-LT Eocene Metamorphic Belt, represents the metamorphosed equivalent of the three aforementioned units.

In this chapter we review the large amount of published data on these different units as well as their interpretations. In the literature, both the European Alpine 'Nappe' and circum-Pacific 'Terrane' terms have been used although they have substantially different meanings. A nappe is primarily characterized by its flat-lying geometry whereas a terrane is mainly characterized by its internal tectono-stratigraphic homogeneity, both having clear tectonic boundaries. The terminology which is adopted and recommended in this memoir (Table 1), results more from the history of exploration of the island than from a formal logic, but for the sake of continuity, past terminology has been retained in this chapter.

Formal unit	Nature	Reference	Other obsolete term and reference
Montagnes Blanches Nappe	Sedimentary cover of the thinned continental crust of Zealandia	Maurizot 2011	Koumac Terrane (Cluzel et al. 1994)
Poya Terrane	Oceanic to continental crust of the South Loyalty Basin	Cluzel et al. 1994	Basalt Formation (Paris 1981)
Poya Terrane Basalts	Genuine oceanic crust	Cluzel et al. 2017	
Koné Facies	Ocean-continent transitional crust	Cluzel et al. 2017	
Eocene Metamorphic Belt	HP-LT subduction complex	This chapter	
Diahot-Panié Metamorphic Complex	Metamorphosed sedimentary cover of the thinned continental crust of Zealandia	This chapter	Diahot-Panié Terrane (Cluzel et al. 2001) Diahot Blueschists (Spandler et al. 2004)
Pouébo Terrane	Ophiolitic melange	Cluzel et al. 2001	Pouébo Eclogite (Aitchison et al. 1995)
Peridotite Nappe	Ophiolitic mantle lithosphere	Avias 1967	

Table 1 Terminology of formal tectonostratigraphic units used and recommended in this memoir, in their order of presentation in this chapter.

In this chapter the terms “Loyalty Basin” and “South Loyalty Basin” are defined as below. At present, the Loyalty Basin (LB) is the oceanic basin located between the Grande Terre and the Loyalty Islands, in which the Peridotite Nappe is rooted (Collot et al. 1987). The term South Loyalty Basin (SLB) has been created (Cluzel et al. 2001) and is used in this chapter, to account for the pre-obduction history and especially, the origin of the oceanic material partly or totally involved in the Eocene subduction. Thus, the oceanic (marginal) basin that opened to the E or NE of the Norfolk Ridge during the Late Cretaceous-Paleocene is termed Loyalty/South Loyalty Basin (LB/SLB). After the Early Eocene subduction inception, the LB represented the upper plate and the SLB the lower plate of the subduction/obduction system. The obducted part of the LB (upper plate) is now represented by the Peridotite Nappe (Collot et al. 1987), while the SLB is only known by its obducted (Poya Terrane Basalts), metamorphosed and exhumed remains (Pouébo terrane, Cluzel et al. 2001). According to this interpretation, the North Loyalty Basin is in part the remaining (rear-arc) part of the original LB and in part the back-arc basin of the Eocene Loyalty Arc, coeval to the South Fiji Basin, which is involved in the active subduction of the Vanuatu Arc (Monzier 1993).

Parts of the sedimentary units are already described in chapter 4 (this memoir) from a stratigraphic and lithologic point of view. Proposed models of evolution and coeval units in Papua-New-Guinea and New Zealand are presented and discussed in the final part of this chapter. Whenever unpublished information is newly brought into the present chapter it is referred to as “this work”.

Montagnes Blanches Nappe

In the Koumac area, a Late Cretaceous to Eocene sedimentary succession displays large southwest-verging overturned folds and thrust folds. Although its base is not known, due to a general décollement in sheared Late Cretaceous black argillite, the succession is supposed to correlate with the sedimentary cover lying on the basement greywackes (cf. chapter 3, this memoir) which are exposed to the southwest. The unit, in the Koumac area, has been called Koumac Terrane (Cluzel *et al.* 1994; Cluzel *et al.* 1995b). It is rooted in the north, and clearly allochthonous farther south, thrust over the top of the Eocene Bourail Group turbidites, and structurally sandwiched between it and the overlying Poya Terrane. In this area the Montagnes Blanches Nappe is so-named after the local name of the white coloured ranges marking the limbs of the Bourail anticline (Maurizot 2011).

Except for a few slices of basement greywackes in the Bourail area, the sedimentary succession is very consistent throughout the whole terrane (chapter 4, this memoir). The lowermost levels comprise the ‘Mamelons Rouges’ Formation (Tissot & Noesmoen 1958) of argillite and siltstone with widespread nodules containing Coniacian–Early Campanian fossils (ammonites and inocerams, chapter 4, this memoir). These beds grade into the Black Chert Formation, previously termed “phtanites” (Routhier 1953), a Late Campanian-Maastrichtian silicified equivalent of the underlying ‘Mamelons Rouges’ Formation, owing to remobilisation of its abundant siliceous fossil content of radiolarians and sponge spicules. The black argillites and cherts are rich in organic matter (total organic content > 1 %, Maurizot 2011, and chapter 4, this memoir). The black cherts pass gradually into pelagic micrite deposited from the late Maastrichtian to the Early Eocene. The micrite is overlain by calci-turbidite and calci-debrite of the Early Eocene–base Middle Eocene, which display soft-sediment deformations. The calci-turbidites alternate with an increasing amount of coarsening upward graded breccia beds termed ‘Buadio Breccia’ (Routhier 1953) that rework all the elements of the underlying sedimentary pile, including large blocks surrounded by breccia of the same

composition, interpreted as olistoliths, accumulated in front of a southward propagating fold-thrust belt. Notably, the breccia contains no clasts of Poya Terrane.

The Late Cretaceous to Palaeocene sedimentary succession in the Montagnes Blanches Nappe is essentially made of pelagic to hemipelagic deep-sea deposits (argillite, chert, micrite), with dominant biogenic input (radiolarians, sponge spicule, planktonic foraminifera), and subordinate terrestrial contribution. It can be interpreted as having been deposited on the thinned north-eastern margin of Zealandia. During the Late Cretaceous, reduced sedimentation, deposited in anoxic conditions, took place during post-rift thermal subsidence. During the Palaeocene, micrite deposition marked a return to normal oxygenated conditions and possibly warmer climate. During the Early Eocene, the same pelagic carbonate material records a dynamic depositional regime, with turbidites and breccia, marking a change from stable conditions to a syn-tectonic regime. The entire succession was subsequently thrust over the top of the younger turbidites of the southward-propagating Eocene flysch basin (Maurizot 2011, and chapter 4, this memoir).

Poya Terrane

The former autochthonous 'Formation des Basaltes' (Basalt Formation) of Paris (1981) is now universally regarded as an allochthonous unit, the Poya Terrane (Aitchison *et al.* 1995; Cluzel *et al.* 1994; Cluzel *et al.* 2001; Cluzel *et al.* 1995b; Cluzel *et al.* 1997; Eissen *et al.* 1998). The Poya Terrane is an imbricate thrust complex which lies between the Peridotite Nappe and the Montagnes Blanches Nappe. It is divided into two units, Poya Terrane Basalts and Koné Facies. The former is made of narrow slices of oceanic material (dominant basalt and rare thin drapes of argillite and chert), while the latter mainly consists of thicker fine-grain sedimentary units intruded by dolerite sills (Cluzel *et al.* 2017).

The main body of the Poya Terrane crops out along the southwest coast of Grande Terre, beneath the klippes of the Peridotite Nappe. To the south and east, smaller and discontinuous slivers of Poya Terrane occur beneath the Massif du Sud and its northeastern extension along the east coast, and above thin slices of Montagnes Blanches Nappe. The southernmost occurrences of the terrane are in Ouen Island, under the Peridotite Nappe; while basalt possibly related to the Poya Terrane has been intersected at the bottom of the Amédée Islet borehole, on the barrier reef, to the southwest of Nouméa (Cabioch *et al.* 2008). Magnetic anomalies have been attributed to the offshore extension of the Poya Terrane, over 200 km below the Northern Lagoon (Collot & Missègue 1986) and over 500 km to the southwest of Nouméa Peninsula (Lagabrielle & Chauvet 2008; Rigolot 1988). However, these anomalies could also be related to Late Cretaceous volcanic rocks or basement terrane rocks. A single sample of enriched mid-ocean ridge basalt (E-MORB), collected during the GEORSTOM cruise, c. 200 km to the SE of Grande Terre, is comparable with Poya Terrane basalts (Daniel *et al.* 1976; Mortimer *et al.* 2014a). Inliers of basalts involved in the Eocene HP-LT metamorphic complex between Hienghène and Poindimié, and metamorphosed into blueschist facies, are correlated with Poya Terrane (Maurizot et al. 1984).

Poya Terrane Basalts (PTB)

The PTB unit consists of upright stacked slices of basalt, only a few m to a few 10 m thick in individual intact stratigraphic sections, and subordinate m to several m-thick beds of red, black, white, and green radiolarian chert, argillite, and ferro-manganiferous jaspers (Fig. 3a, b). Lenses of manganese oxide and low-grade gold-bearing copper sulphide of volcanogenic massive sulphide deposit type, are

associated with the sedimentary inliers. In one of these deposits near Koné, clusters of worm tubes in the sulphide ore represent the remains of a seafloor hydrothermal vent and its associated living community (chapter 9, this memoir, and Oudin *et al.* 1985). Basalts are crosscut by a number of brittle- to semi-brittle shears and tension cracks. Most of sedimentary inliers are fault-bounded, locally folded with steeply dipping fold axes. Basalts are generally massive and locally coarse grained, with apparently only rare pillow basalt occurrences (e.g. Gatope Peninsula or Pandop Peninsula, Fig. 3c). However, pillow structures may have been erased by weathering, and pillow "ghosts" appear locally in deeply weathered basalt. Inter-pillow material is scarce and argillite drapes are commonly 2 to 5 m in thickness, a feature which suggests that abyssal sediments accumulated only after fast eruption of basalt on the ocean floor. Neither a dyke complex, nor mafic or ultramafic cumulates are known from Poya Terrane. The basalts are locally cross cut by a dense network of quartz, calcite, zeolite, chlorite, and/or epidote veins. The basalts are generally affected by hydrothermal-like static metamorphism of zeolite to lower greenschist facies. In addition to static recrystallization, a rough schistosity appears near the base of the Peridotite Nappe within a vertical distance of about 100-200 m in basalt, and 300-500 m in sedimentary rocks.

Pervasive alteration has likely disturbed the K-Ar system of the basalts making age dating based upon this method unreliable (Daniel *et al.* 1976; Eissen *et al.* 1998; Guillon & Gonord 1972; Rodgers 1976). The abyssal argillite of the Poya Terrane has yielded Late Cretaceous (Campanian-Maastrichtian) and Paleogene (Palaeocene to Early Eocene) radiolarians (Aitchison et al. 1995; Cluzel et al. 2001).

Locally, at Foué and Pinjen peninsulas, reddened pillow breccias and vesicular pillow lavas of alkaline affinity (see below) are interbedded with and/or overlain by pinkish micrite (Coudray & Gonord 1966), which yield a mixed planktonic microfauna of Late Cretaceous (Globotruncanids) to mid-(?) Eocene age (*Turborotalia cerroazulensis pomerolii*). Compared with the dominant argillite and chert inliers, these rare carbonate occurrences associated with alkaline or back-arc basin basalt (BABB) lavas might represent shallow parts of the basin in which Poya Terrane basalts were formed originally, possibly seamounts.

Three contrasting magmatic affinities are present within PTB: BABB, E-MORBs, and alkaline basalts. Most Poya Terrane basalts display subalkaline (tholeiite) features; i.e., low K_2O contents ($0.1 < K_2O < 0.5$ %), relatively flat chondrite-normalised rare-earth element (REE) patterns (Fig. 4a) with low $(La/Yb)_n$ ratios ($0.41 < (La/Yb)_n < 1.93$), and Th/Ta ratios (Fig. 4b). Trace elements compositions vary between light REE (LREE)-undepleted and LREE-depleted end-members.

The LREE undepleted type represents about 80 % of the samples analysed. It comprises basalts and dolerites containing low-Ti and Al augite, and plagioclase (An_{30-70}) phenocrysts. The igneous rocks display flat chondrite-normalised LREE patterns ($0.84 < (La/Sm)_n < 1.17$; $0.96 < (La/Yb)_n < 1.43$ (Fig. 4a). They also display enrichment in high field strength (HFS) elements (Th, Ta, Nb) and moderately high Nb/Y and Th/Nb ratios ($0.14 < Nb/Y < 0.23$; $0.05 < Th/Nb < 0.13$, Fig. 4b). εNd values back-calculated to 80 Ma (Campanian) vary from 2.77 to 6.72, within the range of typical E-MORB lavas (Sun & McDonough 1989). Their $^{87}Sr/^{86}Sr$ ratios ($0.70386 < (^{87}Sr/^{86}Sr) < 0.70599$) are also consistent with E-MORB affinities but reveal some Sr mobility due to hydrothermal alteration and weathering (Fig. 4c). E-MORBs were originally considered the dominant type (Cluzel et al. 2001); however, their importance within PTB has been largely overestimated for two reasons: i) E-MORB dolerites are younger, according to their intrusive nature and ages (see below) and better preserved than the bulk

of PTB and have been oversampled, and ii) most E-MORBs actually are sills intruded in the Koné Facies (see below) and have been wrongly taken for oceanic crust basalts.

The LREE depleted (BABB) type has been identified in a few areas of the Poya Terrane: near Koné, Gatope peninsula, Poya, Ouazangou and Koumac (west coast); and in the Canala and Thio areas (east coast); however, its area of extent is probably much larger. The depleted-type rocks (SiO_2 = 46-50 wt %; MgO = 6-8 wt %; TiO_2 = 0.96-1.57 wt %) contain augite microphenocrysts with higher Al and Ti contents than those of enriched type lavas. They display chondrite-normalised REE patterns with marked LREE depletion ($0.45 < (La/Sm)_n < 0.69$; $0.41 < (La/Yb)_n < 0.73$), clearly distinctive of depleted MORBs. Expanded multi-element normalised diagrams display typical MORB-like patterns with respect to HFS elements, with the exception of a slight Nb-Ta depletion. εNd values vary from 7.0 to 11.6, consistent with a depleted mantle source (Fig. 4c). The features of the "depleted type" are transitional between island-arc tholeiite and N-MORB and thus are similar to lavas erupted in a back-arc environment (BABB).

Alkaline volcanic rocks occur in one area on the west coast (Foué and Pinjen peninsulas). They comprise highly vesicular pillow-basalts and pillow breccia with pinkish Al and Ti-rich diopside; plagioclase (An_{30-70}) and Fe-Ti oxides microphenocrysts in a devitrified groundmass. Due to weathering, major element concentrations are unreliable; mineral chemistry, high TiO_2 contents (1.9-2.4 wt %), HREE depleted and LREE enriched patterns ($3.27 < (La/Sm)_n < 3.8$; $10.7 < (La/Yb)_n < 13.9$), and prominent enrichment in Ta, Nb and Th suggest alkaline character. However, elevated εNd = ($6.7 < \varepsilon Nd < 7.8$) are inconsistent with typical oceanic island basalt (OIB) (Fig. 4c).

According to Ali & Aitchison (2000), palaeomagnetic data of the basalts indicate that they have been generated at about 500 km to the north of their present location. However, the highly altered and severely deformed state of the unit (see above description) makes such an interpretation somewhat equivocal.

Koné Facies

Mappable and extensive units of light-coloured sedimentary rocks, dominant over subordinate basalts, have long been distinguished in the Poya Terrane, near Koné area, as the "Koné facies" (Carroué 1972a; Paris 1981; Routhier 1953), and reappraised recently (Cluzel *et al.* 2012b; Cluzel *et al.* 2017; Whitten 2015).

Sedimentary rocks of the Koné Facies display successions of well-bedded volcaniclastic, siliciclastic sandstone, siltstone, argillite, and chert (Fig. 3d). Quartz and feldspar (albite) are dominant as detrital minerals and in lithic clasts. Sandstones dominate near the structural base of the unit where they may be several m thick; their thickness and grain size reduce upward and grade into well-bedded silt-size turbidites with millimetre-thick laminations. Soft sediment deformation features such as slumps and syn-sedimentary boudinage are common, as expected in gravity-driven slope deposits. These rocks are locally intruded by dolerite and transformed by contact metamorphism into whitish massive recrystallized cherts, hornfels, and spotted schists bearing millimetre-size spheroidal aggregates of chlorite and albite (Fig. 3f). In the Koné area, sedimentary rocks are dominant and dolerite subordinate; in contrast, near Temala 100 m thick dolerite sills represent about one half of the bulk formation. Cross-cutting dykes are rare.

The highly disrupted nature of the Poya Terrane makes it impossible to draw an accurate contact between Koné Facies and PTB. Some intermediate facies occurrences (e.g. abyssal draping alternating with turbidites) suggest former continuity, later disrupted by tectonic slicing. At a regional scale, e.g. on the West Coast, most occurrences of Koné Facies are located to the northeast of PTB, i.e. structurally below it. It is therefore likely that Koné facies rocks are structurally below PTB and above the Montagnes Blanches Nappe.

Hemipelagic sediments of the Koné Facies yield numerous large inoceramid casts (Fig. 3e), notably *Inoceramus bicorrugatus* (Carroué 1972a, b), *I. (Sphaenoceramus) angustus,* and *I. australis* (Paris 1981) indicating a Late Turonian to Santonian age (Cooper 2004). These assignments partially make the Koné Facies a time correlative of Formation à Charbon (Coniacian-Campanian; chapter 4, this memoir). Radiolarians are widespread in thin sections of fine-grained sediments; however, identifying them has so far been unsuccessful as a consequence of recrystallization that has only left silica "ghosts".

Detrital zircon data and sediment provenance

Cluzel *et al.* 2017 undertook a detrital zircon study on representative samples of siliciclastic, volcaniclastic and greywacke-like sandstones of the Koné Facies and compared them to those from the autochthonous Late Cretaceous Formation à Charbon. All analysed populations contained relatively young, euhedral (presumed young) zircon and rounded (presumed older) crystals.

The bulk Koné Facies age distribution shows a main Cretaceous population, a lesser Early Mesozoic group and a minor Paleozoic- Precambrian group. The distribution of Cretaceous zircons shows two distinct age peaks at 104 Ma (Albian) and 83 Ma (Coniacian-Santonian). Age-probability plots for individual samples show that all of the Koné Facies sandstones have similar detrital zircon patterns differing mostly in the magnitude of the youngest Coniacian-Santonian population with respect to the Albian and older zircon populations (Fig. 5). The youngest Coniacian-Santonian zircon population is very close to the depositional age determined upon paleontological grounds and likely related to synchronous magmatic activity, consistent with the volcaniclastic character of most of the sandstones. The prominent Albian zircon population is widespread in Late Cretaceous sedimentary rocks of New Caledonia (Cluzel *et al.* 2011) and New Zealand (Adams *et al.* 2013a, b, 2016). Albian rocks are only poorly represented in New Caledonia by scarce volcaniclastic turbidites that share the same origin as the rest of Mesozoic greywackes from the basement terranes (Adams *et al.* 2009; Cluzel *et al.* 2011). Therefore, Early Cretaceous zircons may locally be derived from volcanic or volcaniclastic rocks, which were eroded before the Late Cretaceous; or alternatively, from an external source of this age such as the silicic Eastern Australian Whitsunday Province (Bryan *et al.* 2012; Bryan *et al.* 2000). In the locally derived 'Formation a Charbon', the relative abundance of 250-150 Ma detrital zircons and scarcity of Paleozoic zircons is similar to the bulk age distribution in greywackes of basement terranes (Adams et al. 2009; Cluzel et al. 2011), thus a similar local origin is likely.

Dolerite age and geochemistry

Dolerite dating has been undertaken by *in situ* LA-ICPMS U-Pb geochronology on micro-zircons. Most zircons display concordant U-Pb ages, and all the analyzed dolerite dykes/sills crystallized during a relatively narrow time interval in the latest Palaeocene and Early Eocene (58.4 ± 1.5 - 47.6 ± 4.0 Ma, Cluzel *et al.* 2017). The dolerite U-Pb ages cluster around 54 ± 5 Ma, almost the same age as the

youngest fossil ages from the PTB unit of the Poya Terrane, and approximately coeval (within error) with pre-obduction ~53 Ma dykes from the Peridotite Nappe (Cluzel *et al.* 2006), and ~56 Ma inferred subduction inception (Cluzel *et al.* 2012a). Therefore, at variance with previous interpretations (Cluzel et al. 2001), mafic rocks of the Koné Facies are chronologically and thus genetically unrelated to the enclosing sediments and to passive margin evolution.

All dolerite samples have very similar sub alkaline basalt major and trace element compositions and display almost flat chondrite-normalized REE patterns (Evensen *et al.* 1978; Pearce 1982, $(La/Yb)_n$ = 1.2 ± 0.1) without depletion in LREE ($(La/Sm)_n$ = 1.0 ± 0.2), and are diagnostic of E-MORBs (enriched MORBs), e.g. subalkaline basalts slightly enriched in LREE and large-ion lithophile element (LILE) incompatible elements with respect to N-MORB (Fig. 3a). A negative slope of LREE undepleted patterns and fractionation of LILE with respect to high field-strength elements (HFSEs) of some samples probably signal source heterogeneity, which may be due to near-ridge re-enrichment of the mantle source, or source mixing. Dolerite sills in the Koné Facies commonly display a weak Nb negative anomaly, which is not present in E-MORB dykes crosscutting the PTB, and is likely due to slight contamination by wallrock terrigenous sedimentary rocks. The scarce occurrence of inherited older zircons (~100 Ma) in some dolerites (Cluzel *et al.* 2017) supports this interpretation.

On the Hf/3-Th-Ta triangular diagram (Vermeesch 2006; Wood 1980) Koné Facies dolerites plot in a restricted area similar to that of E-MORB flow and pillow basalts of the PTB. Thus, Koné Facies dolerites correlate with PTB E-MORBs, suggesting one single magmatic affinity (Fig. 4b), however, they neither display the typical BABB, nor OIB-like features of the PTB.

Eocene Metamorphic Belt

The Eocene HP-LT metamorphic domain in the northeast of Grande Terre (Fig. 6) is a NW-SE trending belt, 20 km wide and 200 km long. It is considered as one of the largest in the world (Clarke et al. 1997), and as such, it has been the object of a great number of descriptive and interpretive publications. The belt underlies the most elevated ridge of Grande Terre, with Mont Panié (1628 m) as its highest point.

Since the early mentions and descriptions of glaucophane schists and eclogites (Brière 1919; Garnier 1867a, b; Lacroix 1897, 1941), the metamorphic belt has been the subject of numerous detailed petrological and mineralogical studies (e.g. Bell & Brothers 1985; Black 1970a, b, c; Black *et al.* 1993; Black 1973; Black 1975, 1977; Black & Brothers 1977; Black *et al.* 1988; Blake *et al.* 1977; Briggs 1975, 1977, 1978; Briggs *et al.* 1978; Brothers 1970, 1974, 1985; Brothers & Black 1973; Coleman 1967; Diessel *et al.* 1978; Ghent *et al.* 1987a; Ghent *et al.* 1987b; Itaya *et al.* 1985; Yokoyama *et al.* 1986). More recently, modern thermodynamic approaches and plate tectonic concepts have been applied (e.g. Agard & Vitale-Brovarone 2013; Baldwin *et al.* 2007; Carson *et al.* 2000; Clarke *et al.* 1997; Cluzel *et al.* 2001; Cluzel *et al.* 1995b; Fitzherbert *et al.* 2004; Pirard & Spandler 2017; Potel *et al.* 2006; Rawling & Lister 2002; Spandler *et al.* 2005; Taetz *et al.* 2016; Vitale Brovarone & Agard 2013, and references therein).

The belt has been extensively studied along the Koumac-Ouégoa provincial road N° 7 (PR 7) transect, and along the NE coast. Conversely, the remote area of the Mont Panié has been largely overlooked. The south-eastern termination of the belt is in the Touho-Poindimié area where lawsonite and blueschist facies rocks were identified in the 1980s (Maurizot *et al.* 1984; Maurizot & Vendé-Leclerc 2009).

The belt consists of blueschist and eclogite facies metamorphic rocks. The metamorphic grade increases from southwest to northeast, as does the metamorphic grain size. In this direction, successive lawsonite, glaucophane, garnet, epidote, and omphacite pseudo-isograds are crossed. The deformation is polyphase. Broad late foliation antiforms and synforms have been noted by several authors (Lister & Forster 2009; Maurizot *et al.* 1989; Rawling & Lister 1999b; Rawling & Lister 2002).

Various classifications have been used to subdivide the belt, based either on metamorphic grade (Black *et al.* 1993; Ghent *et al.* 1987a; Ghent *et al.* 1994; Maurizot *et al.* 1989; Paris 1981; Vitale Brovarone & Agard 2013; Yokoyama *et al.* 1986), or on protolith composition (Agard & Vitale-Brovarone 2013; Aitchison *et al.* 1995; Baldwin *et al.* 2007; Carson *et al.* 1999; Clarke *et al.* 1997; Clarke *et al.* 2006; Cluzel *et al.* 1994; Cluzel *et al.* 2001; Cluzel *et al.* 2012b; Fitzherbert *et al.* 2003; Fitzherbert *et al.* 2004; Gautier *et al.* 2016; Potel *et al.* 2006; Spandler *et al.* 2005; Taetz *et al.* 2016). The two most frequently used terms are:

- The Diahot - Panié Terrane, dominated by metasediments and metavolcanic rocks.

- The Pouébo Terrane, an ophiolitic melange.

The two terranes have also been termed Diahot Blueschists and Pouébo Eclogite Melange (Pirard & Spandler 2017; Spandler *et al.* 2004a; Spandler *et al.* 2008) in reference to their dominant metamorphic grades. This distinction has been used mainly in the most accessible Ouégoa-Pouébo area, and the coincidence of structural and metamorphic boundaries does not necessarily apply at the scale of the entire belt.

To the northeast, in the Ouégoa-Pam Peninsula area, the boundary between the Diahot and Pouébo terranes has long been recognized as fault-bounded (Briggs *et al.* 1978; Clarke *et al.* 1997; Cluzel *et al.* 1994; Maurizot *et al.* 1989) with obvious metamorphic (pressure, temperature, and fabric) breaks, justifying subdivision as distinct terranes separated by major structural contacts. To the southwest, the boundary between the Diahot – Panié Terrane and the Montagnes Blanches Nappe (previously referred to as the Koumac Terrane, Cluzel *et al.* 1994) is less obvious, and its delineation is variable from one author to another. Along the Koumac-Ouégoa section, despite a number of important along-strike faults, lithology, stratigraphy, and low-grade metamorphism, in both Diahot- Panié Terrane and Montagnes Blanches Nappe are similar (Potel 2001; Potel *et al.* 2004; Potel *et al.* 2006; Potel *et al.* 2002). The terrane concept seems difficult to apply for such a transitional contact.

To the southeast, from Hienghène to Poindimié, various units are included into the Diahot-Panié Terrane. The following elements are identifiable despite the metamorphic overprint: i) basement greywackes; ii) Late Cretaceous to Palaeocene sedimentary cover similar to the Montagnes Blanches Nappe; and, iii) basalt equivalent to the Poya Terrane. All of them are recrystallized in the lawsonite-glaucophane blueschist facies (e.g. Maurizot *et al.* 1984). Outside the metamorphic belt, these units constitute different terranes so it is inappropriate to regard them as a single terrane within the metamorphic belt.

Such disparate structural and metamorphic terminology clearly results from insufficient data and this issue can only be solved by further detailed investigations. Meanwhile, it is proposed here to use the new and more comprehensive term Diahot-Panié Metamorphic Complex instead of Diahot-Panié Terrane, and to retain the Pouébo Terrane. The southwestern limit of the Diahot-Panié Metamorphic

Complex approximately corresponds to the lower grade, lawsonite-in isograd of the HP-LT belt. This is complexly faulted and its delineation needs to be improved.

Diahot-Panié Metamorphic Complex

Basement (cf. chapter 3, this memoir) and cover (cf. chapter 4, this memoir) lithologies, comparable with unmetamorphosed units of Grande Terre, can be recognized in the Diahot-Panié Metamorphic complex.

Basement in the Poindimié area is mostly fine-grained greywackes and black siltstones which are part of the Ponérihouen-Goipin unit of the Koh-Central Terrane. Despite the metamorphic overprint, identifiable macrofossils have been found in lawsonite-glaucophane schists, including Late Triassic *Monotis* and Late Jurassic inoceramids (Maurizot *et al.* 1984) to the south of Poindimié. Inoceramids of the Late Jurassic have been collected at Kavatch (Paris 1981). Upstream the Diahot River (Paimboas), blueschist facies rocks have yielded an unimodal Early Cretaceous zircon population (102 ± 3 Ma, Albian) some of them with an Eocene recrystallization rim. This rock has been interpreted as a meta-greywacke of the Koh-Central Terrane (Cluzel *et al.* 2010a).

On both sides of the Diahot River, typical lithologies of the Late Cretaceous sedimentary succession are present, some are still fossiliferous. The base of the syn-rift sequence is not exposed. Most of the sedimentary rocks consist of silty to sandy black shale and rare microconglomerates, without coal beds. Bimodal volcanism, of volcanic-arc affinity (Diahot Volcanic Rocks, cf. chapter 4, this memoir) is represented, by meta-basalts/andesites and meta-rhyodacites/rhyolites. Felsic lavas and their pyroclastic equivalents are closely associated with small polymetallic massive sulphide deposits bearing base metals and gold (cf. chapter 9, this memoir). The metamorphosed post-rift succession includes equivalents of the 'Mamelons Rouges' and Black Cherts formations, which are metamorphosed to black schists and black siliceous schists (Fig. 7a). Fossiliferous nodules from schistose ‘Mamelons Rouges’ beds have yielded Late Cretaceous Inoceramids of Late Turonian to Santonian age (Espirat & Milon 1965; Maurizot *et al.* 1989; Paris 1981). Youngest detrital zircon ages in meta-sandstones are in the range of 76-97 Ma (Cluzel *et al.* 2011) and 67-88 Ma (Pirard & Spandler 2017), thus confirming the Late Cretaceous age (and stratigraphic equivalence) of the protolith. Zircon age spectra are similar to those of the Late Cretaceous ‘Formation a charbon’, and suggest a similar local provenance.

To the north of Pam Peninsula, the Bouehndép massif, 5 km long and 1 km wide, consists of eclogitic felsic gneisses with large (5 mm) albite porphyroblasts, epidote, and omphacite. This unit, originally referred to as "leptynite" (Espirat 1963) has been interpreted as a metamorphosed hypabyssal intrusion of rhyolite composition (Black *et al.* 1988; Clarke *et al.* 1997; Maurizot *et al.* 1989). U-Pb on zircon ages of this rock are 83 ± 2 Ma (Cluzel *et al.* 2011) and 90 to 75 Ma (Pirard & Spandler 2017). U-Pb ages on zircons at 108 and 202 Ma are mentioned by Baldwin (2007). The diversity of ages in these rocks, some of them being comparable with ages of detrital zircons of the Late Cretaceous ‘Formation a charbon’, suggests a possible meta-sedimentary, mixed volcano-sedimentary origin; or alternatively, zircon heritage and contamination of a shallow level intrusion by late Cretaceous surrounding rocks.

In the area of Hienghène the renowned tourist sites of the ‘Hen’, Sphinx and Lindéralique Rocks, are composed of chert, micrite with chert, micrite, and pink calciturbidite, similar to that of the Montagnes Blanches Nappe, recrystallised into quartzite and microsparite by the Eocene

metamorphism. Globigerinid and discocyclinid ‘‘ghosts’’ were reported in metamorphosed limestone lenses and boulders, north of Hienghéne, at the Tao Waterfall (Arnould 1958, p. 351 and plate XX - XXI; Arnould & Routhier 1957; Carroué 1971), however the sampling locality has never been found again.

Pouébo Terrane

The Pouébo Terrane is a typical ophiolitic mélange (Fig. 7b), a heterogeneous and chaotic association of 10 cm to 1 km size boulders of mainly meta-basaltic rocks with rarer felsic meta-sedimentary rocks, intimately associated with a serpentinite matrix. Generally, the metabasic rocks form competent blocks or lenses more or less rotated within the sheared soft serpentinite matrix. A few blocks of ferro-manganiferous meta-chert are also present. Serpentinite is typically associated with talc, chlorite, and phengite. Metamorphic grade is eclogite, blueschist, and garnet amphibolite facies (Maurizot *et al.* 1989).

There is substantial evidence that the Pouébo Terrane protolith is in part derived from the Poya Terrane. Mafic rocks from both terranes are geochemically and isotopically identical (Cluzel *et al.* 2001; Spandler *et al.* 2004b). Mineral phases of low-temperature seafloor alteration by sea water, which are common in the Poya Terrane, have been reported within the recrystalisation rim of eclogite facies zircons of the Pouébo Terrane (Spandler *et al.* 2004b). Eclogite blocks of the Pouébo Terrane have yielded Late Cretaceous and Palaeocene magmatic zircons dated at 85 Ma and 50-55 Ma (Pirard & Spandler 2017; Spandler *et al.* 2005) which correlate with the paleontological age of the Poya Terrane Basalts and U-Pb age of dolerites of the Koné Facies.

The Pouébo Terrane is restricted to the northwest part of the metamorphic belt. To the southeast, only one occurrence of melange-like high grade metamorphic rock is mentioned at Anse Ponandou, between Poindimé and Touho, where stretched conglomerate, glaucophane schists and eclogite are exposed (Black & Brothers 1977; Maurizot *et al.* 1984); however, it is not associated there with serpentinite.

Metamorphism, structure, and age

The Diahot-Panié and Pouébo terranes have contrasting lithologies and tectonic facies. Gneisses and schists of both terranes display generally a well-developed foliation and stretching lineation. The number of interpreted deformation-metamorphism stages invoked for the metamorphic rocks is varied. It ranges from two (Maurizot *et al.* 1989), three (Cluzel *et al.* 1995a), four (Bell & Brothers 1985; Fitzherbert *et al.* 2004), three to seven (Clarke *et al.* 1997), and eight (Rawling & Lister 2002). This diversity of interpretations is unlikely to fit into a single consistent model, and probably reflects the discontinuous perception of a more or less continuous process.

Field observations, mineral relationships, and geothermobarometry indicate a clockwise pressure-temperature-time path (P-T-t) in both terranes (Fig. 8c), starting with prograde metamorphism in the blueschist facies, peak metamorphism in the eclogite facies, then retrogression through blueschist and greenschist facies. The prograde path is attributed to progressive burial and subduction of the protolith. The retrograde path corresponds to its exhumation (see below).

In the Diahot-Panié Metamorphic Complex, crystallinity of organic matter and illite show a progressive increase in metamorphism from a diagenetic zone, through very low grade to low grade metamorphic zones (Diessel *et al.* 1978; Potel 2001; Potel *et al.* 2004; Potel *et al.* 2006; Potel *et al.*

2002). For convenience, the first appearance of lawsonite is commonly used as marking the southwestern limit of the complex.

In the Pouébo Terrane, common rocks are gneiss and amphibolite (with barroisitic amphibole, omphacite and garnet diagnostic of the eclogite-facies peak metamorphism). Garnet commonly preserves complex curved to spiral-shaped inclusion trails (Clarke *et al.* 1997). Complex vein networks, composed of garnet–quartz–phengite assemblage, in blueschist and eclogite, represent channelized fluids collected by dehydration processes of hydrous phases of the host rock during prograde metamorphism (Spandler & Hermann 2006; Taetz *et al.* 2016). Decussate aggregates of actinolite-tremolite laths (up to 10 cm in length), associated with phengite and magnetite, which form rims, a few cm to a few dm-thick around eclogite boulders indicate static retrogression into the greenschist facies.

Geothermobarometry of various mineral assemblages (Agard & Vitale-Brovarone 2013; Carson *et al.* 1999; Clarke *et al.* 1997; Fitzherbert 2002; Fitzherbert *et al.* 2003; Fitzherbert *et al.* 2004; Taetz *et al.* 2016; Vitale Brovarone & Agard 2013), Raman spectroscopy of carbonaceous material (Agard & Vitale-Brovarone 2013; Vitale Brovarone & Agard 2013), and oxygen isotope ($^{18}O/^{16}O$) fractionation in quartz, calcite, muscovite, pyroxene and amphibole (Black 1974), have been used to constrain the metamorphic P-T conditions. These estimates are summarized in Fig. 8c. The P-T conditions for the lawsonite-in isograd of the Diahot-Panié Metamorphic Complex are assessed at c. 300 °C and 0.8 GPa. The peak metamorphism of eclogite in the Pouébo Terrane is constrained to a maximum temperature of 550-650 °C at a range of maximum pressure of 1.6-2.4 GPa. The most recent estimates based on pseudosection modelling and Tmax value of Raman spectroscopy suggest maximum temperatures of 550 °C (Vitale Brovarone & Agard 2013). P-T values for the two units point to a maximum of c. 70-80 km of burial (Agard & Vitale-Brovarone 2013).

Spatial discontinuities are revealed by contrasting deformation styles and metamorphic gaps through major faults, especially between the Pouébo Terrane and the Diahot-Panié Metamorphic Complex. Along the northeastern coast and in the Ouégoa area, the Pouébo Terrane, which has the higher metamorphic grade, forms the core of a regional foliation antiform, wrapped by the Diahot-Panié complex (Cluzel *et al.* 1995a). The regional foliation bears a penetrative stretching lineation, trending ENE-WSW; it is marked by stretched pebbles, quartz rods, aligned amphibole needles, pressure shadows around phenocrysts, and sheath folds (Fig. 8a). Synkinematic minerals related to the stretching lineation belong generally to retrograde metamorphic events (e.g. blueschist after eclogite assemblage, quartz-chlorite pressure shadows around garnets).

There are many radiometric ages from both terranes. Ages measured on whole rocks are much dispersed and are difficult to interpret due to mixing of mineral phases of different ages (Blake *et al.* 1977; Ghent *et al.* 1994; Taetz *et al.* 2016). Ages measured on single minerals are more pertinent and have allowed reconstruction of the P-T-t path (Fig. 8c).

Newly formed zircon rims are only developed in the higher-grade rocks (beyond garnet-in grade). In the Ouégoa area of the Diahot-Panié Metamorphic Complex, zircon rims yielded U-Pb ages of 39.1 ± 1.0 and 37.2 ± 1.8 Ma (Pirard & Spandler 2017). In the Early Cretaceous meta-greywacke of Paimboas area, thin recrystallization rims are dated at 38 ± 3 Ma (Cluzel et al. 2010a). Therefore, peak metamorphic age of the Diahot-Panié blueschist could be close to c. 38 Ma. In the Pouébo Terrane, zircon rims in eclogites yielded ages of 44.1 ± 0.9, 44.5 ± 1.2, and 47.9 ± 5.3 Ma (Spandler *et al.* 2005)

and 40.4 ± 5.2 Ma (Pirard & Spandler 2017). The former age has been obtained in zircon rim containing preserved inclusions of barroisite, diagnostic of eclogite facies. A non-retrograde eclogite of the same terrane yielded a poorly constrained Rb-Sr rock-mineral isochron age of c. 38 Ma, (Taetz *et al.* 2016). On average, the age of the peak metamorphism of Diahot-Panié Metamorphic Complex is centred on 38 Ma, and that of Pouébo Terrane on 46-40 Ma, although some of these values overlap within error.

More than 50 $^{40}Ar/^{39}Ar$ ages (Baldwin *et al.* 2007; Ghent *et al.* 1994; Rawling 1998) and a few K/Ar ages (Blake *et al.* 1977; Coleman 1967) on phengite, fuschite, and K-feldspar have been published. They span the 28 to 40 Ma period, but cluster at about 38 Ma (Fig. 8d). Phengite is considered as a retrogressive phase that formed during cooling and decompression at 350–450 °C and 0.8–0.5 GPa. Apatite fission track on one sample of the Bouhendép felsic eclogite yielded an age of 34 ± 4 Ma for an estimated closure temperature of 150 °C (Baldwin *et al.* 2007); whereas in the same sample locality, K-feldspar and phengite yielded age of c. 35.5 Ma.

On the whole, these data provide a consistent picture of the metamorphic evolution through Eocene of the metamorphic belt. The basement and its Late Cretaceous - Palaeocene cover (Diahot-Panié Metamorphic Complex) as well as part of the Pouébo Terrane, were progressively subducted towards the northeast (see "Discussion" below), at a maximum depth of 70-80 km, then exhumed, as indicated by the P-T-t path. The oldest preserved metamorphic minerals are Middle Eocene, whilst the youngest are Late Eocene. Distinct P-T-t paths for the two terranes indicate independent evolution, albeit at about the same time. The peak metamorphism, which preceded exhumation inception, was delayed for about 6 My in Diahot-Panié Metamorphic Complex compared to Pouébo Terrane, and record the time elapsed by Pouébo eclogites to travel the vertical distance of about 30 km that originally separated them from the Diahot-Panié schists. In contrast, tight clustering phengite ages at 36-38 Ma in both terranes suggest synchronous retrogression and cooling, and advocate for their exhumation as a coherent single block. Although it has to be confirmed by additional work, the single fission track on apatite (AFT) age at 34 Ma suggests fast final exhumation at the end of Eocene.

Peridotite Nappe

The Peridotite Nappe (Avias 1967), is a major element in the geology and economy of New Caledonia. Together with other large ophiolitic complexes, such as Oman ophiolite, the New Caledonia Peridotite Nappe hosts one of the largest and best-preserved mantle sections in the world, and offers important insights on upper mantle processes. The ultramafic unit is particularly well preserved because it has not suffered subsequent collision and unlike many other ophiolites worldwide still lies close to its original oceanic basin (Collot et al. 1987; Patriat et al. 2018).

Located structurally above all the accreted terranes of Grande Terre, the peridotite massifs topographically overlie all other formations (Fig. 9 and Fig. 2). Altogether, the ultramafic sheet represents an area of 5500 km^2, out of the 16500 km^2 of Grande Terre. Along the continuation of the Grande Terre axis, the north westernmost (Bélep) and south easternmost (Ile des Pins) islands are the most remote exposures of the Peridotite Nappe. The ultramafic unit has been recognised by positive gravity anomalies (Fig. 1) as far as 300 km northwest of Grande Terre (Collot & Missègue 1986; Collot *et al.* 1988). Geophysical and seismic data show that the Peridotite Nappe is also present farther South of Grande Terre, from the Ile des Pins to as far as the Cook Fracture Zone, 300 km further South (Auzende *et al.* 2000a; Patriat *et al.* 2018, see below). Geophysical modelling based on

seismic data and free air positive gravity anomalies suggests that beyond the East Coast, the Peridotite Nappe is rooted in the Loyalty Basin and merges with its lithospheric mantle (Bitoun & Récy 1982; Collot *et al.* 1987; Patriat et al. 2018).

The Peridotite Nappe overlies a variety of terranes, including basement terranes (cf. chapter 3, this memoir), cover (cf. chapter 4, this memoir), Montagnes Blanches Nappe and, especially, Poya Terrane. The basal contact is commonly a shallow dipping thrust, marked by a sole of foliated and brecciated serpentinite mylonite 10 m to 200 m thick. Post-obduction tectonic events and erosion have disrupted the Peridotite Nappe into several units and klippes of different sizes, and morphologies, showing variable relationships to underlying terranes (Fig. 10a, b):

1) The absence of ultramafic klippes overlying the HP-LT Metamorphic Belt is noteworthy. The only apparent exceptions are the Yambé Massif, an inlier of a few km^2 included in the Pouébo Terrane, with which it shares deformation and metamorphic grade (Fitzherbert *et al.* 2002), and smaller peridotite lenses, which appear locally along the northeast coast.
2) In the low-grade part of the metamorphic belt, in the Pic Ougne Zone, kilometre-scale elongated lenses of peridotite are associated with serpentinite, and basalt of the Poya Terrane. Peridotite form a series of asymmetric synforms, overturned to the southwest (Gautier *et al.* 2016; Maurizot *et al.* 1989). Serpentinites are tightly pinched and deeply rooted in the schists, with which they share the same deformation, pending some differences due to contrasting shear strength. Intricate slivers of serpentinite, basalt, dolerite, and red chert form lenses in local tectonic melange. Both serpentinite and peridotite contain Early Eocene supra-subduction dykes identical to those of Peridotite Nappe (see below “Dykes”).
3) Km-size Central Chain Klippes overlie the basement terranes of that backbone part of Grande Terre. Their serpentinite soles are characteristically complex and pinched in a number of upright tectonic slices within the basement.
4) Larger klippes (5-10 km) are aligned along the southwestern coast. They dominantly overlie the Poya Terrane. However, their northeastern flank locally rests directly over the Central Chain terrane. The serpentinite sole of most of these massifs, e.g. from Thiébagi to Kopéto massifs, is asymmetric: a few tens of metres to the northeast and steeply dipping, whereas it commonly reaches 200 to 300m to the southwest with a shallower dip.
5) The largest and most continuous area of Peridotite Nappe (3800 km^2) lies in the south of Grande Terre. It comprises the Massif du Sud and its coastal extension, Massifs Côte Est.

In general, the Peridotite Nappe lies undeformed above its sole, in contrast with the complexity of underlying terranes and especially the imbricate structure of Poya Terrane. Along the West Coast, the flat-lying ultramafic klippes clearly truncate major tectonic features, notably the boundaries between basement-cover and allochthon units (e.g. Kopéto and Mé Maoya klippes). On the East Coast the basal thrust dips 30° toward the Loyalty Basin (Guillon 1975). Kinematic indicators in the serpentinite sole in the well-exposed human-made outcrops at the base of Koniambo Massif indicate top to the southwest motion (Gautier et al. 2016; Quesnel et al. 2013; Quesnel et al. 2016). The intensity of brecciation decreases upwards as well as spacing of the shear zones. Post-obduction faulting is widespread (cf. chapter 7, this memoir).

The continuity and consistency of structural markers, notably the mantle fabric (see below), suggests that there is no large duplexing or thrusting within the nappe. Morphologically, above the basal sole,

the ultramafic unit constitutes a mountain front with steep slopes, commonly reaching 500 to 1 000 m in height. Assuming that the Peridotite Nappe is a horizontal sheet (see below), the maximum thickness of the mantle section, measured in the Massif du Sud (Tontouta River), between the base (close to sea level) and the highest summit of the Peridotite Nappe (Mont Humboldt, 1 618 m), does not exceed 2 000 m, although originally, before post-obduction dismantling, erosion, and weathering it was possibly much thicker.

Regolith surfaces and associated lateritic weathering profiles, where are located a number of supergene nickel deposits (laterite type, cf. chapters 7 and 10, this memoir) are mostly on top of the nappe. At large scale, the main regolith surface, dated at ca. 25 Ma by palaeomagnetic methods (Sevin et al. 2014), displays a double longitudinal and transversal upwarp, roughly parallel to the basal sole of the Peridotite Nappe (Fig. 10f).

Lithology

The Peridotite Nappe is dominantly formed of upper mantle rocks (Fig. 13, 14, 15), mostly harzburgite, dunite, and rare lherzolite, the latter restricted to the northernmost massifs of the Southwestern Coast Klippes (i.e. Tiébaghi, Poum, Yandé, and Bélep massifs; Moutte 1982; Nicolas 1989; Sécher 1981; Ulrich *et al.* 2010). Harzburgites are composed of olivine (~ 75-85 vol%), orthopyroxene (~ 15-25 vol%) and spinel (< 1 vol%). Spinel-pyroxene symplectitic aggregates are common (Secchiari et al. 2019). Dunite lenses, dykes and/or pods are always present, with higher concentration of chrome-spinel (< 10 vol%). Chromite concentrations are associated with dunite (cf. chapter 10, this memoir). Lherzolites of the northernmost massifs are spinel lherzolite (clinopyroxene 5-10 vol%) and plagioclase lherzolite (clinopyroxene 15 vol%). Clinopyroxene and plagioclase are interstitial or sometimes forms coronas around other orthopyroxene, olivine or spinel (Ulrich et al. 2010).

The only remnants of the crustal sequence are limited to minor mafic and ultramafic cumulate rocks (i.e. dunites, wehrlites, rare pyroxenites and gabbros) overlying the peridotite in the Massif du Sud and Ile Ouen (Fig. 11, Fig. 12). Field relationships for the Massif du Sud have been described in detail by the pioneering works of Prinzhofer et al. (1980) and Nicolas and Prinzhofer (1983), and more recently by Pirard *et al.* (2013). The shallow dip of the peridotite-cumulate interface matches the general attitude of the nappe and its basal sole.

The geometry of the mafic-ultramafic sequence is not well constrained and detailed mapping has still to be improved. The best known and most studied section of Montagne des Sources plateau (Massif du Sud) culminates at c. 1000 m a.s.l. and is implicitly considered as the highest level of the ophiolite (Guillon 1975; Nicolas 1989; Prinzhofer *et al.* 1980), either horizontal or gently dipping to the southwest.

An important horizon of dunite, 300 to 500 m thick, which can be traced for more than 50 km across the Massif du Sud, forms a transition between harzburgites and cumulates. Based on prevailing rock texture, the dunite zone can be subdivided into two distinct members: a lower massive dunite zone, displaying a tectonite texture, and a layered upper dunite zone (Pirard et al., 2013). Layered dunites, alternated with orthopyroxenites, are believed to be formed from cumulus processes (e.g. Pirard et al., 2013) whereas lower dunites likely own a replacive origin, resulting from melt-rock reactions among the residual harzburgite and olivine-saturated melts (Pirard *et al.* 2013).

Up section, the transition to wehrlites, pyroxenites and, finally, gabbros is marked by the progressive appearance of clinopyroxene, orthopyroxene and plagioclase (Fig. 14). Wehrlites have been either interpreted as cumulates (Dupuy *et al.* 1981; Pirard *et al.* 2013; Prinzhofer *et al.* 1980) or due to melt-rock reactions, whereby boninite-like melts dissolved olivine and precipitated pyroxenes ± plagioclase in the pre-existing dunites (Nicolas and Prinzhofer, 1983; Marchesi et al., 2009).

Notably, the upper oceanic crust (i.e. pillow lavas and sheeted dyke complex), presumed to once have been on the top of the mafic-ultramafic complex, is completely missing. The scarce dolerite dykes crosscutting dunite and cumulates, mentioned at the Montagne des Sources plateau, and interpreted as part of a dyke complex by Prinzhofer (1981), are actually Early Eocene island arc tholeiite dykes, genetically unrelated to the ophiolite (Cluzel *et al.* 2006 and see below). The reasons of this absence of crustal section are discussed in the last section of this paper.

Fabric

Peridotites usually display porphyroclastic to mylonitic textures, typical of high-temperature ultramafic tectonites, related to oceanic spreading (Nicolas 1989). The foliation is mainly defined by the preferred orientation of orthopyroxene porphyroclasts, and by a compositional banding defined by diffuse variations of pyroxene vs. olivine ratio. The foliation planes bear a mineral/stretching lineation defined by elongated orthopyroxene grains and streaks of chromite/spinel (Moutte 1979; Podvin 1983; Prinzhofer *et al.* 1980; Sécher 1981). Compositional banding, when present, is parallel to the foliation as a result of tectonic transposition, except in the hinges of rare isoclinal folds. Deformation is microscopically defined by the lattice-preferred orientation (LPO) of olivine indicative of high temperature intra-granular plastic flow.

A number of cogenetic dunite and pyroxenite dykes with sharp or diffuse, straight or contorted boundaries are present in the harzburgite, crosscutting or parallel to the foliation. Composite dykes with dunite walls and pyroxenite core, cross-cutting the compositional banding, are common (Fig. 13a, b). They are more abundant towards the aforementioned transitional dunite horizon, dip steeply and are perpendicular to the stretching lineation. Pyroxenite dykes without dunite walls have a similar attitude although more dispersed. Pyroxenite dykes, both with and without dunite walls, are interpreted to be local partial melting zones (Nicolas 1989) opened along channels perpendicular to the ductile flow.

Most kinematic data on mantle fabrics were acquired in the 1980s by analyses of LPO in olivine and pyroxene using U-stage optical microscopy work on oriented thin section. A few more data have been acquired recently using anisotropy of magnetic susceptibility (AMS) methods. The low-field AMS results from secondary magnetite formed during serpentinization, reflects late deformation and hydration of mantle rocks, and therefore does not inform on high temperature plastic flow in the mantle peridotite. The high-field AMS represents the contribution of all olivine, pyroxene and chromite, except magnetite, with a minor contribution from serpentine, and correlates with the anisotropy of high temperature mineral fabrics. Data acquired by this method are yet too scarce to be conclusive (Belley *et al.* 2007; Titus *et al.* 2011, Ferré et al. 2019). No anisotropy measurements by electron microscopy techniques such as the electron backscatter diffraction technique (EBSD) have yet been published.

At the scale of Grand Terre, compositional banding and foliation are generally gently-dipping with a homogeneous pattern, disturbed by kilometre-scale undulations of probable primary origin. Banding

is locally tilted or shifted by later block faulting. The dip to the NE on the East Coast may be related to normal faulting and tilting toward the Loyalty Basin where the nappe is rooted (Collot *et al.* 1987) and/or to post-obduction uplift (cf. chapter 7, this memoir). The foliation generally trends NW-SE with a dip of 0-30° to the SW. Lineation in the Massif du Sud (Fig. 11) has a remarkably homogeneous N-S trend (Prinzhofer *et al.* 1980) and indicates top-to-the-north shearing. Beneath cumulates, in the dunite-wehrlite and immediately underlying harzburgite, kinematic indicators are irregularly distributed, but top-to-the-south shearing dominates. Inversion occurs at about 1 km below the base of cumulates (Fig. 11c).

Compared with Massif du Sud, the southwestern coast klippes display a less consistent fabric pattern and many variations occur within the same massif or from one massif to another (Fig. 10d). Lineations display a N30 to N45°E trend, the only exception being the Bélep islands. The occurrence of lherzolite in northernmost units reinforces the differences between Southwestern Coast klippes and Massif du Sud.

In the Montagne des Sources section, the strain increases upward in peridotites, as shown by elongated grain shape and mosaic tabular structure. It culminates in the transitional dunite horizon, then decreases in wehrlite, and decreases still further upward into the crust section (Prinzhofer *et al.* 1980). Except in a few places (Ile Ouen, Ilot Casy), cumulate gabbros are devoid of ductile deformation and commonly display sedimentary-like structures, as slumps, cross bedding, and channelling, which together with various cumulate structures, suggest turbulent flow during crystal accumulation (Fig. 14c).

High-temperature shear zones

Three zones in the Peridotite Nappe have been interpreted as regional shear zones or possible transform faults: the Bogota transform fault (Prinzhofer & Nicolas 1980; Titus *et al.* 2008; Titus *et al.* 2011), the Bélep Shear Zone (Nicolas 1989; Sécher 1981; Titus *et al.* 2011), and the Humboldt corridor (Ferré *et al.* 2004; Vogt & Podvin 1983). These zones are characterised by steeply dipping foliation and intense deformation.

On the northeast coast of Bogota peninsula (Fig. 16), a N-S striking zone, 15 km long, and 3 km wide, is characterised by highly deformed harzburgite and dunite, with a strong compositional banding associated with tight isoclinal folds (Prinzhofer & Nicolas 1980). The foliation is vertical, N-S trending, and the mineral lineation is horizontal. Shear bands are formed by orthopyroxene porphyroblasts trails, some of them having a shape ratio up to 33:1, and olivine neoblasts. The shape-preferred orientation of orthopyroxene grains increases near the centre of the shear zone. LPOs of olivine indicate plastic flow with activation of high-temperature slip system. Shear criteria consistently indicate dextral motion. Strain decreases away from the central shear zone and foliation rotates accordingly on each side of it. In the south of the peninsula, a moderately deformed unit characterised by shallow dipping foliation bearing a N-S trending lineation, seems to overlie the former, although the contact, assumed to be horizontal, is not well exposed. Pyroxenite dykes are transposed into the foliation and boudinaged in the mylonitic zone. The whole system has been interpreted as a dextral paleo-transform fault, parallel with the widespread N-S trending ductile flow of Massif du Sud. This parallelism emphasizes the consistency of Massif du Sud as a single undeformed block. The depth, position, and distance relative to a spreading ridge of the Bogota Peninsula fault are unknown, but shear sense indicators infer that the ridge from which it was

generated had an EW direction, orthogonal to the present NS stretching lineation. Fluid-rock interaction within the transform system has been recently investigated (Teyssier *et al.* 2016). Interstitial pargasite with increasing modal abundance in the mylonite zone, and occurrence of serpentinite shear zones parallel to the high-temperature foliation, suggest that pervasive fluid flow may have played a role in strain localization in the transform system at decreasing temperature.

In the northern, partly lherzolitic klippes, shear zones have been suggested to exist in the eastern side of Bélep islands, the middle of Yandé Island, and western sides of Poum and Tiébaghi massifs (Fig. 10c). This 120 km long system has been termed the Bélep Shear Zone (Leblanc 1995; Nicolas 1989; Sécher 1981). In the shear zones, the fabric is finely grained, porphyroclastic to mylonitic, although more diffuse than in the Bogota Peninsula (Leblanc 1987; Sécher 1981; Titus *et al.* 2011). Shear zones, where the deformation is maximum, are locally associated with vertical foliations of NW-SE orientation, whereas lineation is horizontal. The majority of shear sense indicators, deduced from LPO, are dextral. Within the shear zone, the foliation rotates by 90° over a few kilometres and the lineation plunges steeply or is vertical, a feature similar to that of small-scale mantle diapirs (Sécher 1981). The whole set has been interpreted as being part or located close to a transform fault (Nicolas 1989), although the hypothetic segments are not well aligned, either due to subsequent rotations or to original complexity. The association of that structure with lherzolite is noteworthy, the largest strain being measured in the steeply dipping plagioclase and spinel lherzolites. According to Titus (2011) it could be a palaeo-spreading ridge, reactivated in a transcurrent setting, an interpretation consistent with the secondary enrichment of lherzolites (Secchiari *et al.* 2016; Ulrich *et al.* 2010, and see below).

The Humboldt corridor (Fig. 11b) in the Massif du Sud (Podvin *et al.* 1985; Vogt & Podvin 1983), is a 40 x 20 km zone of NW-SE trending steep foliation in harzburgite crosscut by Tontouta River. It displays conspicuous cm-scale compositional layering made of boudinaged orthopyroxene-rich and olivine-rich layers. The foliation bears a subhorizontal orthopyroxene mineral lineation in which some porphyroblasts have a shape ratio up to 10:1 (Ferré *et al.* 2004).

The Bogota occurrence is one of the well-exposed and documented transform faults in ophiolites worldwide. In other countries, a number of occurrences are reported in the mafic section of the ophiolite (for a review, see Nicolas 1989), however examples in the ultramafic section are much rarer as in Oman (Nicolas 1989), or Newfoundland (Karson 1984).

Petrology and geochemistry

Peridotites

The geochemically depleted nature of the ultramafic rocks that constitute the Peridotite Nappe has long hampered an adequate geochemical characterisation. Only recently, thanks to the progress of analytical methods, has the study and the characterisation of the Peridotite Nappe progressed (Marchesi *et al.* 2009; Pirard *et al.* 2013; Secchiari *et al.* 2016; Ulrich *et al.* 2010). In this paragraph the main mineralogical and geochemical features displayed by the rocks of Peridotite Nappe will be briefly summarized.

Lherzolites, which are mainly exposed in the northern massifs (Tiébaghi and Poum) and scarcely in Massif du Sud (Marchesi *et al.* 2009), are the most studied ultramafic rocks in New Caledonia. The majority of lherzolites from northern massifs are low-strain porphyroclastic tectonites in which the development of superimposed structures testifies evolution from high-temperature ductile to brittle

deformation, which may be related to the presence of the Belep shear zone (see paragraph above). Lherzolites likely record an asthenospheric origin followed by re-equilibration at lithospheric conditions, as supported by geothermometric estimates (T = 1100–940 °C and 920–890 °C for porphyroclastic and neoblastic spinel-facies assemblages, respectively (Secchiari *et al.* 2016). Olivine composition (Fo = 88.5–90.0 mol %), spinel Cr# ([molar 100 • Cr/(Cr + Al)] = 13–17) and relatively high amounts (7–8 vol %) of Al_2O_3- and Na_2O-rich clinopyroxene (up to 0.5 and 6.5 wt %, respectively) indicate a moderately depleted geochemical signature for the spinel lherzolites (Secchiari *et al.* 2016; Ulrich *et al.* 2010). Bulk rock and clinopyroxene REE patterns display a typical abyssal-type peridotite signature, i.e. steeply plunging LREE accompanied by nearly flat heavy REE (HREE) to middle REE (MREE) (Fig. 17a, b).

Clinopyroxene REE compositions of the spinel lherzolites may be reproduced by small amounts of fractional melting of a garnet lherzolite precursor (~4 %), followed by 4–5 % melting in the spinel peridotite field. The plagioclase lherzolites show melt impregnation microstructures, Cr- and Ti-rich spinel and incompatible trace element enrichments (REE, Ti, Y, and Zr) in bulk rock and clinopyroxene. Geochemical modelling of these elements suggests that the plagioclase lherzolites originated from residual spinel lherzolites by entrapment of highly depleted (non-aggregated) MORB melt fractions in the shallow oceanic lithosphere. This evolution was most likely accomplished in a spreading ridge. Nd isotope compositions of lherzolites from the Babouillat and Poum massifs age-corrected at 53 Ma ($+7.0 < \varepsilon Nd < +11.0$) are in the range of depleted MORB mantle sources (DMM, see Hofmann 2003). Average T_{DM} model age (53 Ma) suggests derivation from an asthenospheric mantle source that experienced a then-recent MORB-producing depletion. Geochemical trace element modelling and Nd isotopic ratios ($+2.5 < \varepsilon Nd < +6.6$) of the dominant E-MORB from the Poya Terrane (Cluzel *et al.* 2001; Cluzel *et al.* 2016; Secchiari *et al.* 2016) do not support a genetic mantle-crust link between the lherzolites and Poya Terrane basalts previously postulated by other authors (Ulrich *et al.* 2010). However, a genetic relationship with Poya Terrane BABBs ($+6.9 < \varepsilon Nd < +11.5$) cannot be excluded although is not yet precisely established (Cluzel *et al.* 2001; Cluzel *et al.* 2016).

The harzburgites are refractory rocks, by definition containing no primary clinopyroxene. They also have very high Fo content of olivine (90.0-92.9 mol. %), high Mg# of orthopyroxene (89.8-94.2) and high Cr# of spinel (44-71, Secchiari et al. submitted). Chondrite-normalized diagrams exhibit low REE concentrations, coupled with “U-shaped” profiles (see Fig. 17a). These features are commonly seen in fore-arc peridotites that experienced high degrees of fluid-assisted melting (Bizimis *et al.* 2000; Parkinson & Pearce 1998). Melting models indicate that the trace element compositions of the harzburgites are consistent with up to 25 % melting degrees of a depleted mantle source in the spinel stability field (Marchesi et al. 2009; Secchiari et al. submitted). However, some petrographic features (i.e. the frequent occurrence of secondary thin films of ortho- and clinopyroxene) as well as selective enrichment in incompatible, fluid-mobile, elements suggest secondary re-enrichment possibly related to metasomatism in a supra-subduction zone setting (e.g. Marchesi et al. 2009; Secchiari et al. submitted).

The contrasting geochemical features displayed by the New Caledonia harzburgites indicate a complex evolution, including several phases of melting, melt-rock reaction, and re-melting, which

finally led to their ultra-depleted compositions (Marchesi et al. 2009; Ulrich et al. 2010; Secchiari et al submitted).

Ultramafic and mafic cumulates

With a few exceptions (Marchesi *et al.* 2009), the geochemical features of ultramafic cumulates have not been accurately determined due to their extreme depletion in most trace elements. In contrast, mafic cumulates, i.e. websterite, mela- and leuco-gabbronorite, which occur at several places in Massif du Sud, have been studied in more detail (Marchesi et al. 2009; Pirard et al. 2013; Secchiari et al. 2018). In general, mafic rocks display the typical features of cumulates however, some isotropic leucogabbro bodies a few cm thick, although parallel to the layering are compositionally different (see below) and may represent slightly younger sills intruded within cumulates.

Gabbronorites are characterized by very low REE concentrations and similar REE patterns with weakly concave upward LREE segments, more or less flat HREE, and variable positive Eu anomalies (Eu/Eu* = 1.13 - 3.91, see Secchiari et al. 2018), related to plagioclase accumulation. LREE and MREE concentrations of gabbronorites are much lower than those of arc cumulates and were in equilibrium with ultra-depleted melts (Marchesi et al. 2009; Pirard et al. 2013; Secchiari et al. 2018). The most evolved samples, which are from intrusive sills, have no Eu anomaly (Fig. 17b) and may represent liquids rather than cumulates. Anhydrous fractional crystallization modeling suggests that the primary melt that generated the cumulates may have a composition close to that of the sills mentioned above; i.e., ultra-depleted, anhydrous melt similar to tholeiite. (Secchiari et al. 2018). Besides, hydrous fractional crystallization modeling suggests that the residual melt left by the crystallization of gabbronorite cumulates had a boninite composition similar to the clinoenstatite boninite of Népoui (Cluzel et al. 2016). Therefore, the missing fore-arc crust could have been composed of ultra-depleted tholeiites and minor boninites; in any case, these rocks drastically differ from the BABBs and EMORBs of the Poya Terrane.

Age

Age constraints on Peridotite Nappe are scarce. Attempts to extract zircons from gabbronorite cumulates have been unsuccessful due to the very low Zr content of these rocks (0.04-0.6 ppm). K-Ar ages between 120–50 Ma (Prinzhofer 1981) are unreliable and include non-cogenetic basalt dykes. Layered gabbros from Montagne des Sources have been dated at 131 ± 16 Ma by the Sm/Nd rock-mineral isochron method (Prinzhofer 1987). This Early Cretaceous age is at odds with the age inferred from tectonic models of the South Loyalty Basin and needs to be confirmed by other methods.

Dykes

The Peridotite Nappe is intruded by a variety of dykes which vary in composition and texture, from ultramafic (pyroxenite) to mafic (hornblendite, basalt, boninite, dolerite), and felsic (diorite, leucodiorite, granite). They are found in all units, independently of geochemical composition of the ultramafic host rock (harzburgite or lherzolite), or structural level (Pic Ougne zone). They are not found in underlying units, notably Poya Terrane, and thus predate obduction, as confirmed by geochronological data (Cluzel *et al.* 2006). The dykes, 10 cm to 10 m thick, are well preserved in the main body of the ultramafic allochthon and are severely disrupted and boudinaged in the serpentinite sole. Clinoenstatite-bearing boninite boudins are only known in the serpentine sole of the Peridotite Nappe, in the Népoui area (Black *et al.* 1994; Cameron 1989; Cluzel *et al.* 2016;

Ohnenstetter & Brown 1992; Ohnenstetter & Brown 1996; Sameshima *et al.* 1983; Solovova *et al.* 2012).

Some dykes underwent ductile deformation (boudinage, mineral preferred orientation, internal folding or microfolding, Fig. 18), and a foliation parallel to dyke walls is locally developed, thus suggesting high-temperature shearing and magma injection in active faults. Some dykes are ultra-mylonitized and depending on original composition, have transformed into nephrite (jade or semi-jade, cf. chapter 9 this memoir). A few dykes have been rodingitized and contain secondary hydro-grossular, pink zoisite, prehnite, and clinochlore, however, they have not been studied in detail. Thin talc-chlorite and anthophyllite reaction rims against peridotite wall rock or xenoliths are common. Dykes were emplaced within an already existing fracture network in the host rock, as shown by straight boundaries and abrupt direction changes. Widespread coarse-grain textures suggest relatively slow cooling, whereas pegmatitic and sub-solvus textures, ductile deformation, and retrograde mineral associations suggest involvement of large amounts of hydrous fluid. In contrast, dolerite dykes display chilled margins, finer grain size, and lack secondary minerals. Dolerites have crystallized immediately or soon after magma injection and were emplaced at lower temperature (i.e. later than most other dyke types, see age constraints below) and in the absence of excess water.

Age constraints

Nineteen samples of representative dyke compositions have been processed for zircon U-Pb dating (Cluzel *et al.* 2006). No inherited cores have been found in the analysed zircons and all ages are concordant and cluster in a narrow span of time at ca. 53 Ma (Fig. 19). There is no significant age difference between the various dyke types.

Two samples of hornblende-bearing dykes, two samples of clinoenstatite-boninite from Népoui, and two samples of dolerite have been dated by the $^{40}Ar/^{39}Ar$ method. All samples yielded apparent $^{40}Ar/^{39}Ar$ ages that cluster at ca. 50-47 Ma (Cluzel *et al.* 2016, and unpublished data). In addition, hornblende $^{40}Ar/^{39}Ar$ apparent ages of 55 Ma have been obtained on sheared diorite dykes (Soret *et al.* 2016), an age closely similar to U-Pb ages obtained from the same type of dykes. Slightly younger Ar/Ar apparent ages compared to U-Pb ages in coarse-grain rocks possibly indicate slow post-crystallization cooling. Small age differences within error bar suggest that all dykes were formed during one single Early Eocene magmatic event, except dolerites which are slightly younger.

Geochemistry

The geochemical classification of early Eocene dykes based on trace-elements compositions allows four main types to be distinguished (Cluzel *et al.* 2006): i) adakite-series (slab melts), ii) boninite-series (ultra-depleted melts), iii) MORB-like diorites to hornblendites, and, iv) island-arc tholeiites (IAT). However, some variability and the occurrence of intermediate types is possibly a consequence of magma mixing. All dyke types display supra-subduction features; i.e., negative Nb-Ta anomalies and low TiO_2 contents. Some felsic dykes display adakite-series features (e.g., high Sr/Y ratio) and were probably due to hydrous melting of a plagioclase-bearing mafic source in HT amphibolite facies conditions. Some of these dykes display a prominent positive Eu anomaly in spite of high SiO_2 contents and were therefore probably generated by melting of plagioclase-rich cumulate gabbro. Boninite-series dykes display average positive slope patterns, with upward concavity of LREE, and downward concavity of HREE, are Cr-rich and have been generated by HT hydrous melting of mantle wedge peridotite, re-enriched by slab-derived fluids and melts; they have been genetically correlated

to Népoui boninite (Cluzel *et al.* 2016). Hornblende-rich dykes are mafic to ultramafic in composition and commonly display average flat patterns, with downward concavity of LREE, and upward concavity of HREE, due to the predominance of hornblende; at variance with aforementioned dyke types, they display MORB-like REE abundances and have probably been generated by a fertile mantle source (note this does not mean that they were generated at a mid-ocean ridge). The dolerites are the only dyke type that crosscuts gabbronorite cumulates, they typically display LREE-depleted REE patterns and substantial Nb-Ta-Ti depletion. They are typical island-arc tholeiite compositions, and likely represent the first indication of "normal" (albeit transient) volcanic-arc activity.

In summary, the dykes that cut the Peridotite Nappe represent Early Eocene supra-subduction magmatic activity implying that subduction was already initiated at ~55Ma. Slab melts and fluids issued from the lower plate modified the mantle wedge and thus generated the boninite-like fore-arc crust, then "normal" (i.e., IAT-like) supra-subduction magmatism (see below 'Discussion' section, and Cluzel *et al.* 2016).

HT amphibolites (metamorphic sole)

A few amphibolite lenses, distinct from the aforementioned amphibole-rich dykes, are present below the serpentinite sole of the Peridotite Nappe, and above unmetamorphosed Poya Terrane Basalts (Cluzel et al. 2012a). The amphibolites crop out in Pinjen, Népoui, Petchecara Pass, Boulouparis areas, and at the base of Koniambo and Poum massifs (Fig. 10d). They display various tectono-metamorphic textures: foliated and fine-grained, coarse grained with compositional banding, porphyroclastic mylonitic with amphibole clasts surrounded by anastomosed ribbons. At the base of the lenses, the texture is generally cataclastic. Some occurrences show a well-defined stretching lineation marked by amphibole needles. The internal foliation generally dips gently and is conformable with tectonic boundaries. Near Boulouparis, amphibolites are associated with centimetre to decimetre-thick quartz-schist lenses. Low grade metamorphic rocks which are present in other ophiolitic basal soles, are not known in New Caledonia so far.

The protolith of amphibolite is basaltic, similar in composition to the BABBs of the Poya Terrane, and the associated quartz schists probably had abyssal argillite/chert protoliths. Various geothermobarometers provide an estimate of peak recrystallization conditions at c. 0.5 GPa and 800–950 C°. Thermochronological data from hornblende ($^{40}Ar/^{39}Ar$), zircon and sphene (U-Pb) indicate that they recrystallized at c. 56 Ma. U-Pb dating of zircon cores/rims from a granulite-facies crosscutting dyke confidently constrain the age of basaltic protolith at >70 Ma and recrystallization at ca. 56 Ma. These mafic metamorphic rocks are interpreted as slices of Poya Terrane basalts that were overthrust and metamorphosed during subduction inception (Cluzel *et al.* 2012a, and see below).

Serpentinization and fracture development

Secondary minerals that have grown in the Peridotite Nappe include serpentines, amphiboles, and phyllosilicates. These are both dispersed and occur in veins, and grew both statically and under ductile and brittle tectonic conditions. As such they are typical of mineral assemblages driven by externally-derived hydrothermal fluids in serpentinite terranes worldwide (Evans *et al.* 2013; Frost *et al.* 2013; Scott *et al.* 2017).

Minerals of the serpentine group (lizardite, antigorite, chrysotile, and polygonal serpentine, Fig. 20) are by far the most common (Cathelineau *et al.* 2016; Lahondère *et al.* 2012; Quesnel 2015; Ulrich 2010). They replace olivine and orthopyroxene, and caused notable volume expansion.

Serpentinization and deformation are intimately associated. Complex polyphase fracture sets filled by minerals of the serpentine family are ubiquitous in the Peridotite Nappe (Legueré 1976). Unravelling their chronology is a challenge since serpentine may form in a wide range of pressure-temperature conditions. The lack of radiogenic elements prevents radiometric dating, however a relative chronology can be interpreted and a few stages may be defined (Iseppi *et al.* 2017).

Thin mesh networks of lizardite in randomly oriented cracks within olivine, banded veins, and tension gashes are sometimes referred to as primary serpentinization, and have been suggested to form during the oceanic seafloor spreading stage (Evans *et al.* 2013; Fritsch *et al.* 2016; Frost *et al.* 2013; Scott *et al.* 2017). Fracturing and serpentinisation associated with the putative transform faults (e.g. Bogota), that could be coeval with the oceanic spreading, remains unstudied as yet.

Chrysotile commonly appears in en-echelon tension gashes reopening lizardite veins. Antigorite, very often associated with minerals of the actinolite-tremolite series and chlorite, forms fibrous crack seal veins walls with fibrous infills oblique to the vein showing limited displacement, partly dilatational. Intimately mixed antigorite and tremolite fibres are common and advocate one single origin. Tremolite occurrences suggest the infiltration of high pressure, Ca-rich fluids (Ca is an uncommon element in ultra-depleted peridotites). The Sr isotopic composition and high REE content of tremolite veins suggests a common origin with the 53 Ma-old supra-subduction felsic dykes (see above 'Dykes - Age constraints', and Cluzel *et al.* submited; Cluzel *et al.* 2006; Lahondère *et al.* 2012; Lesimple *et al.* 2017), which commonly crosscut the peridotite host-rock. The antigorite-tremolite association post-dates the formation of lizardite and chrysotile.

If the relative timing of mineral phases filling fractures seems to be rather well established, the spatial distribution of the fracture and evolution of the dense fracture network is less well known. Measurements in the field or observations by remote sensing, enable a N 135° dominant vertical-dipping trend to be defined, locally associated with subordinate N. 90°, N.45°, and N. 0° directions (Jeanpert *et al.* 2016; Legueré 1976; Moutte & Paris 1977a; Quesnel *et al.* 2016; Robineau *et al.* 2007). The dyke network and associated fractures in the Peridotite Nappe are characteristic of a dextral transtensional or transpressional regime of brittle deformation, as postulated by several authors (Gonord 1977; Moutte & Paris 1977a; Moutte & Paris 1977b; Robineau & Join 2005), although the detailed study of this important features remains to be undertaken. The youngest faults and fractures associated with supergene weathering products (silica, garnierite, cf. chapter 10, this memoir), display multidirectional extension indicating gravitational movements contemporaneous with regolith evolution.

Offshore extent

To the south of New Caledonia, seismic data of the VESPA and FAUST cruises and a reappraisal of dredged rocks (Auzende et al. 2000b; Daniel et al. 1976; Mortimer et al. 2014a; Patriat et al. 2018; Puillandre & Samadi 2016) have led to offshore mapping of the Peridotite Nappe as far as the Cook Fracture Zone. On seismic sections (Fig. 21) the Peridotite Nappe is a c. 150 km wide unit (compared to the 50 km wide exposed on Grande Terre). Its western edge overlies a wedge-shaped fold and thrust belt with clear south western vergence, thrust over the Norfolk Ridge, which is flexured under the nappe load. The nappe is uplifted in its north eastern part by an antiform or dome-shaped ridge (Félicité Ridge), interpreted as the south eastern extension of the exhumed HT-LP belt observed in New Caledonia although this has not yet been confirmed by dredging or drilling. On top of the

Félicité Ridge, the nappe is thinned and unroofed. The nappe roots eastward in the Loyalty Basin along the eastern side of the Félicité Ridge and is crosscut by normal faults.

Geodynamic model

A summary of the available chronological data for Subduction-Obduction Complex of New Caledonia is presented in Fig. 22. All rocks that can be related to convergence, either supra-subduction igneous rocks, HT or HP-LT metamorphic rocks, and syntectonic sedimentary rocks, have well-constrained radiometric or palaeontologic ages of Late Palaeocene – Eocene age (56 - 34 Ma). The oldest age is Late Palaeocene (56 Ma) for the amphibolite of the basal sole of the Peridotite Nappe which is interpreted as marking subduction initiation in an intra-oceanic context (Cluzel et al. 2012a and see below). The youngest age is Late Eocene (34 Ma) which is the age of the topmost sedimentary rocks of the Bourail Group, involved in thrusting by the allochthonous units, and the youngest cooling age of the exhumed rocks of the HP-LT Metamorphic Complex (see below). The synchronicity of Peridotite Nappe emplacement and HP-LT exhumation suggests a genetic link between the two events (Coleman, 1967; Brothers, 1974). There is also a striking similarity in the length of time between the evolution cycle of the metamorphic rocks of the HP Belt and that of syntectonic sedimentation in the foreland basin, both of which took place within the 56-34 Ma interval (c. 22 My). To the south, near Nouméa, the Peridotite Nappe, and its basal thrust and substrate, are crosscut by the Saint-Louis granodiorite intrusion dated at c. 27 Ma (cf. chapter 7, this memoir), which post-dates the final emplacement of Peridotite Nappe.

The convergence period is thus well-constrained in time, but the overall geometry of the convergent system must be specified as well. In the area of Koumac (NW), the Montagne Blanches Nappe is parautochthonous and forms large south-westward overturned folds, whereas in the Bourail area (SE) it is allochthonous and thrust over the top of syntectonic deposits of the Eocene Bourail Group (Maurizot 2011; Maurizot & Cluzel 2014, and Fig. 2). Furthermore, according to gravity models, the Peridotite Nappe is rooted in the Loyalty Basin (Collot et al. 1987) and consequently was emplaced toward the southwest. Seismic sections in the southeastern offshore extent of the nappe clearly locate this root along the NE edge of the Norfolk Ridge (Patriat et al. 2018). At last, the grade of the HP-LT Metamorphic Belt increases from SW to NE. All this features indicate clearly a southwestern vergence of the system. Additionally, the distinctive blueschist and eclogite facies in the HP-LT Metamorphic Belt, supports the interpretation that these units were dragged down to 70 km in a subduction zone.

On this basis, most proposed models consider that the Subduction-Obduction Complex was formed at a convergent plate boundary, during the Palaeogene, and was associated with a north- or northeast-dipping subduction zone (Agard et al. 2010; Lagabrielle et al. 2013; Gautier et al. 2016; Cluzel et al. 1995a; Cluzel et al. 2012; Agard & Vitale-Brovarone 2013; Aitchison et al. 1995; Clarke et al. 1997; Cluzel et al. 2001; Crawford et al. 2003; Lagabrielle et al. 2013; Meffre et al. 2012; Patriat et al. 2018; Schellart et al. 2006; Sdrolias et al. 2003, 2004 ; Ulrich et al. 2010; Whattam et al. 2008). There is a general consensus for a model of continental subduction (Fig. 23), i.e. the shift from intra-oceanic subduction to attempted continental subduction (i.e. obduction), then subduction blocking or collision, and HP-LT metamorphic rock exhumation.

From southwest to northeast, i.e. from Zealandia continental crust to South Loyalty oceanic basin, the units involved (Fig. 23d) and their interpretation are:

1 - The autochthonous basement terranes of the Norfolk Ridge (cf. chapter 3, this memoir) which is the northeasternmost element of Zealandia.

2 - The Eocene syntectonic sediment accumulation of the Bourail Group which is unconformably deposited on this basement, in front of the convergent system (cf. Chapter 4, this memoir).

3 - The Montagnes Blanches Nappe which represents the sedimentary cover of the thinned continental crust of Zealandia (Norfolk Ridge) and is the unmetamorphosed equivalent of the Diahot Panié Metamorphic Complex.

4 - The Poya Terrane which corresponds to the crust of the oceanic South Loyalty Basin scraped off in front of the convergence zone, comprising:

- The Koné Facies, an ocean to continent transition zone (or passive margin) of the Norfolk Ridge and South Loyalty Basin.
- The Poya Terrane Basalts, genuine oceanic crust of the South Loyalty Basin.

5 - The subducted-then-exhumed HP-LT Metamorphic Belt which comprises the following units:

- The Pouébo Terrane, a mafic ultramafic melange scraped off the oceanic crust of the South Loyalty Basin.
- The Diahot-Panié Metamorphic Complex, the thinned continental margin of the Norfolk Ridge.

6 - The uppermost nappe: the Peridotite Nappe which represents the mantle lithosphere of the oceanic Loyalty Basin.

The present order of superposition, from base to top, of these units onto the basement of Grande Terre, reflects their initial spatial order of organisation from continent to ocean (Fig. 23a), and corresponds to an in-sequence stacking. Unit 1 to 5 correspond to the lower underthrust (Australian) plate, whereas unit 6 is the only one to represent the upper (Pacific) overriding plate. Intra-oceanic subduction initiated in the Loyalty/South Loyalty Basin during the Late Palaeocene as attested by metamorphic and magmatic events (Fig. 23b and see below). The subduction zone then retreated towards the southwest, consuming the oceanic lithosphere of the South Loyalty Basin, until the Late Eocene, when the north-easternmost element of Zealandia margin (Norfolk Ridge), arrived at the trench and progressively blocked subduction by introduction of buoyant continental lithosphere in the convergence zone (Fig. 23c). This was followed by the fast exhumation of the previously-subducted HP-LT metamorphic rocks of unit 5. This pronounced and rapid exhumation drove a piece of the overlying and upper plate supra-subduction Loyalty Basin lithosphere upward; whose lithospheric mantle is now exposed as the obducted Peridotite Nappe of unit 6 (Fig. 23d and see below 'Discussion').

The distribution of the diverse elements of the Peridotite Nappe, their different sizes and morphologies, may be explained by this evolution (see below). The most prominent consequence is the absence of ultramafic units overlying the highest-grade rocks of the HP-LT Metamorphic Belt, and is explained by denudation and unroofing. In this scenario, the subduction phase was a long process (56 to 38 Ma) that started in oceanic context and pre-dated obduction which, in comparison, was a climactic and short event (38 to 34 Ma). This scenario thus accounts for the aforementioned synchronism and genetic link between Peridotite Nappe emplacement and exhumation of HP-LT metamorphic rocks.

Discussion

The nature and interpretation of each unit of the Subduction-Obduction Complex, their role in the general continental subduction model and some pending problems are reviewed below.

Foreland basin

The development of a flexural foreland basin on the southwestern parts of Grande Terre in front of the convergence zone, and in response to overthrust-related loading of the lower plate, is represented by syn-tectonic accumulation of the Eocene Bourail Group (cf. chapter 4, this memoir), which unconformably overlies the basement and its cover (Fig. 23c). The earliest sedimentation change is recorded at c. 55 Ma, marking the demise of the post-rift thermal subsidence deposits and the onset of a syn-tectonic, convergence related, sedimentary regime (cf. chapter 4, this memoir). This change led to the unconformity at the base of the Late Palaeocene Adio Limestone, and to the Early to Middle Eocene calci-turbidite and breccia, which are the first sedimentary records of convergence. The sedimentary succession of the whole Bourail Group is an upward coarsening sequence topped by an olistostrome, in turn thrust by the allochthonous units. The syntectonic accumulation spans the whole Eocene period. The youngest sedimentary rocks and the olistostrome are Late Eocene. The Bourail Group thus constitutes an excellent record of the convergence history. The detrital content of the basin shows an increasing amount of coarse clasts coming from the thrust wedge. The nature and proportion of the clasts recorded the progressive accretion of Montagnes Blanches Nappe followed by Poya Terrane (Maurizot 2014; Maurizot & Cluzel 2014, and chapter 4, this memoir). The clasts coming from the thrust wedge bear no imprint of a terrestrial or sub-aerial evolution and were likely formed in a submarine environment. It is worth noting that ultramafic clasts and minerals (chromite), and HP-LT metamorphic lithoclasts are lacking. Therefore, the Peridotite Nappe and Eocene metamorphic belt were not in a position to feed the basin at that time and the emplacement of the Peridotite Nappe occurred after that of the underlying Montagnes Blanches Nappe and Poya Terrane. Syntectonic deposits of Oligocene age are not known so far in onland New Caledonia.

Montagnes Blanches Nappe

The Montagnes Blanches Nappe is the lowermost allochthonous unit stacked over the autochthonous basement and cover of the Norfolk Ridge. It is entirely constituted of sedimentary rocks. The lower part comprises Late Cretaceous to Palaeocene pelagic to hemipelagic passive margin deep-sea deposits whereas the upper part is composed of Eocene active margin calci-turbidites and breccias which represent the earliest of such syntectonic deposits in the Bourail Group Flysch, recording the beginning of convergence regime. The unit is an unmetamorphosed equivalent of the low-grade part of the Diahot-Panié Metamorphic Complex into which it passes gradually northeastward.

Poya Terrane

The terrane originated from an oceanic or marginal basin, the South Loyalty Basin (Cluzel et al. 2001; Eissen et al. 1998). The geological content of the basin is known only from on land outcrops of Grande Terre, the basin not having been drilled offshore. Basalts are dominantly E-MORB and BABB in composition, with minor alkaline basalts. The basin is interpreted to have opened to the northeast of Zealandia during the Late Cretaceous to Palaeocene, almost synchronously with the opening of the Tasman Sea (84-52 Ma, Gaina *et al.* 1998; Hayes & Ringis 1973). The occurrence of basalts of back-arc affinity (BABB) suggests that they were erupted behind an active island arc, although volcaniclastic

and tuffaceous deposits are lacking. For a review of current models and nature of the Loyalty/South Loyalty Basin, see Matthews et al. (2015), Cluzel et al. (2012a), and chapter 2, this memoir. In most models, at least one spreading ridge is supposed to be present.

The PTB unit is exclusively composed of upper oceanic crust material associated with abyssal sediments without any terrigenous component. Thus, it is interpreted to have been formed away from the continental margin of Zealandia. In contrast, the Koné Facies is dominated by terrigenous turbidites that originally accumulated on the continental rise of the eastern margin of the Norfolk Ridge. Volumetrically significant dolerite sills, which intrude the turbidites, are much younger than their host rocks; in contrast, they are synchronous with subduction inception (see below), and might have a link with that.

PTBs have been scraped off a subducting slab, sliced in an intra-oceanic accretionary wedge, piled up with more coherent units of Koné Facies, and eventually thrust south-westward on to the Montagne Blanche Nappe. The present position of the Koné Facies zone below the PTB is consistent with their former proximal and distal locations with respect to the passive continental margin of the Norfolk Ridge. Frictional forces due to shallow dip of young and buoyant 'oceanic' lithosphere at subduction inception were probably the reason why slices of the uppermost part of the oceanic crust were detached from the lower plate (Cluzel et al. 2001). At variance with some assertions, the Poya Terrane does not contain any mantle peridotite or cumulate (Lagabrielle *et al.* 2013), nor contains or is intruded by boninitic supra-subduction melts (Crawford et al. 2003; Eissen et al. 1998; Lagabrielle et al. 2013).

HP-LT Metamorphic Belt

The Eocene metamorphic belt is composed of two contrasting units in terms of lithology, deformation, and metamorphism. Some aspects of the nature, geometry, and significance of these units are still debated.

The Diahot-Panié Metamorphic Complex encompasses basement and cover terranes. Part of it has been dragged deep into the subduction zone and metamorphosed to eclogite facies. The protolith of the Diahot-Panié Metamorphic Complex is similar to that of the Late Cretaceous cover in the rest of Grande Terre (e.g. Southwestern Coast), but with a larger amount of fine-grained carbonaceous argillite however denoting a deeper water setting (cf. chapter 4, this memoir). The geochemical features of associated volcanic rocks differ as well. They are subduction-related in the Diahot-Panié Metamorphic Complex whereas they are rift-related in the Noumea area.

The Pouébo Terrane is a typical ophiolitic mélange, an usual feature of exhumed oceanic material (Agard et al. 2009). The mafic blocks of the melange are equivalent to the Poya Terrane in terms of lithology, geochemistry, and age. Both Poya and Pouébo terranes are interpreted to have been scraped off the upper crust of the South Loyalty Basin, the former having been pushed in front of the convergence zone, and the latter having been dragged and buried down the subduction interface. The serpentinite of the Pouébo Terrane corresponds to hydrated mantle altered by seawater hydrothermal fluids, then mixed with HP-LT rocks during subduction (Spandler et al. 2008). The serpentinite matrix of the Pouébo Terrane may belong either to the previously exhumed mantle of the lower plate (Agard & Vitale-Brovarone 2013; Spandler *et al.* 2008) or more likely to the mantle wedge of the upper plate (this work) detached by subduction erosion. Exhumation of ophiolitic melange would be facilitated by the low density of serpentinite counterbalancing the negative

buoyancy of eclogitic material and enhancing mechanical decoupling. Exhumation of oceanic material would be impossible at depth greater than 70 km due to the breakdown of serpentinite by dehydration (Agard et al. 2009).

Diahot-Panié Metamorphic Complex and Pouébo Terrane underwent distinct tectono-thermal histories, before being exhumed together. The occurrence of eclogitic rocks recrystallized at about 70 km depth (Clarke *et al.* 1997) on the northeastern coast, now exposed at an horizontal distance of only 20 km from unmetamorphosed equivalent rocks on the southwestern coast, is an apparent paradox that was noted some time ago (Brothers 1974, Coleman 1967) and was explained by major tectonic disruptions. More recently, the concepts of tectonic exhumation and metamorphic core complexes have been proposed by most authors to explain this juxtaposition (Agard & Vitale-Brovarone 2013; Aitchison *et al.* 1995; Baldwin *et al.* 2007; Clarke *et al.* 1997; Cluzel *et al.* 1995a; Cluzel *et al.* 2001; Cluzel *et al.* 1995b). Exhumation accounts for the geometry of the metamorphic belt along the northeastern coast where the Pouébo Terrane forms the core of a regional foliation antiform, wrapped by the Diahot-Panié complex. It also accounts for the final metamorphic retrogression stage of both units. Only the part which has been buried to a depth ≤70 km was returned to the surface by exhumation. A review of HP-LT belts worldwide suggests that 70 km could be a maximum burial depth in similar contexts (Agard & Vitale-Brovarone 2013).

The P-T-t analysis of the HP-LT rocks provides important information on the evolution of the convergence history. Similar ages within error for the peak metamorphism of the Diahot-Panié Metamorphic Complex (38 Ma), and its retrogression (36-38 Ma) suggest that there was a causal link between the beginning of continental subduction (of the light material of the thinned continental margin of Zealandia) and exhumation. Peak metamorphism of the Pouébo Terrane at 44 Ma, was followed rapidly by cooling and decompression at 38 Ma. This represents a rapid exhumation rate of c. 1 cm/yr. Assuming that 34 Ma (based on a single sample) is an age representative of the end of exhumation then, furthermore, the exhumation phase was seemingly short compared with the rest of the convergence history.

Peridotite Nappe

The ultramafic unit, which represents the mantle lithosphere of the Loyalty Basin, has long been considered as a single homogeneous sheet, albeit subsequently dismembered into massifs by erosion (Nicolas, 1989, Paris, 1981). Recent investigations have shown much more diversity in its composition and structure.

Protolith

Protolith of the different ultramafic units have a variety of geochemical compositions, and fabrics. All peridotites are characterized by a complex history with multiple partial melting events, and contrasting geochemical signatures (Secchiari et al. 2016, and references therein). The northernmost undepleted lherzolites are abyssal-type, compatible with an origin in a spreading ridge environment. They host larger chromite deposits than those of harzburgite massifs (cf. chapter 10, this memoir). The rest of the units, including the Massif du Sud and their cumulates, are highly refractory ultra-depleted rocks, with supra-subduction geochemical affinity (Marchesi *et al.* 2009; Pirard *et al.* 2013; Prinzhofer 1981; Secchiari 2016; Secchiari *et al.* 2017a; Secchiari *et al.* 2015, 2016, 2017b; Ulrich *et al.* 2010). The homogeneous fabric of the Massif du Sud, which bears a NS striking lineation, contrasts with that of the south western klippes where lineations are more dispersed. Ductile shear

zones, assumed to be transform faults, in the Peridotite Nappe have different orientations, e.g. the strikes of Bogota and Bélep shear zones, and suggests that they were related to spreading centres oriented E-W and NE-SW respectively.

These differences between units may be explained either by different initial settings, by polyphase evolution, or by later (syn- to post-obduction) disruptions. The occurrence of both coeval abyssal- and supra subduction geochemical composition in the same oceanic basin may be expected in the case of intra-oceanic subduction initiation at mid-ocean ridge (Ulrich et al. 2010, Secchiari et al. 2016, and references therein). The association of coeval transform faults and ridges of different orientations might be interpreted as a result of complex patterns like Ridge Ridge Transform (RRT) or triple spreading ridge (RRR) junctions (McKenzie & Morgan 1969). The absence of age constraints in the Peridotite Nappe protolith prevents a refined interpretation. However, all the above features might be expected in a complex back-arc basin setting (Cluzel et al. 2001) comparable to those in the modern North Fiji and Lau back-arc basins.

The absence of a sheeted dyke complex or pillow basalts above the cumulates is a striking feature of the Peridotite Nappe. The crustal part of the ophiolite is only represented by cumulates in the Massif du Sud, and they are boninitic in composition i.e. supra-subduction related. A MORB-like crust that would represent the remnants of the older (Late Cretaceous – Eocene) Loyalty Basin crust, beneath the boninitic cumulates would be expected. This is not the case and this absence is puzzling. A possibility is that the upper plate was uplifted and its crust early eroded or detached when the young and buoyant lower plate had to force its way at subduction inception (at c. 56 Ma), and before the start of fore-arc magmatism (53 Ma).

Supra-subduction magmatism

The chronology of fore-arc magmatic events that affected the Peridotite Nappe after subduction inception and before obduction provides some information on this crucial period. All dykes, except dolerites which are slightly younger, correspond to one single Early Eocene magmatic event, dated at 53 Ma. The ages are not diachronous. They are younger than subduction inception at 56 Ma. This suggests that at 53 Ma, the lower plate crust was still hot enough to partially melt, consistently with a near-ridge origin. It has been proposed that subsequently, slab melts and fluids issued from the lower plate modified the mantle wedge and thus generated the boninite-like fore-arc crust (cumulates of the Massif du Sud). Slightly later (but still Early Eocene), subduction of older and denser lithosphere allowed slab steepening, uplift of fertile asthenosphere and inception of “normal” (i.e., IAT-like) supra-subduction magmatism (Cluzel et al. 2016).

The ubiquitous supra-subduction geochemical fingerprint present in the Massif du Sud, in the mantle and crust rocks, as well as in the crosscutting dyke network, raises fundamental questions as to their geometrical and temporal relationships. Gautier and al. (2016) have questioned the nature and age of the high temperature flow measured in the mantle section (cf. ‘Peridotite Nappe – Fabric’ section, this chapter), suggesting that, instead of being the result of sea floor spreading, it could be the result of the later fore-arc evolution during subduction. However, supra-subduction dykes at 53 Ma clearly cut across the foliation of the ultramafic rocks, post-dating it. The relationship between the cumulate and the dykes is less clear and is not documented so far. The relationship between the peridotite and the overlying cumulate in the Massif du Sud has been described as transitional (Prinzhofer et al. 1980) whereas their geochemical composition points to a possible discontinuity. A reappraisal of all

these elements in light of the new geochemical characterizations would be appropriate, and age constraints for the cumulate would provide essential information on this issue.

Basal sole

At the base of most massifs, the chaotic porphyroclastic mylonite contains boulders of undeformed serpentinized peridotite and Eocene dykes, and is interpreted as forming mainly during obduction. An overall decrease of degree of serpentinization from the base of Peridotite Nappe upward is observed. Serpentinization is generally interpreted as being generated by hydrous fluids along the subduction plane. This suggests that part of the serpentinite sole thus represents the serpentinized mantle wedge of the Eocene subduction (Iseppi et al. 2017; Mothersole et al. 2017).

Amphibolite, whose parent rock composition is comparable with BABB of Poya Terrane, in the basal sole of the Peridotite Nappe, is interpreted as the best indicator of intra-oceanic subduction initiation. In the amphibolite, the rare occurrence of quartz-schist lenses, derived from argillite/chert protolith, is consistent with an origin in an oceanic domain, far from any terrigenous source.

In the literature, infra-ophiolite metamorphic soles are slices of crustal material scraped off from lower plate, and underplated below the upper plate. They have very comparable characteristics worldwide (for a review, see Robertson et al. 2004, and references therein). The metamorphism is generally interpreted as the result of downward heat transfer from hot oceanic lithosphere thrust over colder lithosphere. They are formed during the first 1 to 2 My of the subduction history. A range of tectonic settings have been proposed for their formation. Most involve thrusting at or near a ridge or a transform fault. In New Caledonia, the scarce occurrences of amphibolite do not allow a unique interpretation. Speculatively, different authors have proposed that subduction have nucleated by inversion at (or near) an active spreading centre of the Loyalty/South Loyalty Basin (Cluzel et al. 2012a; Cluzel et al. 2012b; Ulrich et al. 2010), or a (then-recently) extinct spreading centre (Crawford et al. 2003; Eissen et al. 1998; Whattam 2009). Subsequently, amphibolite would have been detached from the down-going plate and underplated at the base of the Peridotite Nappe, the whole being eventually thrust over the unmetamorphosed Poya Terrane.

Mechanism

New Caledonia bears strong resemblances with other Subduction-Obduction complexes, particularly with Tethyan occurrences. A comparison with Corsica or Oman, which have also not undergone substantial post-obduction deformation, is presented by Agard et al. 2013. Despite distinct geodynamic contexts (New Caledonia is a narrow thinned continental ribbon, Corsica is located in between two large continents, Oman is on the edge of a large continent), there are similarities between the three ophiolitic complexes in terms of tectono-metamorphic organization, size of units, thermal regime, and duration of processes. They all comprise three fundamental units:

- a partly subducted continental margin including cover and basement (equivalent to Montagnes Blanches Nappe);

- a HP-LT belt comprising i) a metasedimentary unit formed in a thinned continental margin (comparable to the Diahot-Panié Metamorphic Complex) and ii) ophiolitic rocks deriving from the lower plate (comparable to the Pouébo Terrane);

- non metamorphic ophiolite klippe (like Poya Terrane and Peridotite Nappe).

In all three areas, the HP-LT belt has a typical antiformal stack structure where the metamorphic grade increases gradually downward. P–T estimates indicate similar conditions with P_{max} of c. 2.4 GPa (c. 70 km), and T_{max} of c. 550 °C, the P-T-t path aligning along a similar paleo-geothermal gradient of 8–10 °C/km. The elapsed time from initial intra-oceanic subduction inception to continental subduction choking is 10 - 20 My. These key parameters seems to be independent of convergence velocities, thicknesses and ages of the subducted oceanic lithosphere, nature of the subducted ocean to continent transition, and nature of the upper plate (partly continental or only oceanic).

In New Caledonia, the intra-oceanic plate motion inversion, oceanic subduction, then attempted continental subduction, are the best-constrained stages of the total continental-subduction model because they are recorded by several kinds of data (amphibolite sole, fore-arc magmatic activity, HP-LT metamorphic P-T-t path, foreland basin sedimentation). These stages are also the longest, covering a period of 18 My, from 56 to c. 38 Ma. In contrast, the final collision-exhumation-obduction stage seemingly was a telescoped short event for which age data are scarce (e.g. one single FTA age, Baldwin et al. 2007), or inaccurate (Late Eocene paleontological age of turbidites). As presently understood, the final collisional stage covers a period of c. 4 My, from 38 to 34 Ma during which allochthonous units became stacked over the Norfolk Ridge basement. There is no sedimentary record of the emplacement of the Peridotite Nappe and HP-LT metamorphic rocks, the two fundamental units of the Subduction-Obduction Complex.

The wider mechanism (cause) of Peridotite Nappe emplacement in New Caledonia involves different tectonic regimes and different timing. Four scenarios or models have been proposed: (1) the dextral oblique convergence model (Cluzel *et al.* 2001; Gautier *et al.* 2016); (2) the passive obduction of Lagabrielle et al. (2013); (3) the force applied to the rear of Gautier et al. (2016); (4) the multi-phase structural evolution model (Rawling & Lister 1999a; Rawling & Lister 1999b; Rawling & Lister 2002, Spandler et al. 2005). Some of these are considered in more detail below.

1) The oblique convergence model arises from the interpretation of southeastward foreland basin propagation (cf. chapter 4, this memoir). It also follows from the dextral transcurrent pattern of fractures and associated supra-subduction dykes that crosscut the Peridotite Nappe (see above, Peridotite Nappe – Serpentinization and fracture network development). Assuming that the foliation of the peridotite was acquired at spreading ridge, this configuration is supported by the NS stretching lineation mantle fabric observed in the Massif du Sud, which implies an EW spreading ridge, that would have been inverted at subduction inception giving rise to north-dipping subduction. The present NW-SE orientation of Grande Terre could subsequently have been acquired by an anticlockwise rotation during convergence (Cluzel et al. 2001) or reflect an original geometry (Gautier et al. 2016).
2) The passive obduction scenarion considers that much of the emplacement of the Peridotite Nappe occurred in an extensional regime dominated by gravity-driven units sliding away from a culminating exhumed metamorphic core. The scenario is based primarily on the fact that the Peridotite Nappe is generally flat lying over a more disrupted substrate, suggesting that its main body has been thrust without major dislocations or duplexing, and did not experienced thickening during its emplacement. Several authors have proposed that the alignment of the west coast klippes could represent the remains of a once-single unit detached from the front of the main body of the Peridotite Nappe (Cluzel *et al.* 1995a; Lagabrielle *et al.* 2013). This setting is reminiscent of the structures visible on seismic lines,

on the southeastern offshore extent of the Peridotite Nappe (syn-exhumation/obduction models of Patriat *et al.* 2018, and Fig. 21). Such a configuration is plausible because of the dispersed orientations of the mantle fabric of the West Coast klippes, compared to the Massif du Sud.

The passive obduction scenario has been developed even further. The absence of basaltic crust above the Peridotite Nappe, but the presence of oceanic crust in the nappe beneath it, has prompted many geologists to seek a relationship between them. This relationship has been variously interpreted as the result of recumbent folding, out of sequence detachment, or fore-arc accretion (Avias 1967; Cameron 1989; Challis & Guillon 1971; Lagabrielle et al. 2013). REE modelling of fractional melting of re-enriched lherzolite may result in E-MORB melt compositions similar to some Poya Terrane Basalts (Ulrich et al. 2010). This model has been taken as evidence that Poya Terrane basalts do petrogenetically belong to the missing upper part of the mantle peridotite, and were once attached to it (Lagabrielle et al. 2013). However, Nd isotope composition of the lherzolites ($+6.98 < \varepsilon Nd < +10.97$) do not fit that of E-MORBs of the Poya Terrane ($+2.5 < \varepsilon Nd < +6.6$). This, together with the absence of supra-subduction dykes and cumulates within Poya Terrane, seems to exclude any genetic link between the two ophiolitic terranes (Secchiari et al. 2016). That said, the absence of sheeted dyke complex and pillow basalts above the cumulates of Massid du Sud remains a major issue.

3) The force applied to the rear scenario emphasises ubiquitous reverse faults observed in the serpentinite sole of the Koniambo and Kopéto massifs, as well as ultramafic klippes of Pic Ougne zone which are deeply pinched, and severely folded within HP-LT schists (Gautier et al. 2016; Quesnel et al. 2016). This scenario states that the Peridotite Nappe and the HP-LT exhumed metamorphic rocks were mostly emplaced through horizontal contraction sustained by plate convergence.
4) In the multi-phase structural evolution model, alternating periods of contractional and extensional tectonics, account for the antiformal and synformal structures present in the HP metamorphic belt. In this model, exhumation results from a short period of interruption of the convergence process.

Seismic profiles of the south eastward offshore extension of the Subduction-Obduction Complex, do not provide additional conclusive information to choose between the four models. Assuming that the Félicité Ridge is indeed the continuation of the HP-LT metamorphic belt, it is difficult to decide from these sections whether the prominent extension observed in the Peridotite Nappe has a syn- or post-obduction origin.

Regional correlations

The existence of a discontinuous SW Pacific ophiolitic belt, emplaced during the Palaeogene, from Papua New Guinea, through New Caledonia, to northern New Zealand (Fig. 24), has been recognised since the 1970s. This is the the “Papuan and New Caledonia ultramafic belt” of Rodgers (1975), the “Periaustralian ophiolitic crown” of Auboin et al. (1977), and the “Disrupted ophiolitic belt” of Parrot & Dugas (1980).

In Papua New Guinea, the Papuan Ultramafic Belt ophiolite (PUB, 400 km x 40 km) comprises 4-8 km of tectonite ultramafics (refractory harzburgite, dunite and pyroxenite), overlain by 4 km of (partly

cumulate) gabbro, in turn overlain by 4 km of basalt and pillow basalt which are resting over a discontinuous and thin sheeted dyke complex (Davies 1971). Pelagic sediments associated with the basalt have yielded Maastrichtian foraminifers; one basalt K-Ar age is c. 56 Ma (Davies 2012). Dipping to the northeast, the ophiolite rests at shallow angle over the Owen Stanley Metamorphic Complex (OSMC) composed of blueschist to greenschist metamorphic rocks. The OSMC protolith is mid-Cretaceous, and the metamorphic ages cluster in the Late Cretaceous to Paleocene, and the Eocene. The OSMC comprises the Emo Metamorphics composed of tholeiitic basalts of N- to E-MORB composition, with foraminifera indicating a Maastrichtian age (Davies 2012; Whattam 2009; Whattam et al. 2008). The base of the ophiolite is underlain by a granulite and amphibolite-facies sole, deriving from high-temperature metamorphism of the Emo Metamorphics, with Ar/Ar cooling ages on hornblende of c. 58 Ma (Lus et al. 2004). To the east of PUB, lies the Cape Vogel island arc which comprises 59–58 Ma boninites and tholeiites (König et al. 2010; Walker & McDougall 1982). The whole PUB is interpreted as a Subduction-Obduction Complex, associated with a northeast-dipping subduction zone.

It is a quite remarkable fact that New Caledonia and PUB Subduction-Obduction complexes, separated by c. 2000 km, have similar (though not identical) ages of events, although the connection between them is obscured by the complex opening of the eastern Coral Sea (Seton et al. 2016) and by a lack of data over the D'Entrecasteaux Zone, whose interpretation is still a matter of debate (cf. chapter 6, this memoir).

Farther south, dredges to the west of Three Kings Ridge, in the Cagou Trough, have recovered ultramafic rocks, HP-LT metamorphic rocks of Late Eocene Ar/Ar age (38 Ma), and Miocene terrestrial sandstones with Gondwana-derived detrital zircons (Meffre et al. 2006). In the same area Early Oligocene boninites have been dredged (Bernardel 2002; Mauffret et al. 2001; Sdrolias et al. 2004).

In the northern part of New Zealand, allochthonous units are known onshore and offshore as the Northland Allochthon (Ballance & Spörli 1979) and the East Cape Allochthon. The Northland Allochthon comprises a series of thrust sheets composed of sedimentary rocks, mostly mélange and broken formations, and a structurally uppermost igneous unit. In the Northland Allochthon, the oceanic crust rocks are referred to as the Tangihua Volcanics or Ophiolite (Malpas et al. 1992; Nicholson 1999; Nicholson et al. 2000; Whattam et al. 2005). Coeval rocks of the East Cape Allochthon are referred to as the Matakaoa Volcanics (Cluzel et al. 2010b). The oceanic crustal part of the ophiolite is well developed, with pillowed and massive basalts. There are only small occurrences of sheeted dykes and layered gabbros, and a few harzburgites and lherzolites, mostly associated with serpentinite slices. Basalts are mainly tholeiitic, with N-MORB, BABB and IAT affinities, which suggest a supra-subduction zone origin (Cluzel et al. 2010b; Malpas et al. 1992; Nicholson 1999; Nicholson et al. 2000; Whattam et al. 2005). The age range, based on fossils in the Tangihua and Matakoa volcanics is Late Cretaceous to Palaeogene. The detailed structural mapping suggests tectonic emplacement from northeast to southwest. Offshore Northland, the allochthon front is clearly visible to the west, on seismic profiles (Isaac et al. 1994). The age of the emplacement is latest Oligocene to earliest Miocene (Ballance & Spörli 1979; Rait 2000) i.e. slightly younger than in New Caledonia. To the northeast of the Northland Peninsula lies the Cavalli Seamount interpreted as an Early Miocene metamorphic core complex (Mortimer et al. 2003).

Conclusions

The Subduction-Obduction Complex of New Caledonia comprises a HP-LT Metamorphic Belt and three stacked allochthonous units. Reconstruction allows to locate each unit in a context of a NE dipping continental subduction during Eocene. From bottom to top, the allochthonous units comprises the Montagnes Blanches Nappe (thinned continental crust of the Norfolk Ridge), the Poya Terrane (scraped-off shallow crust of the South Loyalty Basin) and the Peridotite Nappe (mantle lithosphere of the Loyalty Basin). These allochthonous units were stacked from NE to SW over the autochthonous Norfolk Ridge, the north easternmost continental margin of Zealandia. The HP-LT Eocene Metamorphic Belt, represents the metamorphosed and subducted equivalent of these three units which were exhumed in Late Eocene. Intra-oceanic subduction started in the Loyalty/South Loyalty Basin in the Late Palaeocene, as indicated by amphibolite (56 Ma), boninite- and adakite-series dykes (55-50 Ma), and changes in sedimentation regime (55 Ma). Convergence in the Eocene first consumed the oceanic South Loyalty Basin, and then the Norfolk Ridge. The South Loyalty Basin and its margin were dragged to a maximum depth of 70 km, forming the HO-LT Pouébo Terrane and the Diahot-Panié Metamorphic Complex. Continental subduction attempt led to collision, exhumation, and eventually obduction in the Late Eocene at 38-34 Ma.

At the SW Pacific scale, the New Caledonia Subduction-Obduction Complex and its northward and southwards continuations delineate a major diachronous Palaeogene arc-continent collision belt from 8°S to 38°S. The entire belt from Papua New Guinea to New Zealand is marked out by ophiolites and HP-LT metamorphic units, is thrust over continental Australia (PNG) and Zealandia, and roots eastward towards the oceanic basins from which the ophiolites presumably came. This ocean/continent collision belt is diachronous, being older in Papua-New Guinea and reaching Northern New Zealand in the Miocene.

Acknowledgements

Special thanks are due to A.H.F. Robertson for an extensive and constructive review of this article and very useful comments. The authors acknowledge the accurate review and improvement of the first version of the manuscript by N. Mortimer.

Figure captions

Fig. 1 a) Simplified geological map of New Caledonia showing the main terranes related to the Eocene Subduction-Obduction Complexx. Offshore gravity data after Collot (1989) and Van de Beuque et al. (1998). b) Legend.

Fig. 2 Geological cross sections across Grande Terre showing the relationships of allochthonous units (Peridotite Nappe, Poya Terrane, Montagnes Blanches Nappe), and autochthonous units (basement, cover). Same legend as figure 1. No vertical exaggeration. Long dashes: basal contact of Peridotite Nappe; short dashes: basal contact of Poya Terrane. Section 7: Imaging by heliborne electromagnetic survey and interpretation of a section through the south eastern extremity of the Koniambo klippe showing the main basal thrust of the Peridotite Nappe over its substrate (Iseppi 2019).

Fig. 3 Typical Poya Terrane outcrops and rocks (a,b, and c) : a) Littoral cliff of the Poya Terrane Basalts showing an inliers of b) abyssal manganese-rich sediment (north of Parseval Island). c) Pillow basalts (Pandop Peninsula, Koumac). Typical Koné Facies (d,e, and f): d) Fine-grained turbiditic siltstone (Koumac). e) Inoceramid cast at the surface of a turbidite bed North of Pouembout, (along road cut of RP N2). f) Photomicrograph (plane polarized light) of a spotted schist in the Koné Facies with millimetric aggregates of oxy-chlorite and albite (same locality).

Fig. 4 Geochemical features of Poya Terrane Basalts and dolerites of Koné Facies: a) C1 Chondrite-normalized REE patterns (Evensen et al. 1978). b) Hf/3-Th-Ta ternary diagram (Vermeesch 2006; Wood 1980). c) Nd-Sr isotopic compositions, reference data from Zindler & Hart (1986).

Fig. 5 Comparison of zircon ages from a) Formation à Charbon and b) Koné Facies. N = number of samples, n = number of grain analyzed.

Fig. 6 a) Geological map of the HP-LT Metamorphic Belt (metamorphic grades after Maurizot et al. 1989 and Vitale Brovarone & Agard 2013). b) Idealized crosssection (no horizontal scale) through the South-western Coast – Koumac- Pouébo - North-eastern Coast, showing the relationships of the different subduction-obduction units.

Fig. 7 Typical Eocene Metamorphic Belt outcrops and rocks: a) Diahot-Panié Metamorphic Complex siliceous schist with prominent stretching lineation (Amos Pass). b) Heterogeneous mélange of the Pouébo Terrane (shoreline of Balade).

Fig. 8 a) Simplified geological map of the HP-LT Metamorphic Belt with structural elements (Cluzel et al. 1995b), $^{40}Ar/^{39}Ar$ ages on phengite rounded up to the nearest whole number (red circles), U-Pb ages of zircon rims (yellow circles). b) Enlargement of the former in the Ouégoa area. c) Estimated Pressure-Temperature paths for the metamorphic rocks after different authors, and radiometric ages of the main stages. Abbreviation: AFT: Apatite Fission Track. Vertical labels on x axis indicate approximate temperature of formation for some key mineral phases. d) Histogram of $^{40}Ar/^{39}Ar$ age values. P-T parameters of the basal sole amphibolite are given for comparison with HP-LT conditions. Thick dashed grey line indicates the estimate T-gradient of subduction after Agard & Vitale-Brovarone 2013.

Fig. 9 View from the north of Poya village. Overthrust of the Peridotite Nappe (Mé Maoya klippe) over the Poya Terrane.

Fig. 10 Distribution of the Peridotite Nappe units. a) Geographical names. b) Zonation of units. c) Association of harzburgite and lherzolites in northern klippes. d) Foliations and e) lineations (modified after Nicolas 1989). f) Longitudinal and transversal sections showing the large-scale double up warp of the basal sole and main regolith surfaces of the Peridotite Nappe. Large red stars indicate occurrences of High Temperature (HT) amphibolite of the 'metamorphic sole' after Cluzel et al. 2012. Small red stars indicate other occurrences not studied. Green star indicates clinoenstatite-bearing boninite occurrences.

Fig. 11 a) Foliations and b) lineations in the Massif du Sud. c) Montagne des Sources upper mantle to crust section: left, strain variation versus elevation; right, idealized cross section of the high-temperature foliation Prinzhofer et al. (1980).

Fig. 12 a) Geological map and b) cross section of dunite and cumulates in the south of Massif du Sud.

Fig. 13 Typical Peridotite Nappe outcrops and rocks: a) Flat lying harzburgite – dunite compositional layering crosscut by a d) dunite dyke with a pyroxenitic core (Massif du Sud). c) Lineation on a dunite surface marked by the stretching (black dotted arrow) of chromite grain spindles and orthogonal pulling-apart.

Fig. 14 Typical outcrops and rocks of the cumulate of the Peridotite Nappe: a, b) Bedded olivine gabbros and pyroxenite (Prony area). c) Gabbronorite cumulate with cross-bedding and slump sedimentary-like structures (Plum area, in Secchiari 2016). d) Cumulus texture of plagioclase bearing olivine gabbros. Ol: olivine (serpentinized); Px: pyroxene. Pl: plagioclase. Ol and Px are cumulus crystals, Pl is intercumulus.

Fig. 15 Photomicrograph (cross-polarized light) of typical Peridotite Nappe rocks. a) Lherzolite: Deformed orthopyroxene porphyroclast showing thin exsolution lamellae of clinopyroxene (Babouillat). b) Harzburgite: Strongly exsolved orthopyroxene porphyroclast in harzburgite tectonite (Poya). c) Wehrlite: Poikiloblastic clinopyroxene with orthopyroxene and olivine inclusions (Montagne des Sources). d) Gabbronorite: Exsolved clinopyroxene crystals displaying evidence of chemical instability (Col de Mouirange). Opx: Orthopyroxene. Cpx: Clinopyroxene; Ol: olivine.

Fig. 16 Geological map of Bogota Peninsula with structural elements: a) Foliation; b) Lineation.

Fig. 17 Geochemical features of peridotites and mafic cumulates: a) Compared chondrite-normalized REE patterns of New Caledonia peridotites (data from Secchiari et al. 2016). REE patterns from Tiébaghi harzburgites display some similarity with lherzolites and differ from the rest of Peridotite Nappe. b) Chondrite-normalized REE patterns for gabbronorites (data from Garrido et al. 2009; Marchesi et al. 2009; Secchiari et al. 2016). Normalizing values from Sun and McDonough (1989).

Fig. 18 a) Horizontal dyke at Col de N'go (Massid du Sud) showing complex relationships of the partly ductile gabbroic intrusion against the brittle peridotite wall rock. The dyke is intruded in a top to the west thrust zone. b) Line drawing. c) Detail of a shear zone on polished section. d) Possible interpretation as i) pre-faulted peridotite, ii) intrusion by gabbros developing chilled margins (pegmatoid texture) with large amphiboles growing orthogonally against the wall rock, and getting progressively more strained and rotated toward the shear zone, iii) final domino like structure consistent with the top to west shear context.

Fig. 19 Combined U-Pb zircon age plot of 19 representative dyke samples of the Peridotite Nappe (3 diorites, 5 granitoids, 3 hornblendites, 5 leucodiorites, 2 leucogabbros, 1 gabbro).

Fig. 20 a) Polished section of serpentinized harzburgite (Massif du Sud) showing different habitus of serpentinite (Serp) as diffuse mesh structure or brittle fracture infills. b) Detail of the mantle fabric (foliation S1) marked by the the mylonitic textures, flattened, and stretched porphyroclasts of orthopyroxene (Opx). c, d): Photomicrograph (plane-polarized and cross-polarized light) showing a porphyroclast of ortopyroxene (Opx) and chromite (Cr) within olivine (Ol) mylonite. Olivine is crosscut by a dense static mesh of serpentine (lizardite).

Fig. 21 Line drawing interpretation of seismic profile VESPA 19 modified from Patriat et al. (2018), location on Fig. 24. VE: Vertical Exaggeration.

Fig. 22Time-unit-event diagram summarizing the available age data, with corresponding method, reference, and geodynamic interpretations.

Fig. 23 Sketch reconstruction of the north easternmost margin of Zealandia (Norfolk Ridge) from Late Cretaceous to Late Eocene period. Out of plane transcurrent dextral displacement is indicated by circular symbols with cross (away from the viewer) and point (toward the viewer). Locations of cross sections vary in latitude through time.

Fig. 24 Major tectonic features of the Southwest Pacific.

References

Adams, C.J., Campbell, H.J., Mortimer, N. & Griffin, W.L. 2013a. Detrital zircon geochronology and sandstone provenance of basement Waipapa Terrane (Triassic-Cretaceous) and Cretaceous cover rocks (Northland Allochthon and Houhora Complex) in northern North Island, New Zealand. *Geological Magazine*, **150**, 455-478, doi: 10.1017/S0016756812000611.

Adams, C.J., Campbell, H.J., Mortimer, N. & Griffin, W.L. 2013b. The mid-Cretaceous transition from basement to cover within sedimentary rocks in eastern New Zealand: evidence from detrital zircon age patterns. *Geological Magazine*, **150**, 89-109, doi: 10.1017/S0016756812000258.

Adams, C.J., Campbell, H.J., Mortimer, N. & Griffin, W.L. 2016. Perspectives on Cretaceous Gondwana break-up from detrital zircon provenance of southern Zealandia sandstones. *Geological Magazine*, **154**, 661-682, doi: 10.1017/S0016756816000285.

Adams, C.J., Cluzel, D. & Griffin, W.L. 2009. Detrital-zircon ages and geochemistry of sedimentary rocks in basement Mesozoic terranes and their cover rocks in New Caledonia, and provenances at the Eastern Gondwanaland margin. *Australian Journal of Earth Sciences*, **56**, 1023-1047, doi: 10.1080/08120090903246162.

Agard, P., Searle, Alsop, G.I. & Dubacq, B. 2010. Crustal stacking and expulsion tectonics during continental subduction: P-T deformation constraints from Oman. *Tectonics*, **29**, 1-19, doi: 10.1029/2010TC002669.

Agard, P. & Vitale-Brovarone, A. 2013. Thermal regime of continental subduction: The record from exhumed HP–LT terranes (New Caledonia, Oman, Corsica). *Tectonophysics*, **601**, 206-215, doi: 10.1016/j.tecto.2013.05.011.

Agard, P., Yamato, P., Jolivet, L. & Burov, B. 2009. Exhumation of oceanic blueschists and eclogites in subduction zones: Timing and mechanisms. *Earth-Science Reviews*, **92**, 53–79, doi: 10.1016/j.earscirev.2008.11.002.

Aitchison, J., Clarke, G., Meffre, S. & Cluzel, D. 1995. Eocene arc-continent collision in New Caledonia and implications for regional southwest Pacific tectonic evolution. *Geology*, **23**, 161-164.

Amstutz, A. 1951. Sur l'évolution des structures alpines. *Archives Sciences*, **4** (5), 323-329.

Arnould, A. 1958. Etude géologique de la partie Nord-Est de la Nouvelle-Calédonie. Thèse Doctorat Etat, 436 p., 28 pl..*Université de Paris*.

Arnould, A. & Routhier, P. 1957. Carte Géologique et notice explicative de la Nouvelle-Calédonie à l'échelle du 1:100 000: Feuille Hienghène-Voh, Paris.

Auboin, J., Mattauer, M. & Allègre, C. 1977. La couronne ophiolitique péri-australienne: un charriage océanique représentatif des stads précoces de l'évolution alpine. *Compte Rendus de l'Académie des Sciences*, **285**.

Auzende, J.-M., Van de Beuque, S., Régnier, M., Lafoy, Y. & Symonds, P. 2000a. Origin of the New Caledonian ophiolites based on a French–Australian seismic transect. *Marine Geology*, **162**, 225-236.

Auzende, J.M., Van de Beuque, S., Régnier, M., Lafoy, Y. & Symonds, P. 2000b. Origin of the New Caledonian ophiolites based on a French–Australian Seismic Transect. *Marine Geology*, **162**, 225-236, doi: 10.1016/S0025-3227(99)00082-1.

Avias, J. 1967. Overthrust structure of the main ultrabasic new caledonian massives. *Tectonophysics*, **4**, 531-541, doi: 10.1016/0040-1951(67)90017-0.

Baldwin, S.L., Rawling, T. & Fitzgerald, P.G. 2007. Thermochronology of the New Caledonian high-pressure terrane: Implications for middle Tertiary plate boundary processes in the southwest Pacific. *Geological Society of America Special Papers*, **419**, 117-134.

Ballance, P.F. & Spörli, K.B. 1979. Northland Allochton. *Journal of the Royal Society of the New Zealand*, **9**, 259-275.

Bell, T. & Brothers, R. 1985. Development of P-T prograde and P- retrograde, T- prograde isogradic surfaces during blueschist to eclogite regional deformation/metamorphism in New Caledonia, as indicated by progressively developed porphyroblast microstructures. *Journal of Metamorphic Geology*, **3**, 59-78.

Belley, F., Ferré, E.C., Martín-Hernández, F., Tikoff, B., Maurizot, P., Garrido, C.J. & Vauchez, A. 2007. Strain localization in the oceanic lithospheric mantle : the Humboldt shear zone of the New Caledonia ophiolite. *Geophysical Resaerch Abstracts, European Geosciences Union*, **9**.

Bernardel, G. 2002. Geological and morphological framework of the Norfolk Ridge and Three Kings Ridge region. Geoscience Australia.

Bitoun, G. & Récy, J. 1982. Origine et évolution du bassin des Loyauté et de ses bordures après la mise en place de la série ophiolitique de Nouvelle-Calédonie. *In: Contribution à l'étude géodynamique du Sud-Ouest Pacifique. Travaux et Documents de l'ORSTOM*, **147**, 505-539.

Bizimis, M., Salters, V.J.M. & Bonatti, E. 2000. Trace and REE content of clinopyroxenes from supra-subduction zone peridotites. Implications for melting and enrichment processes in island arcs. *Chemical Geology*, **165**, 67-85.

Black, P. 1970a. Coexisting glaucophane and riebeckite-arfredsonite from New Caledonia. Mineralogical Soc. Amer. 1015 18th ST, NW Suite 601, Washington, DC 20036, 1061-&.

Black, P. 1970b. Ferroglaucophane from New-Caledonia. Mineralogical Society of America, 1015 Eighteen street, NW Suite 601, Washington, DC 20036, 508-&.

Black, P. 1970c. P2 omphacite, intermediate in composition between jadeite and hedenbergite, from metamorphosed acid volcanics, Bouehndep, New Caledonia. **55**, 512.

Black, P., Maurizot, P., Ghent, E. & Stout, M. 1993. Mg–Fe carpholites from aluminous schists in the Diahot region and implications for preservation of high-pressure/low- temperature schists, northern New Caledonia. *Journal of Metamorphic Geology*, **11**, 455-460.

Black, P.M. 1973. Geology of New Caledonian metamorphic rocks:II Amphiboles from the Ouegoa district. *Contribution to Mineralogy and Petrology*, **39**, 55-64, doi: 10.1007/BF00374767.

Black, P.M. 1974. Oxygen isotope study of metamorphic rocks from the Ouégoa district, New Caledonia. *Contribution to Mineralogy and Petrology*, **47**, 197-206.

Black, P.M. 1975. Mineralogy of New Caledonia metamorphic rocks. IV. Sheet silicates from Ouégoa district. *Contributions to Mineralogy and Petrology*, **49**, 269-284.

Black, P.M. 1977. Regional high-pressure metamorphism in New Caledonia: phase equilibria in the Ouégoa district. *Tectonophysics*, **43**, 83-107.

Black, P.M. & Brothers, R.N. 1977. Blueschist ophiolites in the melange zone, northern New Caledonia. *Contributions to Mineralogy and Petrology*, **65**, 69-78.

Black, P.M., Brothers, R.N. & Yokoyama, K. 1988. Mineral parageneses in eclogite-facies meta-acidites in northern New Caledonia. *In: Smith D. C., editor. Eclogites and Eclogite-Facies Rocks. Amsterdam: Elsevier*, 271-289.

Black, P.M., Itaya, T., Ohira, T., Smith, I.E. & Takagi, M. 1994. Mid-Tertiary magmatic events in New Caledonia: K-Ar dating of boninitic volcanism and granitoid intrusives. *Geoscience reports of Shizuoka University*, **20**, 49-53.

Blake, M.C., Brothers, R.N. & Lanphère, M.A. 1977. Radiometric ages of blueschists in New Caledonia. *International Symposium on Geodynamic in South-West Pacific, Nouméa, 1976, Technip Ed.*, 279-282.

Bradshaw, J.D. 2004. Northland Allochthon: An alternative hypothesis of origin. *Journal of Geology and Geophysics*, **47**, 375-382.

Brière, Y. 1919. Les eclogites françaises: Leur composition minéralogique et chimique; leur origine. *Bulletin de la Société Française de Minéralogie*, **41**, 72-222.

Briggs, R.M. 1975. Structure, metamorphism and mineral deposits in the Diahot region, northern New Caledonia. *PhD Thesis, Univesity of Auckland, New Zealand*, 486.

Briggs, R.M. 1977. High-pressure metamorphism of stratiform sulphide deposits from the Diahot region New Caledonia. *Mineralium Deposita*, **12**, 263-279.

Briggs, R.M. 1978. Ferrocarpholite associated with low-grade blueschists, northern New Caledonia. *Mineralogical Magazine*, **42**, 147-148.

Briggs, R.M., Lillie, A.R. & Brothers, R.N. 1978. Structure and high-pressure metamorphism in the Diahot region northern New Caledonia. *Bulletin du BRGM, Section IV*, **3**, 171-189.

Brothers, R.N. 1970. Lawsonie-albite schists from northernmost New Caledonia. *Contribution to Mineralogy and Petrology*, **25**, 185-202.

Brothers, R.N. 1974. High-pressure schists in Northern New Caledonia. *Contributions to Mineralogy and Petrology*, **46**, 109-127, doi: 10.1007/BF00377499.

Brothers, R.N. 1985. Regionnal mid-Tertiary blueschist-eclogite facies in northern New Caledonia. *Géologie de la France*, **1**, 37-44.

Brothers, R.N. & Black, N.C. 1973. Tertiary plate tectonics and high-pressure metamorphism in New Caledonia. *Tectonophysics*, **17**, 337-358.

Brothers, R.N. & Delaloye, M. 1982. Obducted ophiolites of North Island, New Zealand: Origin, age, emplacement and tectonic implications for Tertiary and Quaternary volcanicity. *New Zealand Journal of Geology and Geophysics*, **25**, 257-274, doi: 10.1080/00288306.1982.10421491.

Bryan, S.E., Cook, A.G., Allen, C.M., Siegel, C., Purdy, D.J., Greentree, J.S. & Uysal, I.T. 2012. Early-mid Cretaceous tectonic evolution of eastern Gondwana: From silicic LIP magmatism to continental rupture. *In: Geology in the Oceania Region, Special issue for the 34 IGC, Brisbane, Australia. Episodes*, **35**, 72-86.

Bryan, S.E., Ewart, A., Stephens, C.J., Parianos, J. & Downes, P.J. 2000. The Whitsunday Volcanic Province, Central Queensland, Australia: lithological and stratigraphic investigations of a silicic-dominated large igneous province. *Journal of Volcanology and Geothermal Research*, **99**, 55-78.

Cabioch, G., Montaggioni, L., Thouveny, N., Frank, N., Sato, T., Chazottes, V., Dalamasso, H., Payri, C., Pichon, M. & Sémah, A.-M. 2008. The chronology and structure of the western New Caledonian barrier reef tracts. *Palaeogeography, Palaeoclimatology, Palaeoecology*, **268**, 91-105, doi: 10.1016/j.palaeo.2008.07.014.

Cameron, W.E. 1989. Contrasting boninite - tholeiite associations from New Caledonia. *In: Boninites, edited by A.J. Crawford. Unwin Hyman, Boston, Mass*, 314-336.

Carroué, J.P. 1971. Carte Géologique à l'échelle du 1 / 50 000 et notice explicative: feuille Hienghène. *Territoire de la Nouvelle-Calédonie - Bureau de Recherches Géologiques et Minières*, 1-14.

Carroué, J.P. 1972a. Carte Géologique à l'échelle du 1 / 50 000 et notice explicative: feuille Pouembout. *Territoire de la Nouvelle-Calédonie - Bureau de Recherches Géologiques et Minières*, 1-38.

Carroué, J.P. 1972b. Carte Géologique à l'échelle du 1 / 50 000 et notice explicative: Feuille Voh-Ouaco. *Territoire de la Nouvelle-Calédonie-Bureau de Recherches Géologiques et Minières*, 1-16.

Carson, C., Clarke, G. & Powell, R. 2000. Hydration of eclogite, Pam Peninsula, New Caledonia. *Journal of Metamorphic Geology*, **18**, 79-90.

Carson, C., Powell, R. & Clarke, G. 1999. Calculated mineral equilibria for eclogites in CaO–Na 2 O–FeO–MgO–Al 2 O 3–SiO 2–H 2 O: application to the Pouébo Terrane, Pam Peninsula, New Caledonia. *Journal of Metamorphic Geology*, **17**, 9-24.

Cathelineau, M., Quesnel, B., Gautier, P., Boulvais, P., Couteau, C. & Drouillet, M. 2016. Nickel dispersion and enrichment at the bottom of the regolith: formation of pimelite target-like ores in rock block joints (Koniambo Ni deposit, New Caledonia). *Mineralium Deposita*, **51**, 271-282, doi: 10.1007/s00126-015-0607-y.

Challis, G.A. & Guillon, J.H. 1971. Etude comparative à la microsone électronique du clinopyroxène des basaltes et des péridotites de Nouvelle-Calédonie. *Bulletin BRGM*, **Deuxième série**, 39-46.

Clarke, G.L., Aitchison, J.C. & Cluzel, D. 1997. Eclogites and blueschists of the Pam Peninsula, NE New Caledonia: a reappraisal. *Journal of Petrology*, **38**, 843-876.

Clarke, G.L., Powell, R. & Fitzherbert, J.A. 2006. The lawsonite paradox: a comparison of field evidence and mineral equilibria modelling. *Journal of Metamorphic Geology*, **24**, 715-725, doi: 10.1111/j.1525-1314.2006.00664.x.

Cluzel, D., Adams, C.J., Maurizot, P. & Meffre, S. 2011. Detrital zircon records of Late Cretaceous syn-rift sedimentary sequences of New Caledonia: An Australian provenance questioned. *Tectonophysics*, **501**, 17-27, doi: 10.1016/j.tecto.2011.01.007.

Cluzel, D., Adams, C.J., Meffre, S., Campbell, H.J. & Maurizot, P. 2010a. Discovery of Early Cretaceous Rocks in New Caledonia: New Geochemical and U-Pb Zircon Age Constraints on the Transition from Subduction to Marginal Breakup in the Southwest Pacific. *Journal of Geology*, **118**, 381-397, doi: 10.1086/652779.

Cluzel, D., Aitchison, J., Clarke, G., Meffre, S. & Picard, C. 1994. Point de vue sur l'évolution tectonique et géodynamique de la Nouvelle-Calédonie (Pacifique, France). *Comptes rendus de l'Académie des sciences. Série 2. Sciences de la terre et des planètes*, **319**, 683-690.

Cluzel, D., Aitchison, J., Clarke, G., Meffre, S. & Picard, C. 1995a. Dénudation tectonique du complexe à noyau métamorphique de haute préssion d'âge tertiaire (Nord de la Nouvelle-Calédonie, Pacifique, France). Données cinématiques. *Comptes rendus de l'Académie des sciences. Série 2. Sciences de la terre et des planètes*, **321**, 57-64.

Cluzel, D., Aitchison, J.C. & Picard, C. 2001. Tectonic accretion and underplating of mafic terranes in the Late Eocene intraoceanic fore-arc of New Caledonia (Southwest Pacific): geodynamic implications. *Tectonophysics*, **340**, 23-59, doi: 10.1016/S0040-1951(01)00148-2.

Cluzel, D., Black, P.M., Picard, C. & Nicholson, K.N. 2010b. Geochemistry and tectonic setting of Matakaoa Volcanics, East Coast Allochthon, New Zealand: Suprasubduction zone affinity, regional correlations, and origin. *Tectonics*, **29**, n/a-n/a, doi: 10.1029/2009TC002454.

Cluzel, D., Clarke, G. & Aitchison, J. 1995b. Northern New Caledonia high pressure metamorphic core complex from contintenal subduction to extensional exhumation. *Pacrim Congress 1995, Exploring the Rim, Australian Institute of Mining and Metallurgy Publication Series*, 129-134.

Cluzel, D., Boulvais, P., Tarantola, A., Paquette, J.L., Iseppi, M., Ulrich, M., Lesimple, S., Lahondère, D. & Maurizot, P., submited. Metasomatic, slab-derived origin of tremolite-bearing veins in supra-subduction ophiolites; an appraisal from Peridotite Nappe, New Caledonia. *Lithos*.

Cluzel, D., Jourdan, F., Meffre, S., Maurizot, P. & Lesimple, S. 2012a. The metamorphic sole of New Caledonia ophiolite: 40 Ar/ 39 Ar, U-Pb, and geochemical evidence for subduction inception at a spreading ridge. *Tectonics*, **31**, 1-18, doi: 10.1029/2011TC003085.

Cluzel, D., Maurizot, P., Collot, J. & Sevin, B. 2012b. An outline of the Geology of New Caledonia ; from Permian – Mesozoic Southeast Gondwanaland active margin to Cenozoic obduction and supergene. *Episodes*, 72-86.

Cluzel, D., Meffre, S., Maurizot, P. & Crawford, A.J. 2006. Earliest Eocene (53 Ma) convergence in the Southwest Pacific: evidence from pre-obduction dikes in the ophiolite of New Caledonia. *Terra Nova*, **18**, 395-402, doi: 10.1111/j.1365-3121.2006.00704.x.

Cluzel, D., Picard, C., Aitchison, J.C., Laporte, C., Meffre, S. & Parat, F. 1997. La nappe de Poya (ex. formation des Basaltes) de Nouvelle Calédonie (Pacifique Sud-Ouest): un plateau océanique campanien-paléocène supérieur obducté à l'Eocène supérieur. *CR Acad. Sci., Paris*, **324**, 443-451.

Cluzel, D., Ulrich, B., Jourdan, F., Meffre, S., Paquette, J.L., Audet, M.A., Secchiari, S. & Maurizot, P. 2016. Early Eocene clinoenstatite boninite and boninite-series dikes of the ophiolite of New Caledonia; a witness of slab-derived enrichment of the mantle wedge in a nascent volcanic arc. *Lithos*, **260**, 429–442, doi: 10.1016/j.lithos.2016.04.031.

Cluzel, D., Whitten, M., Meffre, S., Aitchison, J.C. & Maurizot, P. 2017. A reappraisal of the Poya Terrane (New Caledonia): Accreted Late Cretaceous-Paleocene marginal basin upper crust, passive margin sediments and Early Eocene E-MORB sill complex. *Tectonics*, doi: 10.1002/2017TC004579.

Coleman, R.G. 1967. Glaucophane schists from California and New Caledonia *Tectonophysics*, **4**, 479-498.

Coleman, R.G. 1971. Plate tectonic Emplacement of Upper Mantle Peridotites along Continental Edges. Journal of Geophysical Research, 76, 1212-1222.

Collot, J.-Y. 1989. *Obduction et collision: exemples de la Nouvelle-Calédonie et de la zone de subduction des Nouvelles-Hébrides.* PhD, University of Paris Sud - Centre d'Orsay.

Collot, J.-Y. & Missègue, F. 1986. Extension de la formation des basaltes de la côte ouest et de la zone d'enracinement des péridotites dans le Grand Lagon Nord de la Nouvelle-Calédonie: données géophysiques. *Comptes Rendus de l'Académie des Sciences. Série 2: Mécanique...* **303**, 1437-1442.

Collot, J., Rigolot, P. & Missegue, F. 1988. Geologic structure of the northern New Caledonia Ridge, as inferred from magnetic and gravity anomalies. *Tectonics*, **7**, 991-1013.

Collot, J.Y., Malahoff, A., Recy, J., Latham, G. & Missegue, F. 1987. Overthrust emplacement of New Caledonia Ophiolite: Geophysical evidence. *Tectonics*, **6**, 215-232, doi: 10.1029/TC006i003p00215.

Cooper, R.A. 2004. The New Zealand Geological Timescale. *Institute of Geological & Nuclear Sciences Monograph*, **22**, 284.

Coudray, J. & Gonord, H. 1966. Découverte d'une microfaune paléocène dans les formations volcano-sédimentaires de la Nouvelle-Calédonie. *Compte-Rendu de l'Académie des Sciences*, **716**, 716.

Crawford, A.J., Meffre, S. & Symonds, P.A. 2003. 120 to 0 Ma tectonic evolution of the southwest Pacific and analogous geological evolution of the 600 to 220 Ma Tasman Fold Belt System. *Geological Society of Australia Special Publication*, **22**, 377-397.

Daniel, J., Dugas, F., Dupont, J., Jouannic, C., Launay, J., Monzier, M. & Récy, J. 1976. La zone charnière Nouvelle-Calédonie/Ride de Norfolk (SW Pacifique), résultats de dragages et interprétation. *Cah. ORSTOM, ser. Geol. VIII*, 95-105.

Davies, H. 2012. The geology of New Guinea - the cordilleran margin of the Australian continent. *Episodes*, **35**, 87-102.

Davies, H.L. 1971. Peridotite-gabbro-basalt complex in eastern Papua: an overthrust plate of oceanic mantle and crust. *Bureau of Mineral Resources, Geology and geophysics Australia*, 128.

Diessel, C.F.K., Brothers, R.N. & Black, P.M. 1978. Coalification and graphitization in high-pressure schists in New Caledonia. *Contributions to Mineralogy and Petrology*, 63-78.

Dupuy, C., Dostal, J. & Leblanc, M. 1981. Geochemistry of an Ophiolitic Complex from New Caledonia. *Contribution to Mineralogy and Petrology*, **76**, 77-83.

Eissen, J.-P., Crawford, A.J., Cotten, J., Meffre, S., Bellon, H. & Delaune, M. 1998. Geochemistry and tectonic significance of basalts in the Poya Terrane, New Caledonia. *Tectonophysics*, **284**, 203-219.

Espirat, J.J. 1963. Etude géologique de régions de la Nouvelle-Calédonie septentrionale. *Thèse Faculté des Sciences de Clermont-Ferrand*, 1-210.

Espirat, J.J. & Milon, R. 1965. Carte géologique à l'échelle du 1 / 50 000 et notice explicative: feuille Pam-Ouégoa. *Territoire de la Nouvelle-Calédonie - Bureau de Recherches Géologiques et Minières*, 1-45.

Evans, K.A., Powell, R. & Frost, B.R. 2013. Using equilibrium thermodynamics in the study of metasomatic alteration, illustrated by an application to serpentinites. *Lithos*, **168-169**, 67-84, doi: 10.1016/j.lithos.2013.01.016.

Evensen, N.M., Hamilton, P.J. & O'Nions, R.K. 1978. Rare earth abundance in chondritic meteorites. *Geochimical and Cosmochimical Acta*, **42**, 1199-1212, doi: 10.1016/0016-7037(78)90114-X.

Ferré, E.C., Belley, F., Tikoff, B., Martín-Hernández, F., Nzokwe, G. & Ward, C. 2004. Anatomy of an oceanic mantle shear zone deduced from high-field magnetic anisotropy: the Humboldt corridor, New Caledonia. *Eos Trans. AGU, 85(47), Fall Meeting Supplement, Abstract GP23B-04*.

Ferré, E., Biedermann, A.R., Teyssier, C., Chatzaras, V. Kaczmarek, M.A. 2019. Strain, melt extraction, and serpentinization gradients in the Humboldt peridotite shear zone, Massif du Sud, New Caledonia. Workshop on New Caledonia Peridotite Amphibious Drilling Project, Posters and abstracts. January 22-24 2019 – Montpellier France.

Fitzherbert, J.A. 2002. *Eocene high-Pressure metamorphism in NE New Caledonia.* PhD Thesis, The Univrsity of Sydney.

Fitzherbert, J.A., Clarke, G.L. & Powell, R. 2002. P-T evolution of the Yambé peridotite, northern New Caledonia: high-P ultramylonite development during the emplacement of a 'subduction zone' peridotite. *In: PhD Thesis (paper III), The University of Sydney*, doi: 10.1111/j.1525-1314.2006.00673.x.

Fitzherbert, J.A., Clarke, G.L. & Powell, R. 2003. Lawsonite-Omphacite-bearing metabasites of the Pam Peninsula, NE New Caledonia: Evidence for disrupted blueschist- to eclogite-facies conditions. *Journal of Petrology*, **44**, 1805-1831, doi: 10.1093/petrology/egg060.

Fitzherbert, J.A., Clarke, G.L. & Powell, R. 2005. Preferential retrogression of high-P metasediments and the preservation of blueschist to eclogite facies metabasite during exhumation, Diahot terrane, NE New Caledonia. *Lithos*, **83**, 67-96, doi: 10.1016/j.lithos.2005.01.005.

Fitzherbert, P.G., Clarke, G.L., Marmo, B. & Powell, R. 2004. The origin and P-Tevolution of peridotites and serpentinites of NE New Caledonia: prograde interaction between continental margin and the mantle wedge. *Journal of Metamorphic Geology*, **22**, 327-344, doi: 10.1111!j.1525-1314.2004.00517.x.

Fritsch, E., Juillot, F., Dublet, G., Fonteneau, L., Fandeur, D., Martin, E., Caner, L., Auzende, A.L., Grauby, O. & Beaufort, D. 2016. An alternative model for the formation of hydrous Mg/Ni layer silicates ('deweylite'/'garnierite') in faulted peridotites of New Caledonia: I. Texture and mineralogy of a paragenetic succession of silicate infillings. *European Journal of Mineralogy*, **28**, 295-311.

Frost, B.R., Evans, K.A., Swapp, S.M., Beard, J.S. & Mothersole, F.E. 2013. The process of serpentinization in dunite from New Caledonia. *Lithos*, **178**, 24-39, doi: 10.1016/j.lithos.2013.02.002.

Gaina, C., Müller, D.R., Royer, J.Y., Stock, J., Hardebeck, J. & Symonds, P. 1998. The tectonic history of the Tasman Sea: a puzzle with 13 pieces. *Journal of Geophysical Research: Solid Earth (1978–2012)*, **103**, 12413-12433.

Garnier, J. 1867a. Essai sur la géologie et les ressources minérales de la Nouvelle-Calédonie. *Annales des Mines*, **6**, 1-92.

Garnier, J. 1867b. Note sur la géologie de la Nouvelle-Calédonie. *Bulletin de la Societe Geologique de France*, **2**, 438-451.

Garrido, C.J., Marchesi, C., Godard, M., Belley, F. & Ferré, E. 2009. Migration and accumulation of ultra-depleted subduction-related melts in the Massif du Sud ophiolite (New Caledonia). *Goldschmidt Conference Abstracts 2009*.

Gautier, P., Quesnel, B., Boulvais, P. & Cathelineau, M. 2016. The emplacement of the Peridotite Nappe of New Caledonia and its bearing on the tectonics of obduction. *Tectonics*, doi: 10.1002/2016TC004318.

Ghent, E., Black, P., Brothers, R. & Stout, M. 1987a. Eclogites and associated albite-epidote-garnet paragneisses between Yambe and Cape Colnett, New Caledonia. *Journal of Petrology*, **28**, 627-643.

Ghent, E., Roddick, J. & Black, P. 1994. 40Ar/39Ar dating of white micas from the epidote to the omphacite zones, northern New Caledonia: tectonic implications. *Canadian Journal of Earth Sciences*, **31**, 995-1001.

Ghent, E.D., Stout, M.Z., Black, P. & Brothers, R. 1987b. Chloritoid-bearing rocks associated with blueschists and eclogites, northern New Caledonia. *Journal of Metamorphic Geology*, **5**, 239-254.

Gonord, H. 1977. Recherches sur la géologie de la Nouvelle-Calédonie; sa place dans l'ensemble structural du Pacifique sud-ouest. *Thèse Sciences, Université de Montpellier, France*, 1-310.

Guillon, J.H. 1975. Les massifs péridotitiques de Nouvelle-Calédonie; Type d'appareil ultrabasique stratiforme de chaîne récente. *Mémoire ORSTOM, Paris*, **76**, 1-72.

Guillon, J.H. & Gonord, H. 1972. Premières données radiométriques concernant les basaltes de Nouvelle-Calédonie. Leurs relations avec les grands évènements de l'histoire géologique de l'arc mélanésien interne au Cénozoïque. *Compte-Rendu de l'Académie des Sciences*, **275**, 309-312.

Hayes, D.E. & Ringis, J. 1973. Seafloor spreading in the Tasman Sea. *Nature*, **243**, 454-458.

Herzer, R.H., Barker, D.H.N., Roest, W.R. & Mortimer, N. 2011. Oligocene-Miocene spreading history of the northern South Fiji Basin and implications for the evolution of the New Zealand plate boundary. *Geochemistry, Geophysics, Geosystems*, **12**, n/a-n/a, doi: 10.1029/2010gc003291.

Herzer, R.H., Davy, B.W., Mortimer, N., Quilty, P.G., Chaproniere, G.C.H., Jones, C.M., Crawford, A.J. & Hollis, C.J. 2009. Seismic stratigraphy and structure of the Northland Plateau and the development of the Vening Meinesz transform margin, SW Pacific Ocean. *Marine Geophysical Researches*, **30**, 21-60, doi: 10.1007/s11001-009-9065-1.

Hofmann, A.W. 2003. Sampling mantle heterogeneity through oceanic basalts: isotopes and trace elements. *Treatise on Geochemistry*, **2**, 61-101.

Isaac, M.J., Herzer, R.H., Brook, F.J. & Hayward, B.W. 1994. *Cretaceous and Cenozoic basins of Northland, New Zealand*.

Iseppi, M., Lesimple, S., Cluzel, D., Le Bayon, B., Sevin, B. & Maurizot, P. 2017. The exposed roof of a paleo-subduction zone the Peridotite Nappe of New Caledonia. *Subduction interface processes*, Barcelone, Spain.

Iseppi, M. 2019. Fracturation polyphasée et contröles des gisements de nickel supergène de Nouvelle-Calédonie. Nouvelles méthodes d'exploration et modèles de gisements. PhD. thesis, Institut des Sciences Exactes et Appliquées. Université de Nouvelle-Calédonie.

Itaya, T., Brothers, R. & Black, P. 1985. Sulfides, oxides and sphene in high-pressure schists from New Caledonia. *Contributions to Mineralogy and Petrology*, **91**, 151-162.

Jeanpert, J., Genthon, P., Maurizot, P., Folio, J.L., Vendé-Leclerc, M., Sérino, J., Join, J.L. & Iseppi, M. 2016. Morphology and distribution of dolines on ultramafic rocks from airborne LiDAR data: the case of southern Grande Terre in New Caledonia (SW Pacific). *Earth Surface Processes and Landforms*, doi: 10.1002/esp.3952.

Karson, J.A. 1984. Variations in structure and petrology in the Coastal Complex, Newfoundland: anatomy of an oceanic fracture zone. Geological Society London Special Publication, 13, 131-144.

König, S., Münker, C., Schuth, S., Luguet, A., Hoffmann, J.E. & Kuduon, J. 2010. Boninites as windows into trace element mobility in subduction zones. *Geochimica et Cosmochimica Acta*, **74**, 684-704, doi: 10.1016/j.gca.2009.10.011.

Lacroix, A. 1897. Sur la lawsonite de Corse et de Nouvelle-Calédonie. *Bulletin de la Société Française de Minéralogie*, **20**, 309-312.

Lacroix, A. 1941. Les glaucophanites de la Nouvelle-Calédonie et les roches qui les accompagnent, leur composition et leur genèse. *Académie des Sciences de l'Institut. Mémoires*, **65**, 1-103.

Lagabrielle, Y. & Chauvet, A. 2008. The role of extensional tectonics in shaping Cenozoic New-Caledonia. *Bulletin de la Societe Geologique de France*, **179**, 315-329.

Lagabrielle, Y., Chauvet, A., Ulrich, M. & Guillot, S. 2013. Passive obduction and gravity-driven emplacement of large ophiolitic sheets: The New Caledonia ophiolite (SW Pacific) as a case study? *Bulletin de la Societe Geologique de France*, **184**, 545-556.

Lahondère, D., Lesimple, S., Cagnard, F., Lahfid, A., Wille, G. & Maurizot, P. 2012. *Serpentinisation et fibrogenèse dans les massifs de péridotite de Nouvelle-Calédonie.* Bureau de Recherches Géologiques et Minières, Centre National de Recherche et de Technologie Nickel et Environnement.

Leblanc, M. 1987. Chromite in oceanic arc environments: New Caledonia. *in: Evolution of chromium ore fields. Ed. C.W.Stowe*, **12**, 265-296.

Leblanc, M. 1995. Chromitite and Ultramafic Rock Compositional Zoning through a Paleotransform Fault, Poum, New Caledonia. *Economic Geology*, **90**, 2028-2039, doi: 10.2113/gsecongeo.90.7.2028.

Legueré, J. 1976. Des corrélations entre la tectonique cassante et l'altération supergène des péridotites de Nouvelle-Calédonie. *Ph D. Thesis, Université des sciences et techniques du Languedoc, Montpellier, France*, **80**.

Lesimple, S., Lahondère, D., Cluzel, D., Maurizot, P. & Iseppi, M. 2017. Formation of serpentine-bearing fracture network in the mantle wedge at subduction inception. New Caledonia as a case study. *Subduction interface processes*, Barcelone, Spain.

Lister, G. & Forster, M.A. 2009. Tectonic mode switches and the nature of orogenesis. *Lithos*, **113**, 274–291, doi: 10.1016/j.lithos.2008.10.024.

Lus, W.Y., McDougall, I. & Davies, H.L. 2004. Age of the metamorphic sole of the Papuan Ultramafic Belt ophiolite, Papua New Guinea. *Tectonophysics*, **394**, 85-101.

Luyendyk, B.P. 1995. Hypothesis for Cretaceous rifting of east Gondwana caused by subducted slab capture. *Geology* **23**, 373-376.

Malpas, J., Spôrli, K.B., Black, P.M. & Smith, I.E.M. 1992. Northland ophiolite, New Zealand, and implications for plate-tectonic evolution of the southwest Pacific. *Geology*, **20**, 149-152.

Marchesi, C., Garrido, C.J., Godard, M., Belley, F. & Ferré, E. 2009. Migration and accumulation of ultra-depleted subduction-related melts in the Massif du Sud ophiolite (New Caledonia). *Chemical Geology*, **266**, 171-186, doi: 10.1016/j.chemgeo.2009.06.004.

Marmo, B., Clarke, G. & Powell, R. 2002. Fractionation of bulk rock composition due to porphyroblast growth: effects on eclogite facies mineral equilibria, Pam Peninsula, New Caledonia. *Journal of Metamorphic Geology*, **20**, 151-165.

Mauffret, A., Symonds, P., Benkhelil, J., Bemardel, G., Buchanan, C., D'Acremont, E., Gorini, C., Lafoy, Y., Nercessian, A., Ryan, J., Smith, N. & Van de Beuque, S., 2001127. 2001. Collaborative Australia/France Multibeam Seafloor Mapping Survey-Norfolk Ridge to Three Kings Ridge Region: FAUST-2, Preliminary Results. Geoscience Australia.

Maurizot, P. 2011. First sedimentary record of the pre-obduction convergence in New Caledonia : formation of an Early Eocene accretionary complex in the north of Grande Terre and emplacement of the ' Montagnes Blanches ' nappe. *Bulletin de la Société Géologique Française*, **182, 6**, 479-491.

Maurizot, P. 2014. Evolution and sedimentation in a forebulge environment: example of the Late Eocene Uitoé Limestone, New Caledonia, Southwest Pacific. *New Zealand Journal of Geology and Geophysics*, **57**, 390-401, doi: 10.1080/00288306.2014.938085.

Maurizot, P. & Cluzel, D. 2014. Pre-obduction records of Eocene foreland basins in central New Caledonia: an appraisal from surface geology and Cadart-1 borehole data. *New Zealand Journal of Geology and Geophysics*, 1-12.

Maurizot, P., Eberlé, M., Habault, C. & Tessarollo, C. 1989. Carte Géologique à l'échelle du 1 / 50 000 et notice explicative: feuille Pam-Ouégoa. *Territoire de la Nouvelle-Calédonie - Bureau de Recherches Géologiques et Minières*, 1-81.

Maurizot, P., Tessarolo, C. & Feignier, D. 1984. Carte Géologique à l'échelle du 1 / 50 000 et notice explicative: feuille Touho - Poindimié. *Territoire de la Nouvelle-Calédonie - Bureau de Recherches Géologiques et Minières*, 1-43.

Maurizot, P. & Vendé-Leclerc, M. 2009. New-Caledonia geological map, scale 1/500 000. *Direction de l'Industrie, des Mines, et de l'Energie - Service Géologique de Nouvelle-Calédonie, Bureau de Recherches Géologiques et Minières. Nouméa, New Caledonia*, www.dimenc.gouv.nc.

McKenzie, D.P. & Morgan, W.J. 1969. Evolution of Triple Junctions. *Nature*, **224** 125-133, doi: 10.1038/224125a0.

Meffre, S., Crawford, A.J. & Quilty, P.G. 2006. Arc-continent collision forming a large island between New Caledonia and New Zealand in the Oligocene. *ASEG Extended Abstracts*, **2006**, 1-3.

Monzier, M. 1993. Un modèle de collision arc insulaire-ride océanique. Evolution sismotectonique et pétrologie des volcanites de la zone d'affrontement arc des Nouvelles-Hébrides ride des Loyauté. ORSTOM. Thèse, Nouméa, Université Française de Pacifique:0-322.

Mortimer, N., Gans, P.B., Palin, J.M. & Herzer, R.H. 2014a. Eocene and Oligocene basins and ridges of the Coral Sea-New Caledonia region: tectonic link between Melanesia, Fiji and Zealandia. *Tectonics*, **33**, 1386-1407, doi: 10.1002/2014TC003598.

Mortimer, N., Herzer, R.H., Walker, N.W., Calvert, A.T., Seward, D. & Chaproniere, G.C.H. 2003. Cavalli Seamount, Northland Plateau, SW Pacific Ocean: a Miocene metamorphic core complex? *Journal of the Geological Society, London*, **160**, 971-983.

Mothersole, F.E., Evans, K. & Frost, B.R. 2017. Abyssal and hydrated mantle wedge serpentinised peridotites: a comparison of the 15◦20N fracture zone and New Caledonia serpentinites. *Contribution to Mineralogy and Petrology*, **172**, 1-25, doi: 10.1007/s00410-017-1381-x.

Moutte, J. 1979. Le massif de Thiébaghi, Nouvelle-Calédonie, et ses gîtes de chromite. *Ph D. thesis, ENS des Mines de Paris*, 156.

Moutte, J. 1982. Chromite deposits of the Thiébaghi ultramafic massif, NC.pdf. *Economic Geology*, **77**, 576-591.

Moutte, J. & Paris, J. 1977a. Observations nouvelles sur le Grand Massif ultramafique du Sud de la Nouvelle Calédonie. *Bull. Bur. Rech. Géol. Min. sect. IV*, **1**, 43-51.

Moutte, J. & Paris, J.P. 1977b. Anatomy and structure of the Great Southern Massif (New Caledonia) *In*: Edition Technip, P. (ed.) *International Symposium of Geodynamics in Sout-West Pacific. 27 august-2 september 1976*, Noumea, New Caledonia, 229-234.

Nicholson, K.N. 1999. *The Tangihua complex, New Zealand: Implications for Cretaceous-Oligocene convergent margin process in the SW Pacific from comparison with the Poya Terrane, New Caledonia.* PhD, University of Auckland, New Zealand, University Joseph Fourier, Grenoble, France.

Nicholson, K.N.N., Black, P.M.M. & Picard, C. 2000. Geochemistry and tectonic significance of the Tangihua Ophiolite Complex, New Zealand. *Tectonophysics*, **321**, 1-15, doi: 10.1016/S0040-1951(00)00081-0.

Nicolas, A. 1989. Structure of Ophiolites and Dynamics of Oceanic Lithosphere. *Kluwer, Dordrecht*, 367.

Ohnenstetter, D. & Brown, W.L. 1992. Overgrowth textures, disequilibrium zoning, and cooling history of a glassy four-pyroxene boninite dike from New Caledonia. *Journal of Petrology*, **33**, 231–271.

Ohnenstetter, D. & Brown, W.L. 1996. Compositional variation and primary water contents of differentiated interstitial and included glasses in boninites. *Contributions to Mineralogy and Petrology*, **123**, 117-137.

Oudin, E., Bouladon, J. & Paris, J.P. 1985. Vers hydrothermaux fossiles dans une minéralisation sulfurée des ophiolites de Nouvelle-Calédonie. *Comptes Rendus de l'Académie des Sciences*, **301**, 157-162.

Paris, J.P. 1981. Géologie de la Nouvelle-Calédonie. *Mémoire du Bureau de Recherche Géologique et Minière*, **113**, 1-279.

Parkinson, I.J. & Pearce, J. 1998. Peridotites from the Izu-Bonin-Mariana forearc (ODP leg 125): Evidence for mantle melting and melt-mantle interaction in a supra-subduction zone setting. *Journal of Petrology*, **39**, 1577-1618, doi: 10.1093/petroj/39.9.1577.

Parrot, J.F. & Dugas, F. 1980. The disrupted ophiolitic belt of the Southwest Pacific: Evidence of an Eocene subduction zone. *Tectonophysics*, **66**, 349-372.

Patriat, M., Collot, J., Etienne, S., Poli, S., Clerc, C., Mortimer, N., Pattier, F. & Juan, C. 2018. New Caledonia obducted Peridotite Nappe, offshore extent and implications for obduction and post-obduction processes. *Tectonics*, **37**, 1-20, doi: 10.1002/2017TC004722.

Pearce, J.A. 1982. Trace element characteristics of lavas from destructive plate margins. *In Andesites: Orogenic Andesites and Related Rocks, edited by R. S. Thorpe, John Wiley, New York*, 525-548, .

Pirard, C., Hermann, J. & O'Neill, H. 2013. Petrology and geochemistry of the crust-mantle boundary in a nascent arc, Massif du Sud, New Caledonia. *Journal of Petrology*, 1-34, doi: 10.1093/petroloy/egt030.

Pirard, C. & Spandler, C. 2017. The zircon record of high-pressure metasedimentary rocks of New Caledonia: Implications for regional tectonics of the south-west Pacific. *Gondwana research*, **46**, 79-94, doi: 10.1016/j.gr.2017.03.001.

Podvin, P. 1983. Remobilisations chimiques successives dans les tectonites ophiolitiques et leurs gisements de chromite. Exemple du massif du Humboldt (Nouvelle-Calédonie). *Ph D. thesis, ENS des Mines de Paris*, 204.

Podvin, P., Berger, E.T. & Vannier, M. 1985. Interactions géochimiques liées à la mise en place de dikes pyroxénitiques et gabbroïques dans des harzburgites ophiolitiques. Exemple du Massif du Humboldt (Nouvelle-Calédonie). *BULLETIN DE MINERALOGIE*, **108**, 45-62.

Potel, S. 2001. *Very low grade metamorphism in New Caledonia.* PhD, University of Basel, Switzerland.

Potel, S., Ferreiro-Mâblmann, R. & Frey, M. 2004. Low-Grade Metamorphism in Northern New Caledonia: Evolufion of metapelites under HP-LT Condilions. *Diagenesis and Low-Grade Metamorphism*, 230.

Potel, S., Mählmann, R.F., Stern, W., Mullis, J. & Frey, M. 2006. Very low-grade metamorphic evolution of pelitic rocks under high-pressure/low-temperature conditions, NW New Caledonia (SW Pacific). *Journal of Petrology*, **47**, 991-1015.

Potel, S., Schmidt, S.T. & de Capitanil, C. 2002. Composition of pumpellyite, epidote and chlorite from New Caledonia- How important are metamorphic grade and whole-rock composition? *Schweiz. Mineralogy Petrography Mitt.*, **82**, 229-252.

Prinzhofer, A. 1981. *Structure et pétrologie d'un cortège ophiolitique, le massif du sud (Nouvelle-Calédonie). La transition manteau-croûte en milieu océanique.* Docteur-Ingénieur Thesis.

Prinzhofer, A. 1987. *Processus de fusion dans les zones d'extension océaniques et continentales.* PhD, Université de Paris 7.

Prinzhofer, A. & Nicolas, A. 1980. The Bogota peninsula, New Caledonia: A possible oceanic transform fault. *Journal of Geology*, **88**, 387-398, doi: 10.1086/628523.

Prinzhofer, A., Nicolas, A., Cassard, D., Moutte, J., Leblanc, M., Paris, J.P. & Rabinovitch, M. 1980. Structures in the new caledonia peridotites-gabbros: Implications for oceanic mantle and crust. *Tectonophysics*, **69**, 85-112, doi: 10.1016/0040-1951(80)90128-6.

Puillandre, N. & Samadi, S. 2016. KANACONO cruise, RV Alis. doi: 10.17600/16003900.

Quesnel, B. 2015. Altération supergène, circulation des fluides et déformations internes du massif de Koniambo, Nouvelle-Calédonie: implications sur les gisements nickélifères latéritiques. *Université de Rennes 1, Géosciences Rennes, UMR 6118, Université Européenne de Bretagne*, 1-275.

Quesnel, B., Gautier, P., Cathelineau, M., Boulvais, P., Couteau, C. & Drouillet, M. 2016. The internal deformation of the Peridotite Nappe of New Caledonia: a structural study of serpentine-bearing faults and shear zones in the Koniambo Massif. *Journal of Structural Geology*, **85**, 51-67, doi: 10.1016/j.jsg.2016.02.006.

Rait, G. 2000. Thrust transport directions in the Northland allochthon, New Zealand. *New Zealand Journal of Geology and Geophysics*, **43**, 271-288.

Rawling, T. & Lister, G. 1997. The structural evolution of New Caledonia. *Abstracts. Geodynamics and ore deposits conference, 19*, 62-64.

Rawling, T. & Lister, G. 1999a. The high-pressure sole of the New Caledonia ophiolite belt. *Geological Society of Australia, Abstracts*. Geological Society of Australia, 206-207.

Rawling, T. & Lister, G. 1999b. Oscillating modes of orogeny in the Southwest Pacific and the tectonic evolution of New Caledonia. *Geological Society, London, Special Publications*, **154**, 109-127.

Rawling, T.J. 1998. Oscillating orogenesis and exhumation of high-pressure rocks in New Caledonia, SW Pacific. *Ph D. Thesis, Department of Earth Sciences, Monash University, Melbourne Australia*.

Rawling, T.J. & Lister, G.S. 2002. Large-scale structure of the eclogite–blueschist belt of New Caledonia. *Journal of Structural Geology*, **24**, 1239-1258.

Rawling, T.J., Streets, C.J. & Lister, G.S. 1994. The structural evolution and tectonic signifiance of the mid-tertiary blueschist-eclogite belt, northern New Caledonia. *Geological Society of Australia, 1st Australian Geological Convention, Perth. September 1994. Abstracts n° 37*, **37**.

Rigolot, P. 1988. Prolongement méridional des grandes structures géologiques de New Caledonia. *Compte Rendus de l'Académie des Sciences*, **307**, 965-972.

Robineau, B., Join, J.-L., Beauvais, A., Parisot, J.-C. & C., S. 2007. Geoelectrical imaging of a thick regolith developed on ultramafic rocks : groundwater influence. *Australian Journal of Earth Sciences*, **54**, 773-781.

Robineau, B. & Join, J.L. 2005. Tectonique et microtectonique cassante du massif de Tiebaghi. Géométrie des sillons d'altération sous cuirasse imagée par la Tomographie de Résistivité Electrique. *SLN-IRD Internal Report*.

Rodgers, K.A. 1975. A comparison of the geology of the Papuan and New Caledonian ultramafic belts. *Journal of Geology*, **83**, 47-60.

Rodgers, K.A. 1976. Ultramafic and related rocks from Southern New Caledonia. *Bulletin du Bureau de Recherches Géologiques et Miniéres, France*, **1**, 33-55.

Routhier, P. 1953. Etude géologique du versant occidental de la Nouvelle-Calédonie entre le col de Boghen et la pointe d'Arama. *Mémoire de la Société Géologique de France*, **XXXII 1-3** 1-271.

Sameshima, T., Paris, J.P., Black, P.M. & Heming, R.F. 1983. Clinoenstatite-bearing lava from Népoui, New Caledonia. *American Mineralogist*, **68**, 1076–1082.

Schellart, W.P. 2007. North-eastward subduction followed by slab detachment to explain ophiolite obduction and Early Miocene volcanism in Northland, New Zealand. Terra Nova, 19, 211–218, doi: 10.1111/j.1365-3121.2007.00736.x.

Schellart, W.P., Lister, G.S. & Toy, V.G. 2006. A Late Cretaceous and Cenozoic reconstruction of the Southwest Pacific region: Tectonics controlled by subduction and slab rollback processes. *Earth-Science Reviews*, **76**, 191-233, doi: 10.1016/j.earscirev.2006.01.002.

Scott, S.R., Sims, K.W.W., Frost, B.R., Kelemen, P.B., Evans, K.A. & Swapp, S.M. 2017. On the hydration of olivine in ultramafic rocks: Implications from Fe isotopes in serpentinites. *Geochimica et Cosmochimica Acta*, **215**, 105-121, doi: /10.1016/j.gca.2017.07.011.

Sdrolias, M., Müller, R. & Gaina, C. 2003. Tectonic evolution of the southwest Pacific using constraints from backarc basins. Geological Society of America Special Papers, 372, 343-359.

Sdrolias, M., Müller, R.D., Mauffret, A. & Bernardel, G. 2004. Enigmatic formation of the Norfolk Basin, SW Pacific: A plume influence on back-arc extension. *Geochemistry, Geophysics, Geosystems*, **5**.

Secchiari, A. 2016. *Geochemical and Sr, Nd, Pb isotope investigation of the New Caledonia ophiolite.* PhD Course in Earth Sciences, Parma University, Montpellier University.

Secchiari, A., Becker, H., Gleißner, P., Li, C., Montanini, A. & Bosch, D. 2017a. Evidence from the New Caledonia peridotites for contrasting behavior of highly siderophile and chalcophile elements in supra-subduction zone and normal upper mantle. *In*: Italiana, S.G. (ed.) *Congresso SIMP-SGI-SOGEI-AIV 2017*, Roma 2017, 285.

Secchiari, A., Montanini, A., Bosch, D., Macera, P. & Cluzel, D. 2015. Geochemistry and tectonic significance of lherzolites from New Caledonia Ophiolite. *Mineralogica - Special Papers. 2nd European Mantle Workshop. Wrocław, Poland, 25-28 August 2015*.

Secchiari, A., Montanini, A., Bosch, D., Macera, P. & Cluzel, D. 2016. Melt extraction and enrichment processes in the New Caledonia lherzolites: Evidence from geochemical and Sr–Nd isotope data. *Lithos*, **260** 28-43, doi: 10.1016/j.lithos.2016.04.030.

Secchiari, A., Montanini, A., Bosch, D., Macera, P. & Cluzel, D. 2017b. The contrasting geochemical message from the New Caledonia gabbronorites: insights on depletion and contamination processes of the sub-arc mantle in a nascent arc setting. *Congresso SIMP-SGI-SOGEI-AIV 2017*. Società Geologica Italiana, Roma 2017.

Secchiari, A., Montanini, A., Bosch, D., Macera, P. & Cluzel, D. 2018. The contrasting geochemical message from the New Caledonia gabbronorites: insights on depletion and contamination processes of the sub-arc mantle in a nascent arc setting. *Contributions to Mineralogy and Petrology*, 173 66.

Secchiari A., Montanini A., Bosch D., Macera P., Cluzel D., submitted. Sr-Nd-Pb and trace element systematics of the New Caledonia harzburgites: tracking source depletion and contamination processes in a SSZ setting. Geosciences Frontiers, Sp. Issue: Ophiolites.

Secchiari A., Montanini A., Bosch D., Macera P., Cluzel D. 2019. Origin of the spinel-pyroxene symplectites in the harzburgites from the New Caledonia peridotite. Ofioliti, **44**, 1, 31-42-

Sécher, D. 1981. Les lherzolites ophiolitiques de Nouvelle-Calédonie et leurs gisements de chromite. *Ph D. thesis, Université de Nates, France*, 228.

Seton, M., Mortimer, N., Williams, S., Quilty, P., Gans, P.B., Meffre, S., Micklethwaite, S., Zahirovic, S., Moore, J. & Matthews, K. 2016. Melanesian back-arc basin and arc development: Constraints from the eastern Coral Sea. *Gondwana research*, **39**, 77-95, doi: 10.1016/j.gr.2016.06.011.

Solovova, I.P., Ohnenstetter, D. & Girnisa, A.V. 2012. Melt inclusions in olivine from the boninites of New Caledonia: post-entrapment melt modification and estimation of primary magma compositions. *Petrology*, **20**, 529–544.

Soret, M., Agard, P., Dubacq, B., Viale-Brovarone, A., Monié, P. & Chauvet, A. 2016. Strain localization and fluid infiltration in the mantle wedge during subduction initiation; Evidence frome the base of the New Caledonia ophiolite. *Lithos*, **244**, 1-19, doi: 10.1016/j.lithos.2015.11.022.

Spandler, C. & Hermann, J. 2006. High-pressure veins in eclogite from New Caledonia and their significance for fluid migration in subduction zones. *Lithos*, **89**, 135-153.

Spandler, C., Hermann, J., Arculus, R. & Mavrogenes, J. 2004a. Geochemical heterogeneity and element mobility in deeply subducted oceanic crust; insights from high-pressure mafic rocks from New Caledonia. *Chemical Geology*, **206**, 21-42.

Spandler, C., Hermann, J., Arculus, R. & Mavrogenes, J.A. 2003. Redistribution of trace elements during prograde metamorphism from lawsonite blueschist to eclogite facies; implications for deep subduction-zone processes. *Contribution to Mineralogy and Petrology*, **146**, 205-222, doi: 10.1007/s00410-003-0495-5.

Spandler, C., Hermann, J., Faure, K., Mavrogenes, J.A. & Arculus, R.J. 2008. The importance of talc and chlorite ‘‘hybrid’’ rocks for volatile recycling through subduction zones; evidence from the high-pressure subduction me´lange of New Caledonia. *Contribution to Mineralogy and Petrology*, **155**, 181–198, doi: 10.1007/s00410-007-0236-2.

Spandler, C., Hermann, J. & Rubatto, D. 2004b. Exsolution of thortveitite, yttrialite, and xenotime during low-temperature recrystallization of zircon from New Caledonia, and their significance for trace element incorporation in zircon. *American Mineralogist*, **89**, 1795-1806.

Spandler, C. & Pirard, C. 2013. Element recycling from subducting slabs to arc crust: A review. *Lithos*, **170-171**, 208-223, doi: 10.1016/j.lithos.2013.02.016.

Spandler, C., Rubatto, D. & Hermann, J. 2005. Late Cretaceous-Tertiary tectonics of the southwest Pacific: Insights from U-Pb sensitive, high-resolution ion microprobe (SHRIMP) dating of eclogite facies rocks from New Caledonia. *Tectonics*, **24**.

Spandler, C., Yaxley, G., Green, D.H. & Scott, D. 2010. Experimental phase and melting relations of metapelite in the upper mantle: implications for the petrogenesis of intraplate magmas. *Contributions to Mineralogy and Petrology*, **160**, 569-589.

Sun, S.S. & McDonough, W.I. 1989. Chemical and isotopic systematics of oceanic basalts: Implications for mantle composition and processes. *in Magmatism in the Ocean Basins, edited by A. D. Saunders and M. D. Norry, Geological Society Special Publication*, **42**, 313-345.

Taetz, S., John, T., Bröcker, M. & Spandler, C. 2016. Fluid–rock interaction and evolution of a high-pressure/lowtemperature vein system in eclogite from New Caledonia: insights into intraslab fluid flow processes. *Contribution to Mineralogy and Petrology*, **171**, 1-27, doi: 10.1007/s00410-016-1295-z.

Teyssier, C., Chatzaras, V. & Von Der Handt, A. 2016. Microfabrics in depleted mantle plaeotransform (New Caledonia). *Geophysical Research Abstracts, European Geoscience Union, EGU2016-11489*, **18**.

Tissot, B. & Noesmoen, A. 1958. Les bassins de Nouméa et de Bourail (Nouvelle-Calédonie). *Revue de l'Institut Français du Pétrole*, 739-759.

Titus, S., Davis, J.R., Ferré, E.C. & Tikoff, B. 2008. Quantifying strain across a paleotransform fault using incremental deformation, Bogota Peninsula, New Caledonia. *GSA, Annual Meeting, Abstract 3-288-16*, Houston.

Titus, S.J., Maes, S.M., Benford, B., Ferre, E.C. & Tikoff, B. 2011. Fabric development in the mantle section of a paleotransform fault and its effect on ophiolite obduction, New Caledonia. *Lithosphere*, **3**, 221-244, doi: 10.1130/l122.1.

Ulrich, M. 2010. *Péridotites et serpentinites du complexe ophiolitique de la Nouvelle-Calédonie*, Université de Nouvelle Calédonie.

Ulrich, M., Picard, C., Guillot, S., Chauvel, C., Cluzel, D. & Meffre, S. 2010. Multiple melting stages and refertilisation process as indicators for ridge to subduction formation: the New Caledonia Ophiolite. *Lithos*, **115**, 223-236.

Van de Beuque, S., Auzende, J.M., Lafoy, Y., Bernardel, G., Nercessian, A., Régnier, M., Symonds, P.A. & Exon, N.F. 1998. Transect sismique continu entre l'arc des Nouvelles-Hébrides et la marge orientale de l'Australie: programme FAUST (French Australian Seismic Transect). *Comptes Rendus de l'Académie des Sciences - Series IIA - Earth and Planetary Science*, **327**, 761-768, doi: 10.1016/S1251-8050(99)80048-2.

Vermeesch, P. 2006. Tectonic discrimination diagrams revisited. . *Geochemistry, Geophysics, Geosystems 7*, **6**, doi: 10.1029/2005GC001092.

Vitale Brovarone, A. & Agard, P. 2013. True metamorphic isograds or tectonically sliced metamorphic sequence? New high-spatial resolution petrological data for the New Caledonia case study. *Contributions to Mineralogy and Petrology*, **166**, 451-469, doi: 10.1007/s00410-013-0885-2.

Vogt, J. & Podvin, P. 1983. Carte Géologique à l'échelle du 1 / 50 000 et notice explicative: feuille Humboldt-Port-Bouquet. *Territoire de Nouvelle-Calédonie - Bureau de Recherches Géologiques et Minières*, 1-68.

Walker, D.A. & McDougall, I. 1982. $^{40}Ar/^{39}Ar$ and K-Ar dating of altered glassy volcanic rocks: the Dabi volcanics, Papua-New Guinea. *Geochimica et Cosmochimica Acta*, **46**, 2181-2190.

Whattam, S.A. 2009. Arc-continent collisional orogenesis in the SW Pacific and the nature, source and correlation of emplaced ophiolitic nappe components. *Lithos*, **113**, 88-114, doi: 10.1016/j.lithos.2008.11.009.

Whattam, S.A., Malpas, J., Ali, J.R., Lo, C.-H. & Smith, I.E. 2005. Formation and emplacement of the Northland ophiolite, northern New Zealand: SW Pacific tectonic implications. *Journal of the Geological Society*, **162**, 225-241.

Whattam, S.A., Malpas, J., Ali, J.R. & Smith, I.E.M. 2008. New SW Pacific tectonic model: Cyclical intraoceanic magmatic arc construction and near-coeval emplacement along the Australia-Pacific margin in the Cenozoic. *Geochemistry, Geophysics, Geosystems*, **9**, 1-34, doi: 10.1029/2007gc001710.

Whitten, M.D. 2015. Formation de Koné: Recording the final stages of Gondwana breakup in New Caledonia. *BSc. thesis , Uniersity of Tasmania*, 1-130.

Wood, D.A. 1980. The application of a Th-Hf-Ta diagram to problems of tectonomagmatic classification and to establishing the nature of crustal contamination of basaltic lavas of the British Tertiary Volcanic Province. *Earth and Planetary Science Letters*, **50**, 11-30, doi: 10.1016/0012-821X(80)90116-8.

Yokoyama, K., Brothers, R.N. & Black, P.M. 1986. Regional eclogite facies in the high-pressure metamorphic belt of New Caledonia. *Geological Society of America*, **Memoir 164**, 407-421.

Zindler, A. & Hart, S.R. 1986. Chemical geodynamics. *Annual Review of Earth and Planetary Sciences*, **14**, 493-571.

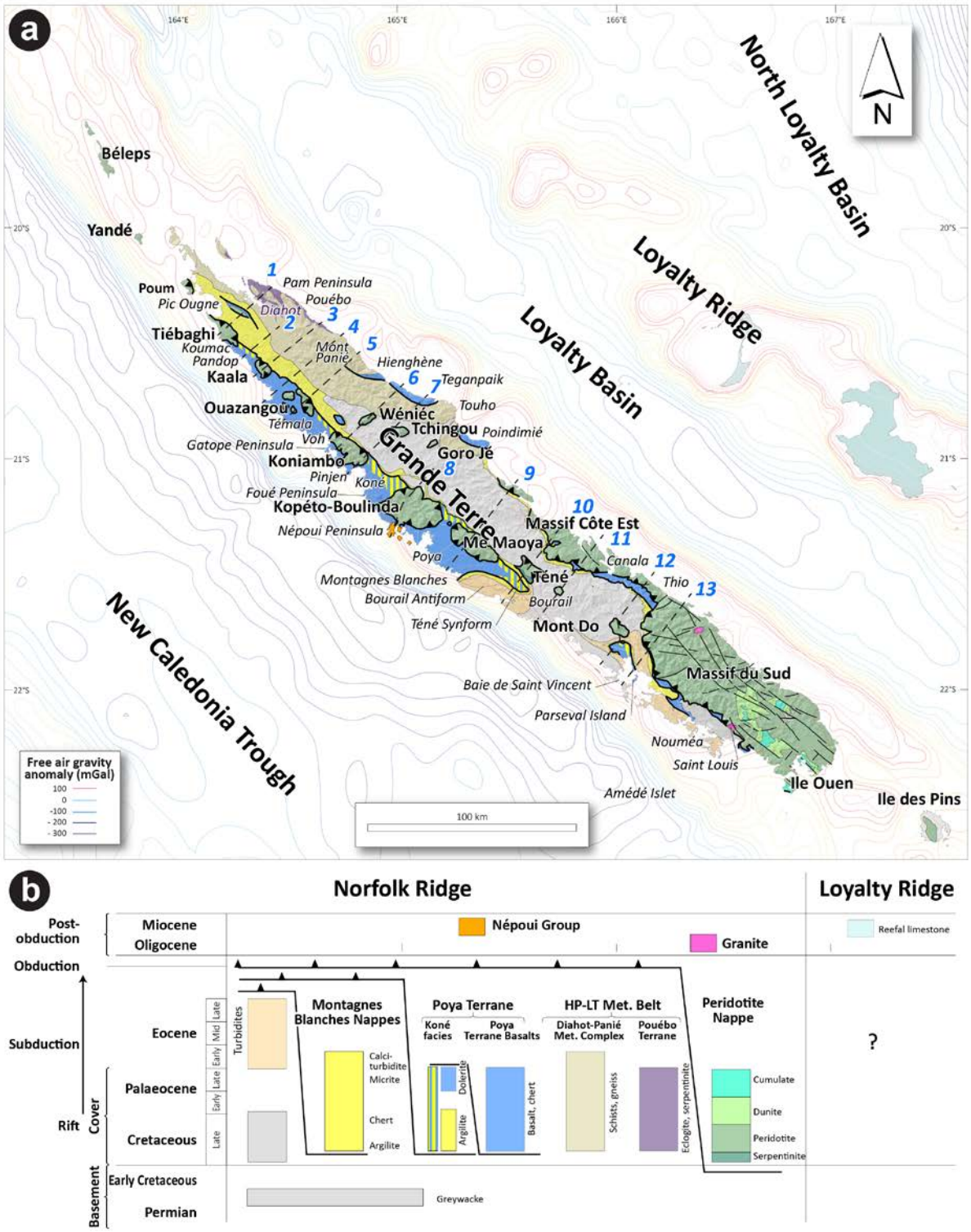

Fig. 1 a) Simplified geological map of New Caledonia showing the main terranes related to the Eocene Subduction-Obduction Complexx. Offshore gravity data after Collot (1989) and Van de Beuque et al. (1998). b) Legend.

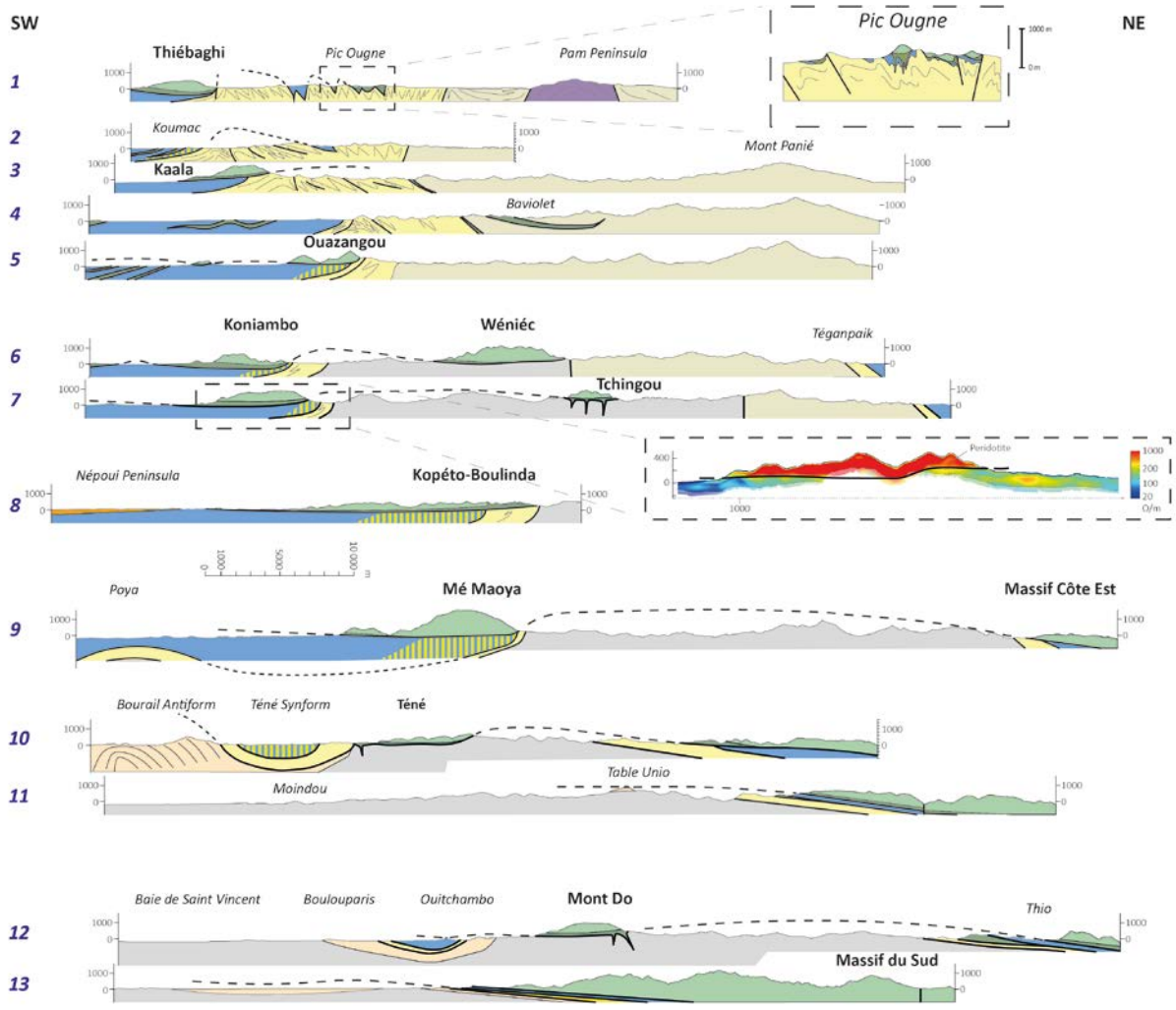

Fig. 2 Geological cross sections across Grande Terre showing the relationships of allochthonous units (Peridotite Nappe, Poya Terrane, Montagnes Blanches Nappe), and autochthonous units (basement, cover). Same legend as figure 1. No vertical exaggeration. Long dashes: basal contact of Peridotite Nappe; short dashes: basal contact of Poya Terrane. Section 7: Imaging by heliborne electromagnetic survey and interpretation of a section through the south eastern extremity of the Koniambo klippe showing the main basal thrust of the Peridotite Nappe over its substrate (Iseppi 2019).

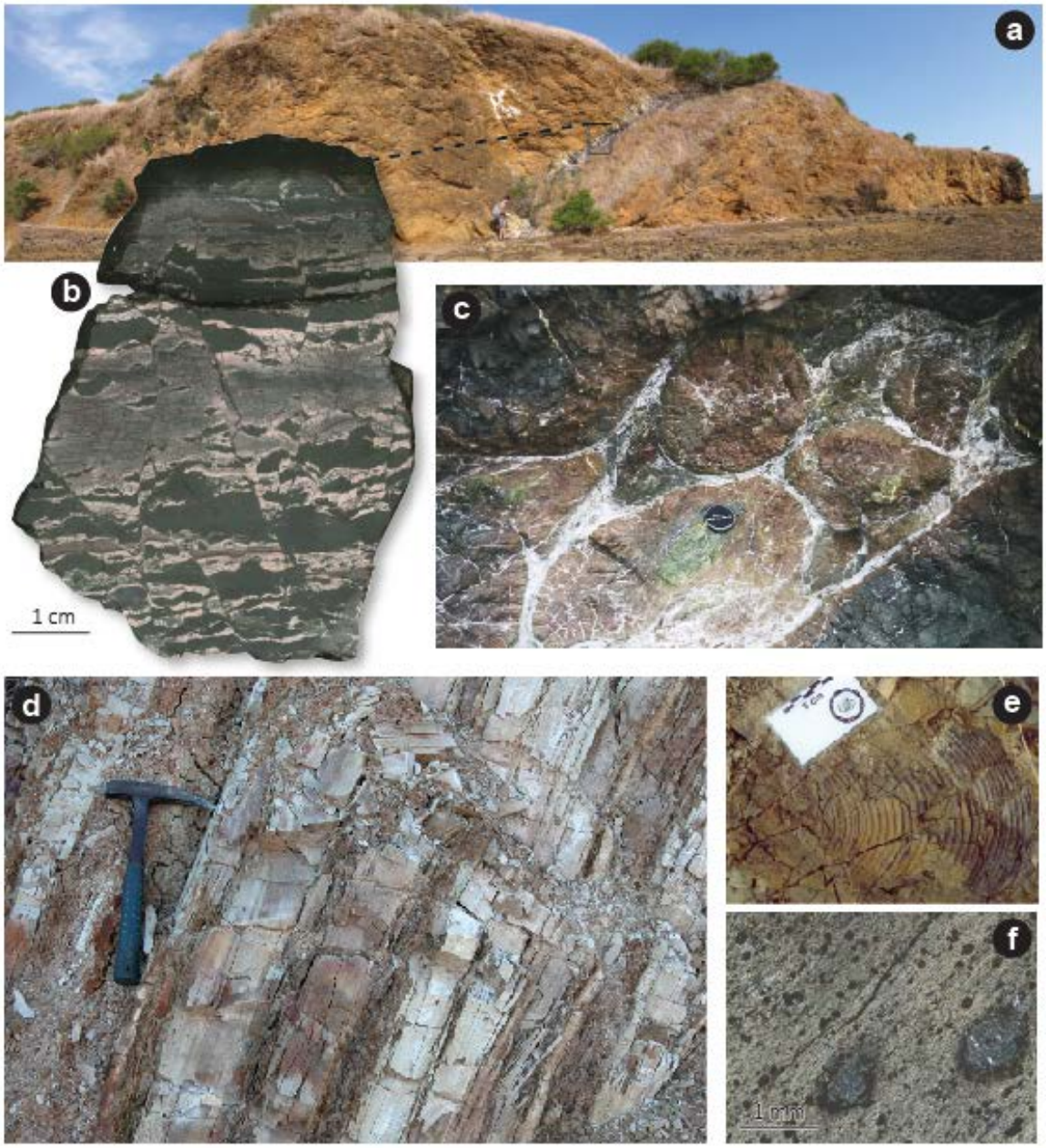

Fig. 3 Typical Poya Terrane outcrops and rocks (a,b, and c) : a) Littoral cliff of the Poya Terrane Basalts showing an inliers of b) abyssal manganese-rich sediment (north of Parseval Island). c) Pillow basalts (Pandop Peninsula, Koumac). Typical Koné Facies (d,e, and f): d) Fine-grained turbiditic siltstone (Koumac). e) Inoceramid cast at the surface of a turbidite bed North of Pouembout, (along road cut of RP N2). f) Photomicrograph (plane polarized light) of a spotted schist in the Koné Facies with millimetric aggregates of oxy-chlorite and albite (same locality).

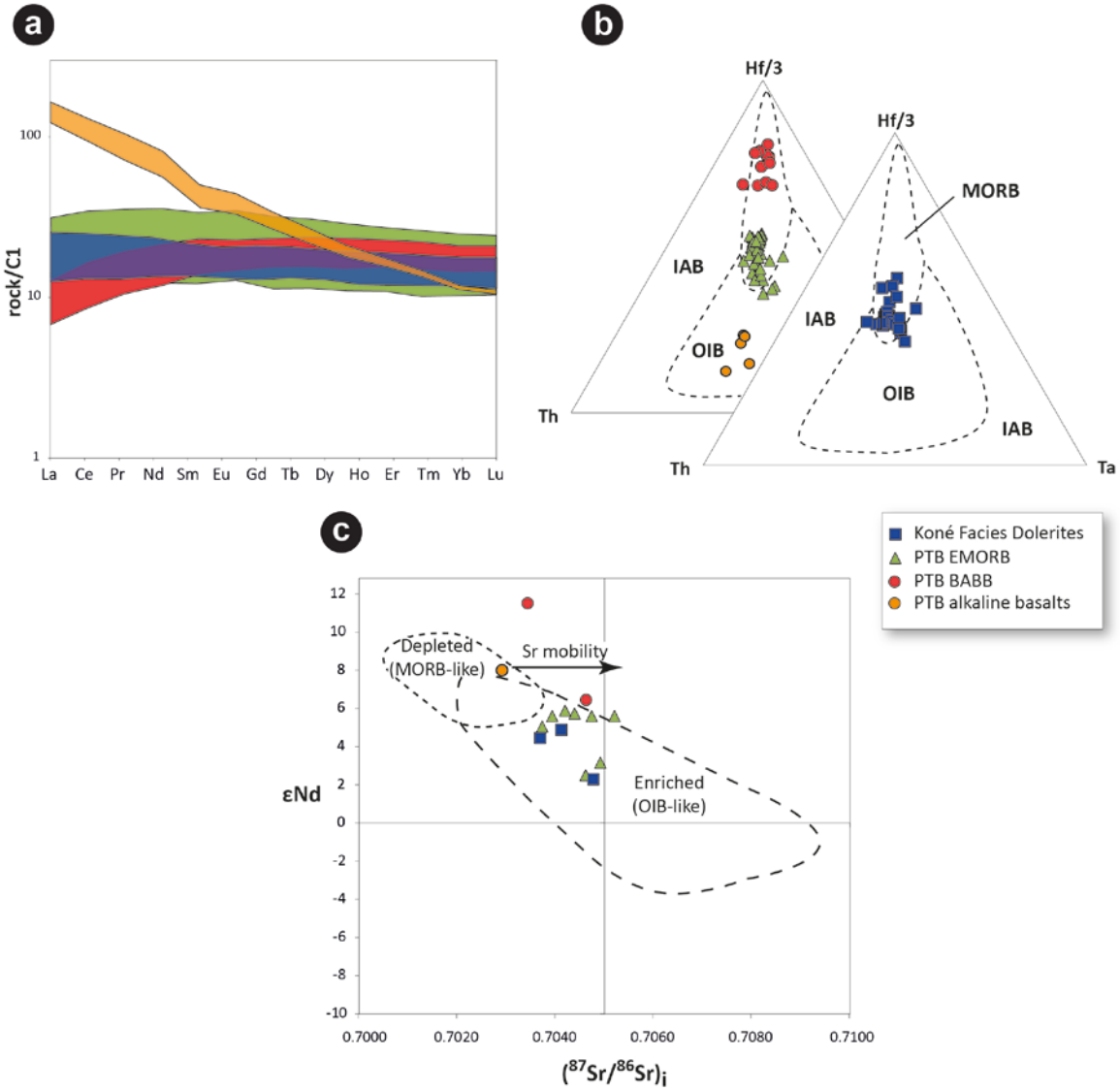

Fig. 4 Geochemical features of Poya Terrane Basalts and dolerites of Koné Facies: a) C1 Chondrite-normalized REE patterns (Evensen et al. 1978). b) Hf/3-Th-Ta ternary diagram (Vermeesch 2006; Wood 1980). c) Nd-Sr isotopic compositions, reference data from Zindler & Hart (1986).

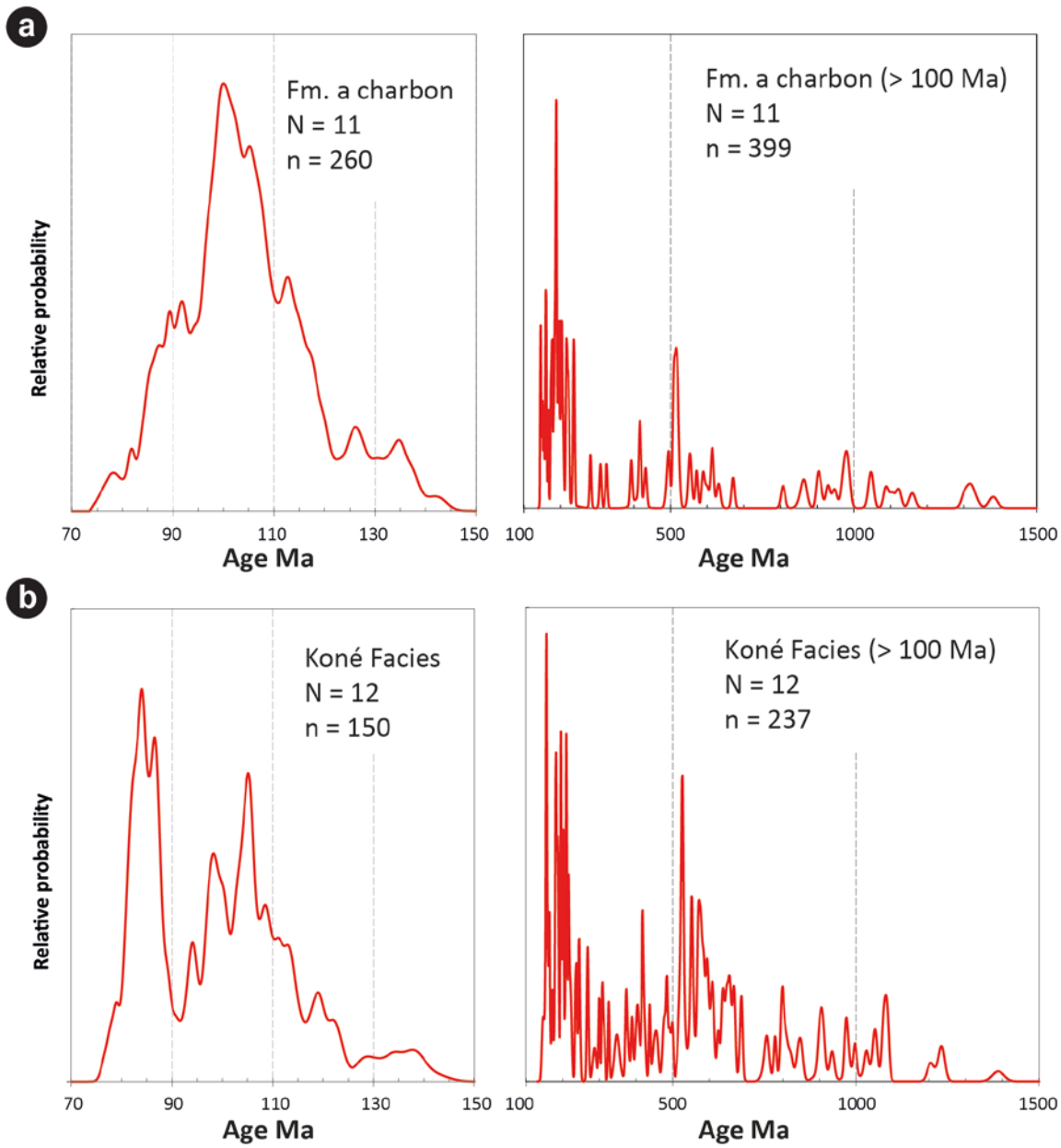

Fig. 5 Comparison of zircon ages from a) Formation à Charbon and b) Koné Facies. N = number of samples, n = number of grain analyzed.

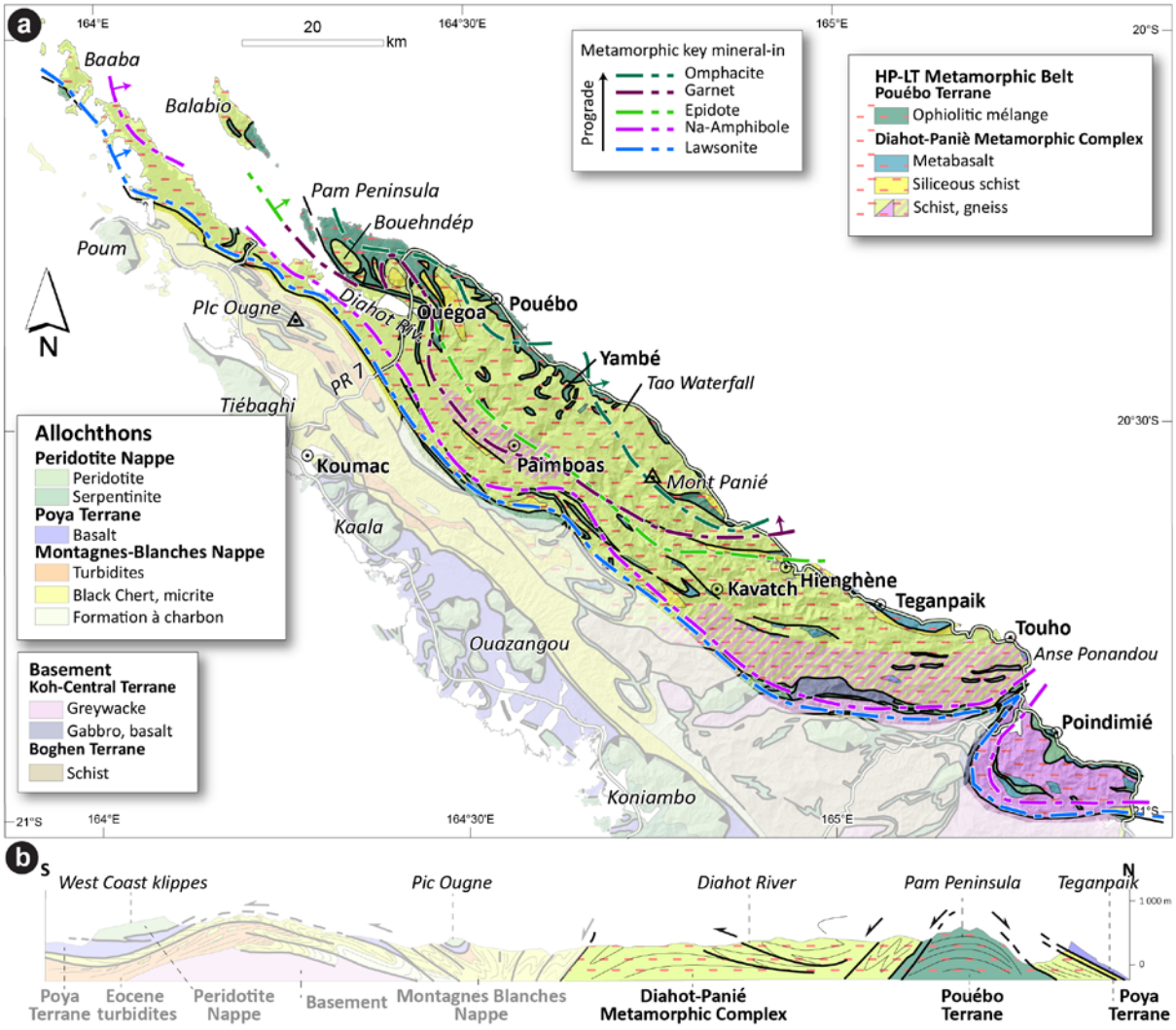

Fig. 6 a) Geological map of the HP-LT Metamorphic Belt (metamorphic grades after Maurizot et al. 1989 and Vitale Brovarone & Agard 2013). b) Idealized crosssection (no horizontal scale) through the South-western Coast – Koumac- Pouébo - North-eastern Coast, showing the relationships of the different subduction-obduction units.

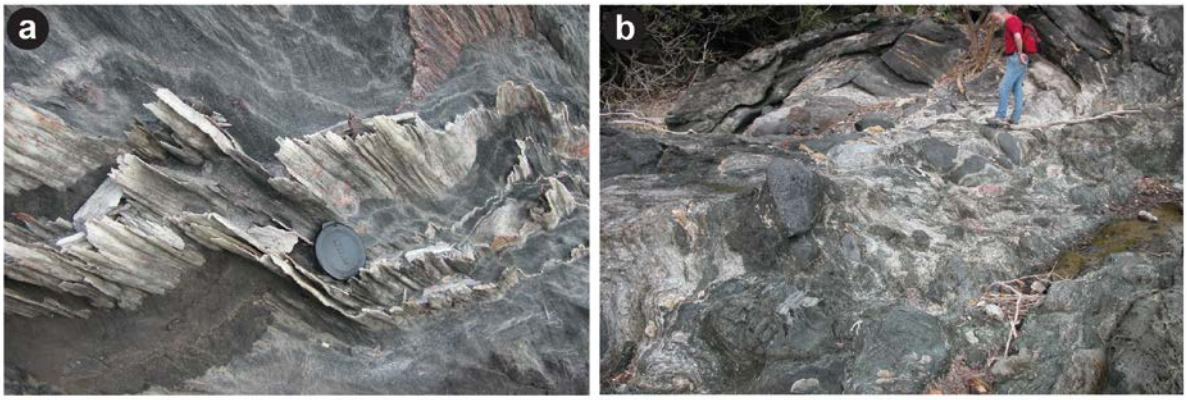

Fig. 7 Typical Eocene Metamorphic Belt outcrops and rocks: a) Diahot-Panié Metamorphic Complex siliceous schist with prominent stretching lineation (Amos Pass). b) Heterogeneous mélange of the Pouébo Terrane (shoreline of Balade).

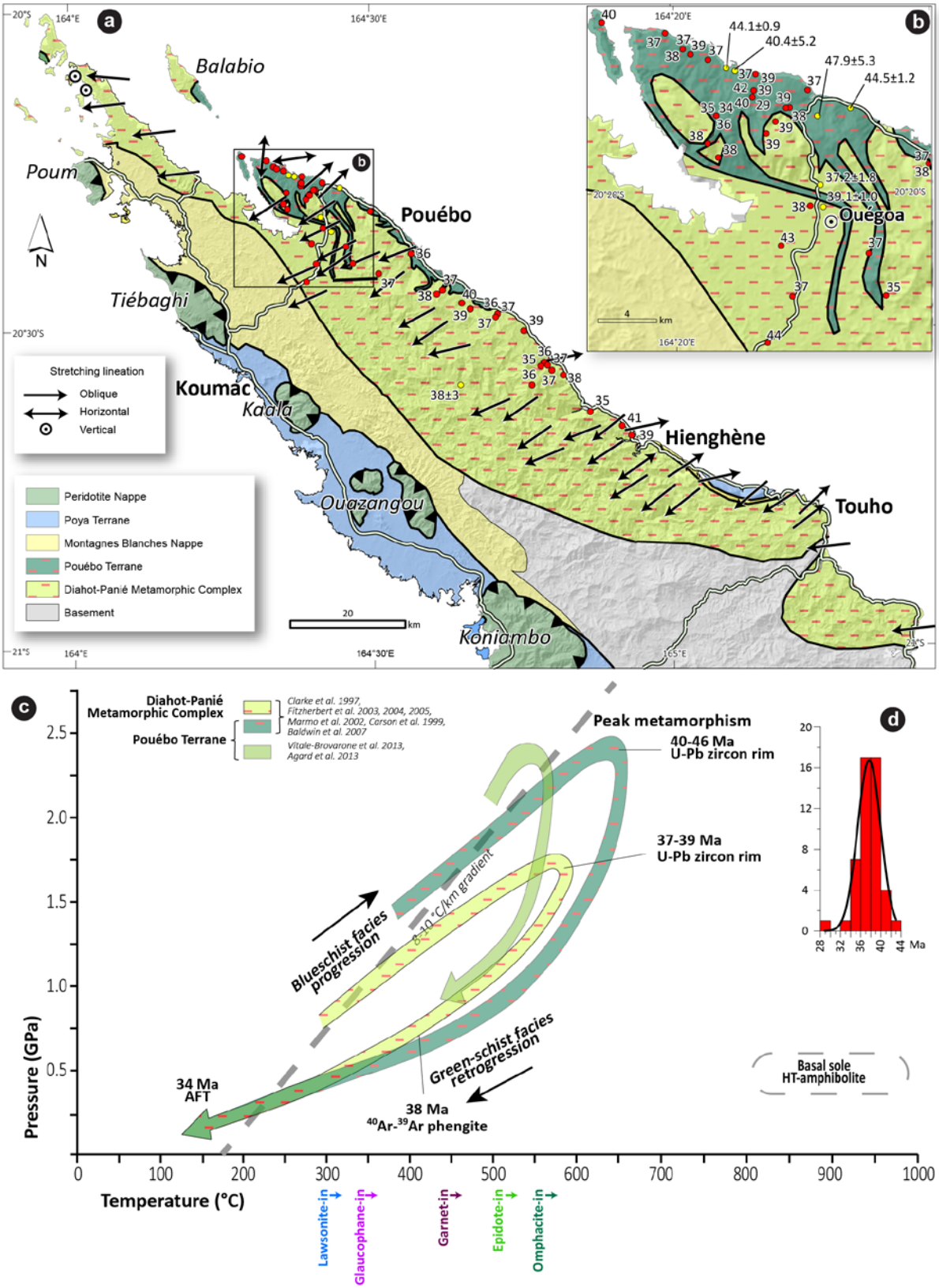

Fig. 8 a) Simplified geological map of the HP-LT Metamorphic Belt with structural elements (Cluzel et al. 1995b), 40Ar/39Ar ages on phengite rounded up to the nearest whole number (red circles), U-Pb ages of zircon rims (yellow circles). b) Enlargement of the former in the Ouégoa area. c) Estimated Pressure-Temperature paths for the metamorphic rocks after different authors, and radiometric ages

of the main stages. Abbreviation: AFT: Apatite Fission Track. Vertical labels on x axis indicate approximate temperature of formation for some key mineral phases. d) Histogram of 40Ar/39Ar age values. P-T parameters of the basal sole amphibolite are given for comparison with HP-LT conditions. Thick dashed grey line indicates the estimate T-gradient of subduction after Agard & Vitale-Brovarone 2013.

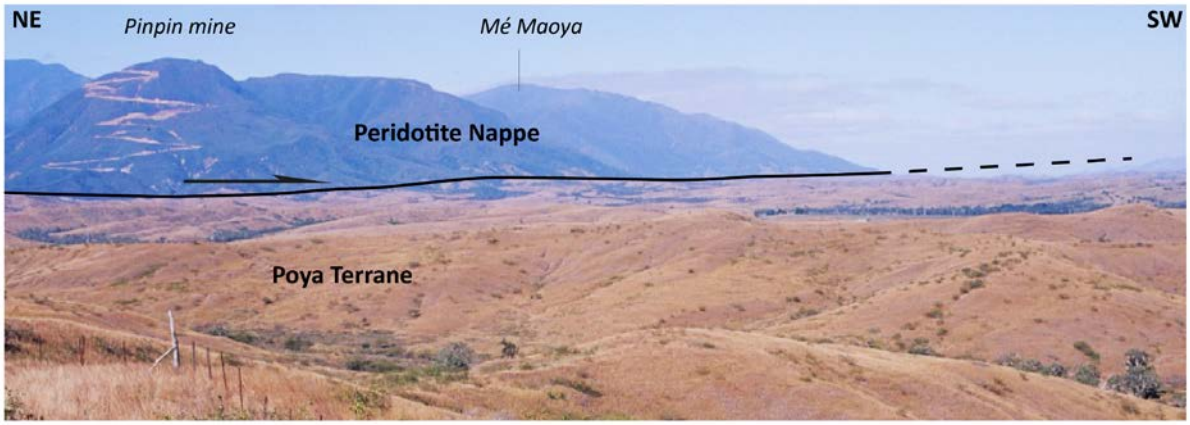

Fig. 9 View from the north of Poya village. Overthrust of the Peridotite Nappe (Mé Maoya klippe) over the Poya Terrane.

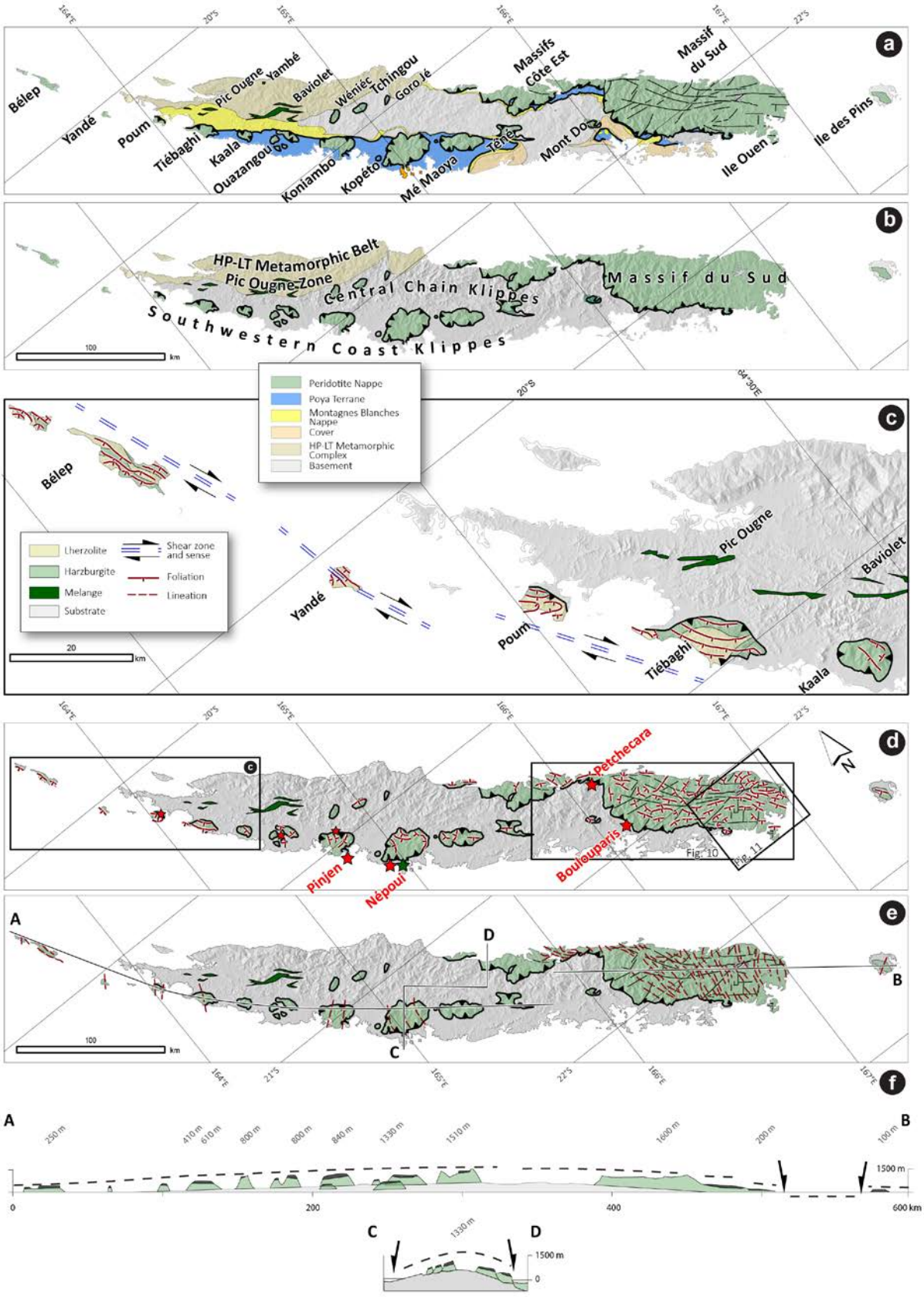

Fig. 10 Distribution of the Peridotite Nappe units. a) Geographical names. b) Zonation of units. c) Association of harzburgite and lherzolites in northern klippes. d) Foliations and e) lineations (modified after Nicolas 1989). f) Longitudinal and transversal sections showing the large-scale double

up warp of the basal sole and main regolith surfaces of the Peridotite Nappe. Large red stars indicate occurrences of High Temperature (HT) amphibolite of the 'metamorphic sole' after Cluzel et al. 2012. Small red stars indicate other occurrences not studied. Green star indicates clinoenstatite-bearing boninite occurrences.

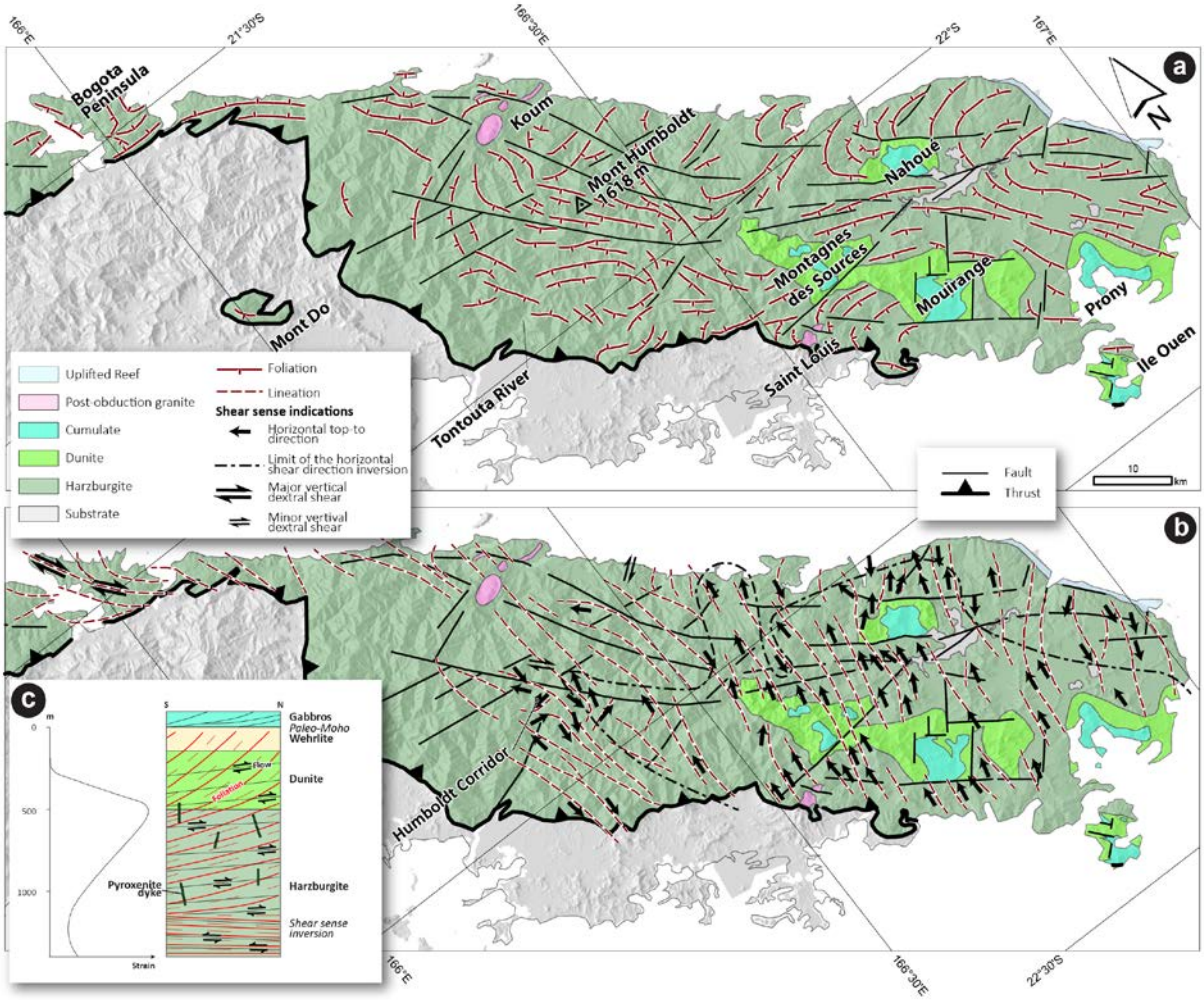

Fig. 11 a) Foliations and b) lineations in the Massif du Sud. c) Montagne des Sources upper mantle to crust section: left, strain variation versus elevation; right, idealized cross section of the high-temperature foliation Prinzhofer et al. (1980).

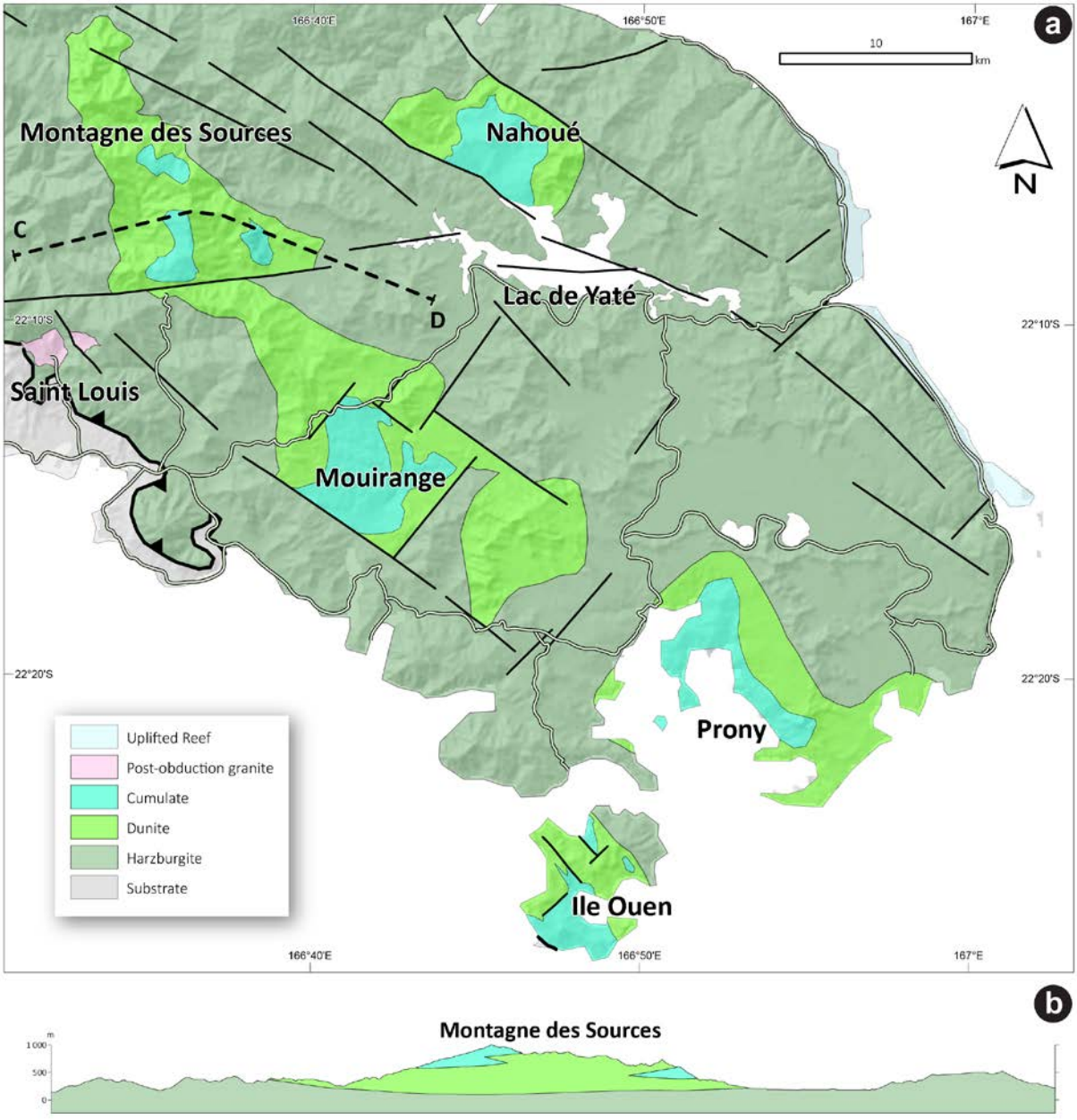

Fig. 12 a) Geological map and b) cross section of dunite and cumulates in the south of Massif du Sud.

Fig. 13 Typical Peridotite Nappe outcrops and rocks: a) Flat lying harzburgite – dunite compositional layering crosscut by a d) dunite dyke with a pyroxenitic core (Massif du Sud). c) Lineation on a dunite surface marked by the stretching (black dotted arrow) of chromite grain spindles and orthogonal pulling-apart.

Fig. 14 Typical outcrops and rocks of the cumulate of the Peridotite Nappe: a, b) Bedded olivine gabbros and pyroxenite (Prony area). c) Gabbronorite cumulate with cross-bedding and slump sedimentary-like structures (Plum area, in Secchiari 2016). d) Cumulus texture of plagioclase bearing olivine gabbros. Ol: olivine (serpentinized); Px: pyroxene. Pl: plagioclase. Ol and Px are cumulus crystals, Pl is intercumulus.

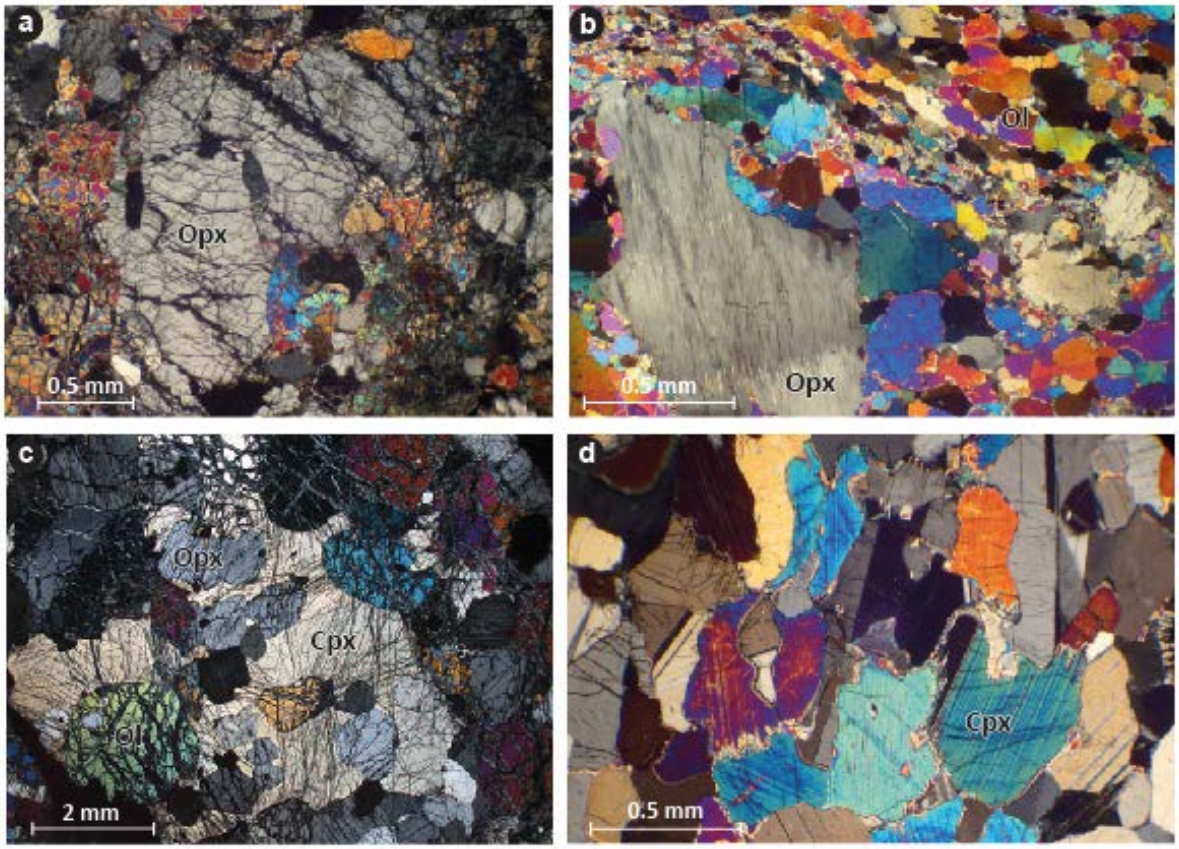

Fig. 15 Photomicrograph (cross-polarized light) of typical Peridotite Nappe rocks. a) Lherzolite: Deformed orthopyroxene porphyroclast showing thin exsolution lamellae of clinopyroxene (Babouillat). b) Harzburgite: Strongly exsolved orthopyroxene porphyroclast in harzburgite tectonite (Poya). c) Wehrlite: Poikiloblastic clinopyroxene with orthopyroxene and olivine inclusions (Montagne des Sources). d) Gabbronorite: Exsolved clinopyroxene crystals displaying evidence of chemical instability (Col de Mouirange). Opx: Orthopyroxene. Cpx: Clinopyroxene; Ol: olivine.

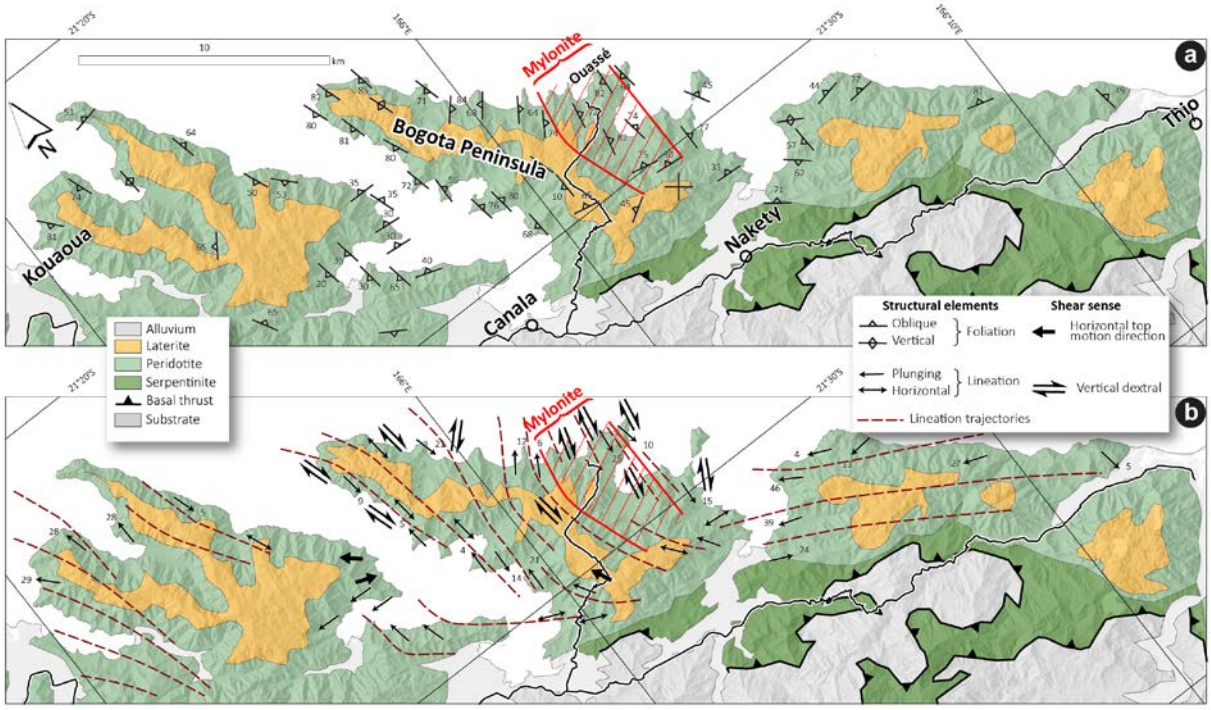

Fig. 16 Geological map of Bogota Peninsula with structural elements: a) Foliation; b) Lineation.

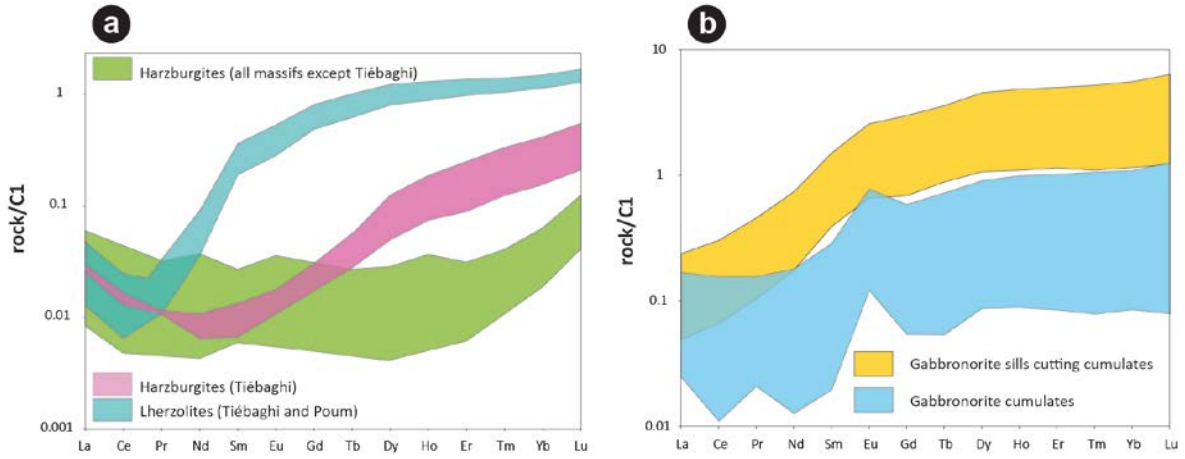

Fig. 17 Geochemical features of peridotites and mafic cumulates: a) Compared chondrite-normalized REE patterns of New Caledonia peridotites (data from Secchiari et al. 2016). REE patterns from Tiébaghi harzburgites display some similarity with lherzolites and differ from the rest of Peridotite Nappe. b) Chondrite-normalized REE patterns for gabbronorites (data from Garrido et al. 2009; Marchesi et al. 2009; Secchiari et al. 2016). Normalizing values from Sun and McDonough (1989).

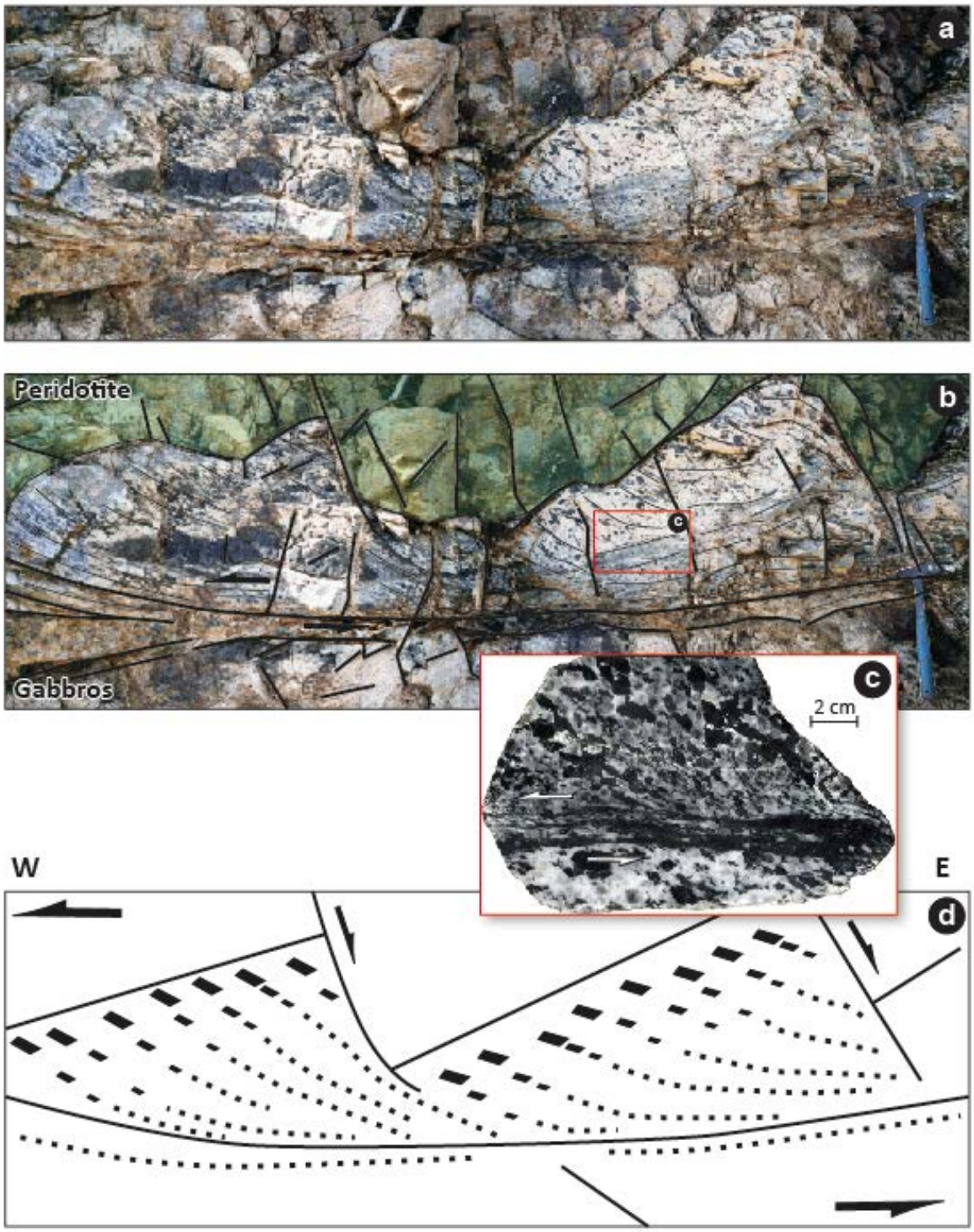

Fig. 18 a) Horizontal dyke at Col de N'go (Massid du Sud) showing complex relationships of the partly ductile gabbroic intrusion against the brittle peridotite wall rock. The dyke is intruded in a top to the west thrust zone. b) Line drawing. c) Detail of a shear zone on polished section. d) Possible interpretation as i) pre-faulted peridotite, ii) intrusion by gabbros developing chilled margins (pegmatoid texture) with large amphiboles growing orthogonally against the wall rock, and getting progressively more strained and rotated toward the shear zone, iii) final domino like structure consistent with the top to west shear context.

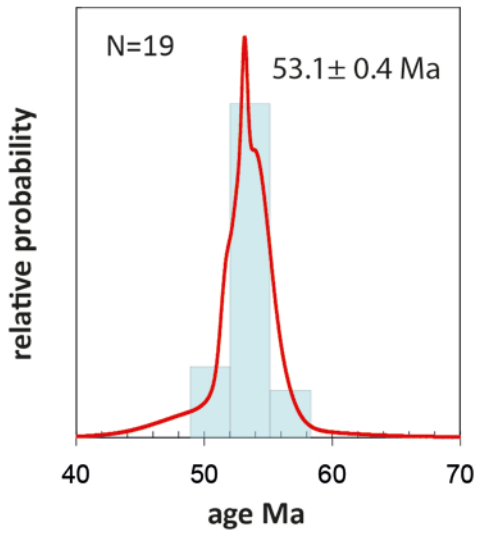

Fig. 19 Combined U-Pb zircon age plot of 19 representative dyke samples of the Peridotite Nappe (3 diorites, 5 granitoids, 3 hornblendites, 5 leucodiorites, 2 leucogabbros, 1 gabbro).

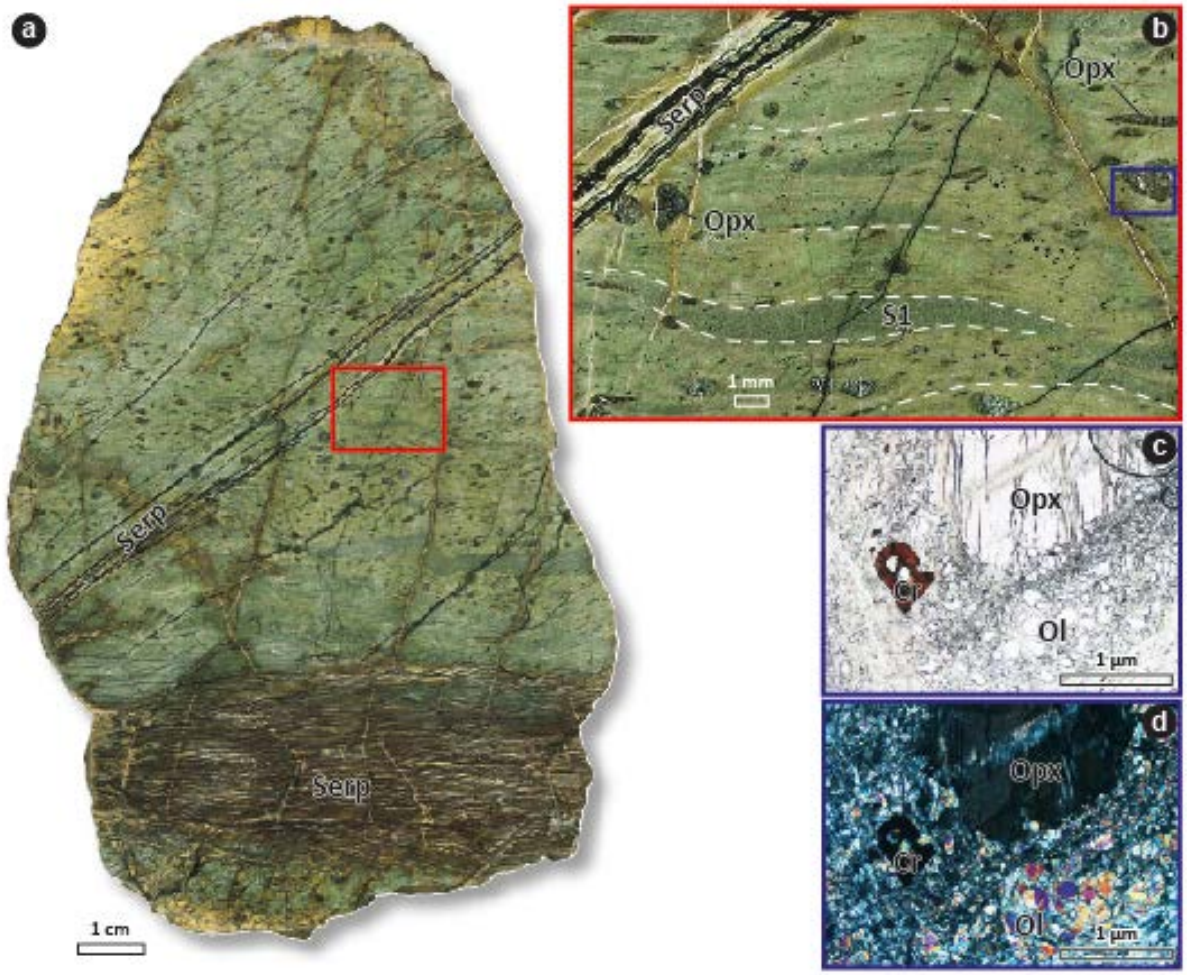

Fig. 20 a) Polished section of serpentinized harzburgite (Massif du Sud) showing different habitus of serpentinite (Serp) as diffuse mesh structure or brittle fracture infills. b) Detail of the mantle fabric (foliation S1) marked by the the mylonitic textures, flattened, and stretched porphyroclasts of orthopyroxene (Opx). c, d): Photomicrograph (plane-polarized and cross-polarized light) showing a porphyroclast of ortopyroxene (Opx) and chromite (Cr) within olivine (Ol) mylonite. Olivine is crosscut by a dense static mesh of serpentine (lizardite).

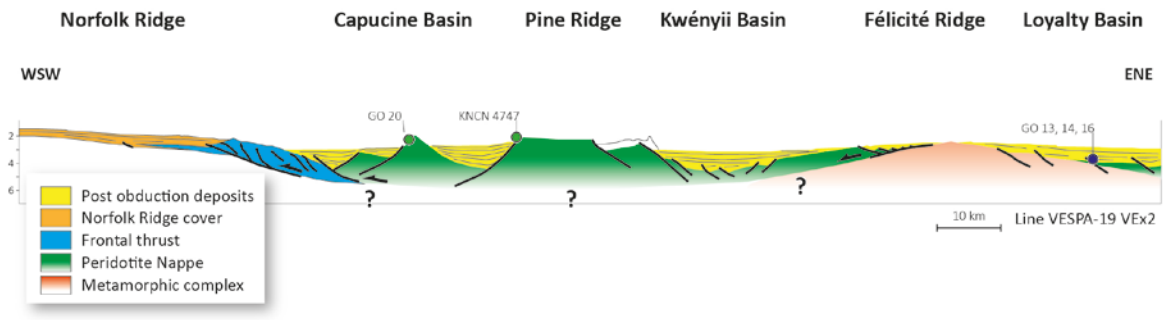

Fig. 21 Line drawing interpretation of seismic profile VESPA 19 modified from Patriat et al. (2018), location on Fig. 24. VE: Vertical Exaggeration.

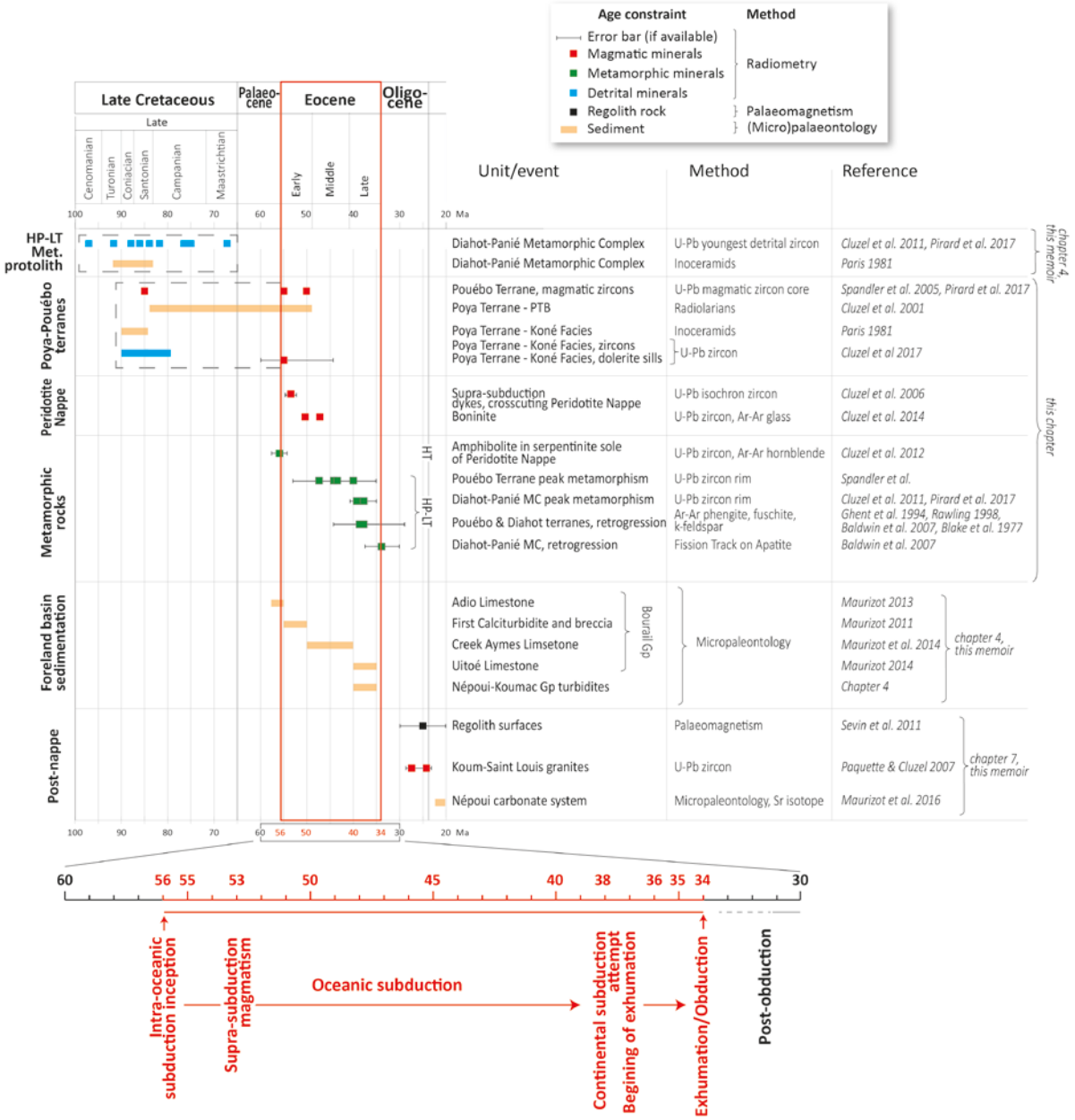

Fig. 22Time-unit-event diagram summarizing the available age data, with corresponding method, reference, and geodynamic interpretations.

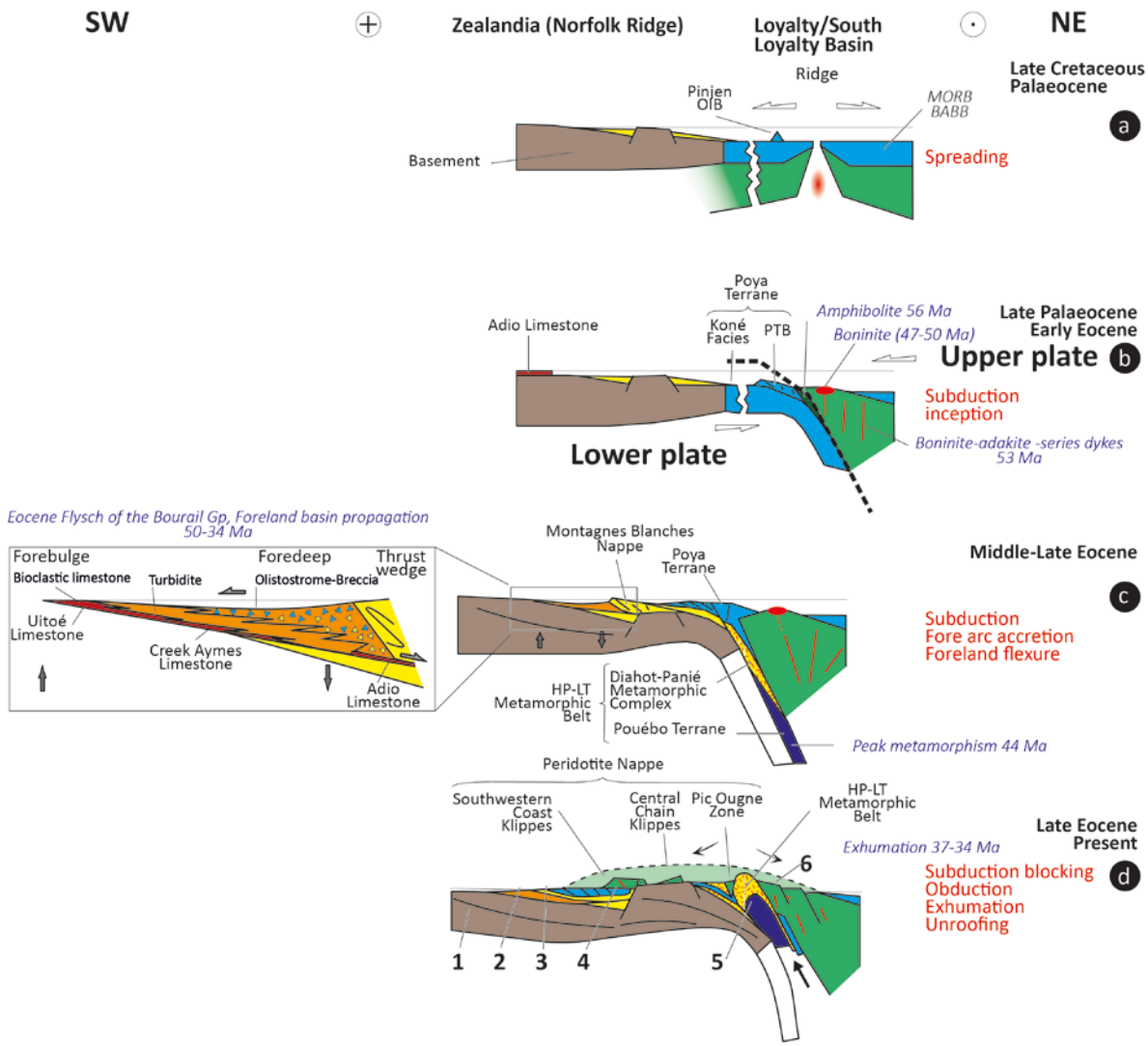

Fig. 23 Sketch reconstruction of the north easternmost margin of Zealandia (Norfolk Ridge) from Late Cretaceous to Late Eocene period. Out of plane transcurrent dextral displacement is indicated by circular symbols with cross (away from the viewer) and point (toward the viewer). Locations of cross sections vary in latitude through time.

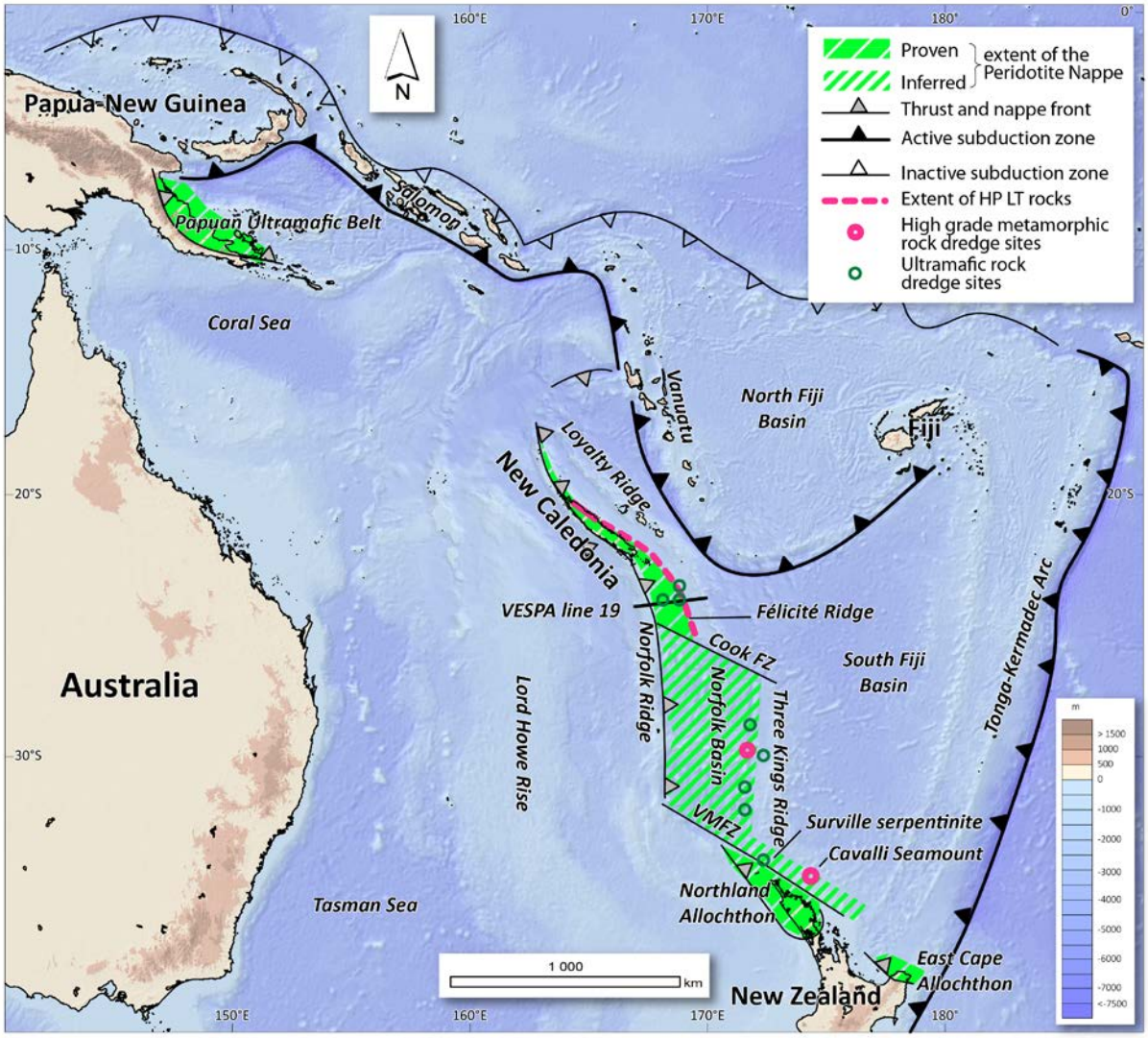

Fig. 24 Major tectonic features of the Southwest Pacific.